ISSN 1007-9327 (print)
ISSN 2219-2840 (online)

World Journal of *Gastroenterology*

World J Gastroenterol 2023 November 28; 29(44): 5872-5944

Published by Baishideng Publishing Group Inc

World Journal of Gastroenterology

Contents

Weekly Volume 29 Number 44 November 28, 2023

ORIGINAL ARTICLE

Clinical and Translational Research

Retrospective Study

Basic Study

CASE REPORT

Contents

NAME OF JOURNAL
World Journal of Gastroenterology

ISSN
ISSN 1007-9327 (print) ISSN 2219-2840 (online)

LAUNCH DATE
October 1, 1995

FREQUENCY
Weekly

EDITORS-IN-CHIEF
Andrzej S Tarnawski

EXECUTIVE ASSOCIATE EDITORS-IN-CHIEF
Xian-Jun Yu (Pancreatic Oncology), Jian-Gao Fan (Chronic Liver Disease), Hou-Bao Liu (Biliary Tract Disease)

EDITORIAL BOARD MEMBERS
http://www.wjgnet.com/1007-9327/editorialboard.htm

PUBLICATION DATE
November 28, 2023

PUBLISHING PARTNER
Shanghai Pancreatic Cancer Institute and Pancreatic Cancer Institute, Fudan University
Biliary Tract Disease Institute, Fudan University

INSTRUCTIONS TO AUTHORS
https://www.wjgnet.com/bpg/gerinfo/204

GUIDELINES FOR ETHICS DOCUMENTS
https://www.wjgnet.com/bpg/GerInfo/287

GUIDELINES FOR NON-NATIVE SPEAKERS OF ENGLISH
https://www.wjgnet.com/bpg/gerinfo/240

PUBLICATION ETHICS
https://www.wjgnet.com/bpg/GerInfo/288

PUBLICATION MISCONDUCT
https://www.wjgnet.com/bpg/gerinfo/208

POLICY OF CO-AUTHORS
https://www.wjgnet.com/bpg/GerInfo/310

ARTICLE PROCESSING CHARGE
https://www.wjgnet.com/bpg/gerinfo/242

STEPS FOR SUBMITTING MANUSCRIPTS
https://www.wjgnet.com/bpg/GerInfo/239

ONLINE SUBMISSION
https://www.f6publishing.com

PUBLISHING PARTNER's OFFICIAL WEBSITE
https://www.shca.org.cn
https://www.zs-hospital.sh.cn

World Journal of Gastroenterology

Submit a Manuscript: https://www.f6publishing.com

World J Gastroenterol 2023 November 28; 29(44): 5872-5881

DOI: 10.3748/wjg.v29.i44.5872

ISSN 1007-9327 (print) ISSN 2219-2840 (online)

ORIGINAL ARTICLE

Clinical and Translational Research

Causal associations between inflammatory bowel disease and anxiety: A bidirectional Mendelian randomization study

Ying He, Chun-Lan Chen, Jian He, Si-De Liu

Specialty type: Gastroenterology and hepatology

Provenance and peer review: Unsolicited article; Externally peer reviewed.

Peer-review model: Single blind

Peer-review report's scientific quality classification

Grade A (Excellent): A
Grade B (Very good): B
Grade C (Good): 0
Grade D (Fair): 0
Grade E (Poor): 0

P-Reviewer: Rodrigues AT, Brazil; Serban ED, Romania

Received: October 8, 2023
Peer-review started: October 8, 2023
First decision: November 1, 2023
Revised: November 6, 2023
Accepted: November 14, 2023
Article in press: November 14, 2023
Published online: November 28, 2023

Ying He, Jian He, Si-De Liu, Department of Gastroenterology, Nanfang Hospital, Southern Medical University, Guangzhou 510515, Guangdong Province, China

Ying He, Department of Infectious Diseases, The Second Xiangya Hospital of Central South University, Changsha 410011, Hunan Province, China

Chun-Lan Chen, Department of Pulmonary and Critical Care Medicine, Guangdong Provincial People's Hospital (Guangdong Academy of Medical Sciences), Southern Medical University, Guangzhou 510080, Guangdong Province, China

Corresponding author: Si-De Liu, PhD, Professor, Department of Gastroenterology, Nanfang Hospital, Southern Medical University, No. 1838 Guangzhou Avenue North, Guangzhou 510515, Guangdong Province, China. liuside2011@163.com

Abstract

BACKGROUND

Anxiety is common in patients with inflammatory bowel disease (IBD), including those with ulcerative colitis (UC) and Crohn's disease (CD); however, the causal relationship between IBD and anxiety remains unknown.

AIM

To investigate the causal relationship between IBD and anxiety by using bidirectional Mendelian randomization analysis.

METHODS

Single nucleotide polymorphisms retrieved from genome-wide association studies (GWAS) of the European population were identified as genetic instrument variants. GWAS statistics for individuals with UC (6968 patients and 20464 controls; adults) and CD (5956 patients and 14927 controls; adults) were obtained from the International IBD Genetics Consortium. GWAS statistics for individuals with anxiety were obtained from the Psychiatric Genomics Consortium (2565 patients and 14745 controls; adults) and FinnGen project (20992 patients and 197800 controls; adults), respectively. Inverse-variance weighted was applied to assess the causal relationship, and the results were strengthened by heterogeneity, pleiotropy and leave-one-out analyses.

RESULTS

Genetic susceptibility to UC was associated with an increased risk of anxiety

[odds ratio: 1.071 (95% confidence interval: 1.009-1.135), P = 0.023], while genetic susceptibility to CD was not associated with anxiety. Genetic susceptibility to anxiety was not associated with UC or CD. No heterogeneity or pleiotropy was observed, and the leave-one-out analysis excluded the potential influence of a particular variant.

CONCLUSION

This study revealed that genetic susceptibility to UC was significantly associated with anxiety and highlighted the importance of early screening for anxiety in patients with UC.

Key Words: Inflammatory bowel disease; Anxiety; Causal effect; Mendelian randomization; Genome-wide association studies

Core Tip: Our study provides evidence that genetic susceptibility to ulcerative colitis (UC) is associated with an increased risk of anxiety [odds ratio: 1.071 (95% confidence interval: 1.009, 1.135), P = 0.023], while genetic susceptibility to Crohn's disease (CD) is not associated with an increased risk of anxiety. No causal effects of anxiety on UC and CD were observed in this study. In conclusion, our study demonstrates the causal effect of UC on anxiety. These findings may be helpful to increase physicians' awareness of the need to recognize anxiety in UC patients and influence the management of anxiety in clinical practice.

Citation: He Y, Chen CL, He J, Liu SD. Causal associations between inflammatory bowel disease and anxiety: A bidirectional Mendelian randomization study. *World J Gastroenterol* 2023; 29(44): 5872-5881
URL: https://www.wjgnet.com/1007-9327/full/v29/i44/5872.htm
DOI: https://dx.doi.org/10.3748/wjg.v29.i44.5872

INTRODUCTION

Inflammatory bowel disease (IBD), mainly composed of ulcerative colitis (UC) and Crohn's disease (CD), is a debilitating chronic inflammatory disease with varying degrees of severity[1,2]. UC and CD influence not only the gastrointestinal tract but also other systems[3]. Emerging evidence has reported the role of the gut-brain axis in the interactions between gastrointestinal diseases and neuropsychiatric disorders[4,5]. Anxiety is a common comorbidity in patients with IBD (prevalence varies from 19.1% to 35.1%) compared with the general population (3.4%)[4,6]. The association between IBD and anxiety, or vice versa, has received considerable attention due to the putative pathophysiological mechanisms regulated by the gut-brain axis.

Some observational studies have investigated the temporal relationship between IBD and anxiety and have suggested that the relationship between IBD and anxiety may be bidirectional[7]. Patients with IBD might be at higher risk for anxiety than control individuals. Specifically, newly diagnosed patients with IBD had a rising prevalence (incidence rate ratio: 1.39) of anxiety when compared with matched control individuals during 10 years of follow-up[7]. However, some observational studies have shown that patients with anxiety are prone to suffering from IBD[8,9]. A cohort study suggested a higher prevalence of IBD in patients with newly diagnosed anxiety compared with control individuals during 6.7 years of follow-up[9]. Collectively, the existing findings from observational studies demonstrated the bidirectional relationships between IBD and anxiety, which is partly influenced by residual confounders. Therefore, more evidence is needed to clarify the causal relationships between IBD and anxiety. A recent Mendelian randomization (MR) study inferred the causal relationships between IBD and depression and demonstrated a causal effect of depression on IBD but no causal effect of IBD on depression[10]. Depression and anxiety are common co-occurrence in IBD, while the causality between IBD and anxiety has not been investigated.

MR is a genetic approach to estimate causality between the exposure and the outcome by using genetic instrument variants (IVs) identified through genome-wide association studies (GWAS), usually using single-nucleotide polymorphisms (SNPs) as IVs. Since genetic makeup is assigned at conception and is unlikely to be affected by disease later in life, unidirectional causality can be deduced by MR analysis. Potential confounders that could affect the outcomes were eliminated from the analysis, effectively forming naturally blinded randomized controlled trials[11]. Therefore, this study aimed to evaluate the causal associations between IBD and anxiety by performing bidirectional two-sample MR analysis.

MATERIALS AND METHODS

GWAS statistics sources for UC, CD and anxiety

The International IBD Genetics Consortium (IIBDGC), a large-scale consortium consisting of hundreds of researchers from more than 20 countries worldwide, collects GWAS data from over 75000 patients with IBD. The IIBDGC is an

authoritative organization aimed at identifying genetic risk factors for IBD. GWAS summary statistics for UC and CD were obtained from the IIBDGC[12], which contains adult individuals of European descent with UC (6968 patients, 20464 control individuals) and CD (5956 patients, 14927 control individuals) (Supplementary Table 1). UC and CD were diagnosed by physicians based on comprehensive evidence of clinical symptoms, endoscopic findings, and histopathological and imaging results.

GWAS summary statistics for anxiety were obtained from two separate databases (Supplementary Table 1): (1): The Psychiatric Genomics Consortium (PGC) (https://pgc.unc.edu/) from Otowa *et al*[13]; and (2) the FinnGen project (https://www.finngen.fi/en). The PGC[14], the largest international psychiatric consortium consisting of more than 800 investigators from 38 countries, is dedicated to finding the genetic variants of psychiatric disorders. The FinnGen project is an academic-industrial collaboration aimed at deciphering genotype-phenotype relationships from more than 500000 Finnish participants. The participants in the GWAS databases for anxiety were adults of European descent. The number of patients and control individuals for anxiety were 2565/14745 in PGC and 20992/197800 in FinnGen, respectively.

We used published GWAS statistics and did not collect initial data. Patient informed consent and ethics approval were not needed for this study, as these materials had already been obtained in each of the preliminary studies.

Genetic IV selection

To select eligible SNPs as IVs from the GWAS statistics, a series of quality control steps were applied. The three following assumptions must be satisfied[11]: (1) Correlation assumption: The IV is strongly correlated with the exposure; (2) independence assumption: The IV does not influence the outcome through the confounding factors; and (3) exclusion assumption: the IV does not directly influence the outcome, but only influences the outcome *via* indirect exposure (Figure 1).

To satisfy the correlation assumption, the following criteria were set for identifying instrumental SNPs: (1): Genome-wide strongly significant ($F > 10$, $P < 5 \times 10^{-8}$) association with the exposure. For a single variant, the F statistic, which should be over 10 to avoid weak instrument bias, was calculated by the following equation[15]: $F = [\beta/se]^2$, where β means estimated effect size and se means standard error of β; and (2) independent SNPs are selected by linkage disequilibrium (LD) clumping ($r^2 < 0.001$, window size = 1 Mb). To satisfy the independence and exclusion assumption, we checked each SNP associated with the exposure at PhenoScanner (http://www.phenoscanner.medschl.cam.ac.uk/) and eliminated SNPs significantly related to the potential confounders and the outcome. The potential confounders that may influence anxiety include smoking, body mass index, neuropsychiatric disease, drinking, and hypertension[16,17]. The potential confounders that may influence UC or CD include smoking, body mass index, and intestinal malabsorption[18,19]. The subsequent harmonization process was used to unify the effect direction and effect allele, ensure SNPs with a minor allele frequency (> 0.01), and remove the palindromic and incompatible SNPs.

For MR estimation from UC or CD to anxiety, the selection criteria of SNPs associated with UC or CD satisfy the abovementioned three assumptions. For MR estimation from anxiety to UC or CD, no eligible SNPs associated with anxiety could be obtained from GWAS statistics in PGC after LD clumping, so we used GWAS statistics from the FinnGen project to extract anxiety-related SNPs. Because anxiety-related SNPs could not be obtained by the statistical P value of $< 5 \times 10^{-8}$, we used a suggested P value of $< 5 \times 10^{-6}$ to extract SNPs, which had been applied in a previous study to decipher bidirectional relationships between prescription opioid use and anxiety risk by MR analysis[20].

The MR-Pleiotropy Residual Sum and Outlier (MR-PRESSO) test was used to detect the outlier SNPs in MR analysis [21]. The MR-PRESSO test consists of three main parts: (1) Detecting horizontal pleiotropy; (2) correcting horizontal pleiotropy by removing the outlier; and (3) testing significant distortion in the causal estimates before and after removing the outlier. The MR-PRESSO test requires that more than 50% of the SNPs are efficient IVs with balanced pleiotropy. The number of distributions was set to 3000 in the MR-PRESSO test.

MR analysis

Three different methods [inverse-variance weighted (IVW), MR Egger, and weighted median] were used in the MR analysis[15]. IVW, the most efficient causal estimation method allowing balanced pleiotropy in MR analysis, was used as the main method[22]. The assessments by the IVW method are efficient, consistent and close to the true effect when the sample size of IVs is large enough and the pleiotropy of IVs is not significant[23]. If no significant heterogeneity (IVW-derived Cochran Q statistic $P \geq 0.05$) was detected, the fixed-effects IVW model was adopted; otherwise, the random-effects IVW model was applied. Since unbalanced pleiotropy may result in bias to the causal estimates by IVW, supplementary MR and sensitivity analyses are usually needed to verify the robustness of causal estimation in MR analysis[24]. MR Egger and weighted median were applied as supplementary MR methods to verify the causal estimates obtained by the IVW method[15,25]. Although they have less statistical power [wider confidence intervals (CIs)], they can provide more robust and reliable causal estimations across a wider range of scenarios. All statistical analyses were conducted using R (version 4.2.1), the Two-Sample MR package (version 0.5.6), and the MR-PRESSO package (version 1). $P < 0.05$ was considered indicative of statistical significance.

Sensitivity analysis

The MR Egger method was applied to assess the potential horizontal pleiotropy of SNPs. If the intercept P value was < 0.05, there was significant pleiotropy. Heterogeneity was tested by the IVW-derived Cochran Q statistic. A Cochran Q statistic P value of < 0.05 was considered to indicate the presence of significant heterogeneity. Scatter plots were used to visualize the results from MR analysis to show efficiency and reliability. The leave-one-out analysis aimed to verify that a single SNP does not affect the results by eliminating a single SNP one by one and performing MR analysis on the remaining SNPs.

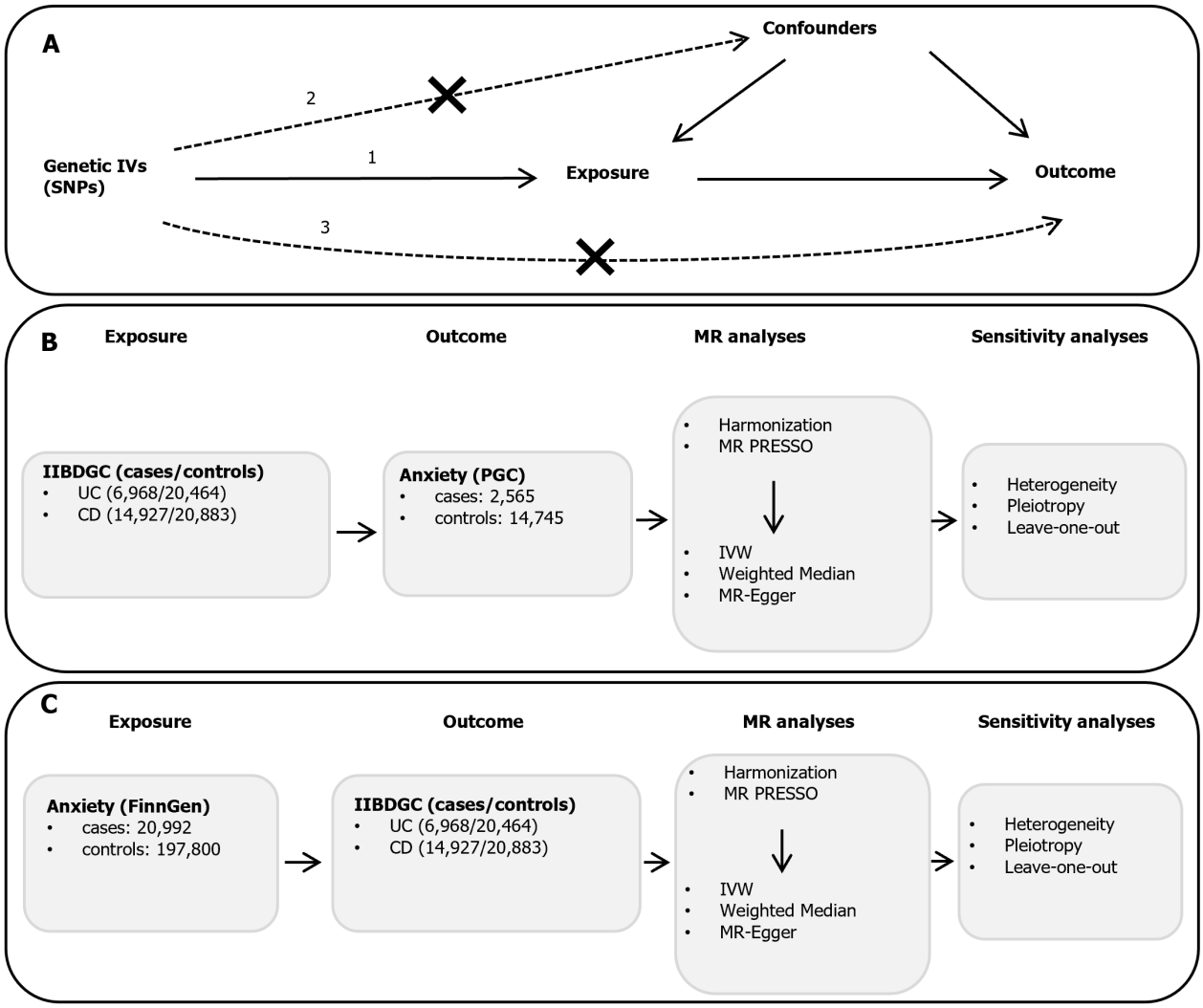

DOI: 10.3748/wjg.v29.i44.5872

Figure 1 Schematic overview of the study design. A: Mendelian randomization (MR) analysis illustration. There are three principal assumptions in MR design: (1) Relevance assumption: the genetic instrument variants (IVs) are strongly associated with the exposure; (2) independence assumption: the genetic IVs do not affect the outcome through the confounders; and (3) exclusion assumption: The genetic IVs do not affect the outcome directly but only *via* indirect exposure; B: MR analysis from ulcerative colitis (UC) or Crohn's disease (CD) to anxiety. UC- or CD-related single-nucleotide polymorphisms (SNPs) obtained from genome-wide association studies (GWAS) statistics in the International Inflammatory Bowel Disease Genetics Consortium (IIBDGC) consortium were identified as IVs, and GWAS summary statistics of anxiety were retrieved from Psychiatric Genomics Consortium; C: MR analysis from anxiety to UC or CD. Anxiety-related SNPs retrieved from FinnGen were identified as IVs, and GWAS statistics for UC and CD were obtained from the IIBDGC consortium. MR analysis was performed after the harmonization process and MR Pleiotropy Residual Sum and Outlier test and subsequently sensitivity analyses to strengthen the MR estimates. MR: Mendelian randomization; IVs: Instrumental variables; UC: Ulcerative colitis; CD: Crohn's disease; PGC: Psychiatric Genomics Consortium; IVW: Inverse-variance weighted; PRESSO: Pleiotropy Residual Sum and Outlier; IIBDGC: International Inflammatory Bowel Disease Genetics Consortium.

MR analysis procedure

First, the abovementioned three assumptions were used to identify the genetic IVs (SNPs) of the exposure. Second, after the harmonization process, MR-PRESSO analysis was applied to detect and remove the outlier SNPs. Third, after the outlier SNPs were removed, MR analysis was performed, and subsequently, sensitivity analyses were conducted to determine whether pleiotropy existed and which IVW model was adopted according to heterogeneity. A schematic overview of the procedure is detailed in Figure 1.

RESULTS

Description of selected genetic IVs

Data for 34652 individuals of European descent who participated in the GWAS cohorts were obtained from seven CD and eight UC collections with combined genome-wide SNP data. After LD clumping and harmonization processes were completed, the MR-PRESSO test did not detect any CD- or UC-related outlier SNPs. Finally, 46-51 confounder-independent CD-related SNPs and 34-36 UC-related SNPs were identified to evaluate the causal effects on anxiety

(Table 1). Twenty-one anxiety-related SNPs from the FinnGen database were obtained to evaluate the causal effects on UC and CD (Table 1). The single-variant F statistic was calculated, and the F statistic values were all over 10, indicating that these selected SNPs were strongly associated with the exposures. Independent UC-related SNPs are listed in Supplementary Table 2, CD-related SNPs are listed in Supplementary Table 3, and anxiety-related SNPs are listed in Supplementary Tables 4 and 5.

Causal estimations from UC or CD to anxiety

We used IVW as the primary method to assess the causal estimates. We only observed a causal effect of UC on anxiety [odds ratio (OR): 1.071, 95%CI: 1.009-1.135, P = 0.0226] (Table 1). However, CD had no causal effect on anxiety. Additionally, MR Egger and weighted median methods verified the reliability of the causality estimated by IVW. Even though the MR Egger-derived P value and weighted median-derived P value were over 0.05, the ORs from MR Egger (OR = 1.138; 95%CI: 0.945-1.371) and weighted median (OR = 1.064; 95%CI: 0.981-1.154) methods were in the same direction as IVW estimation from UC to anxiety, indicating the robustness of causality (Table 1). Moreover, the supplementary MR analysis also did not provide evidence for the causal effect of CD on anxiety.

Heterogeneity was tested by the IVW-derived Cochran's Q statistic. The results showed that no statistically significant heterogeneity (all P > 0.05) was observed for the causal effects of UC and CD on anxiety (Table 1). Thus, we used the fixed-effects IVW model in the MR analysis. In addition, the effects of individual UC- or CD-related SNPs on anxiety are presented in scatter plots (Figure 2). The horizontal pleiotropic effect was performed by the MR Egger method to determine whether genetic IVs associated with UC or CD could affect anxiety through other potential pathways. Significant horizontal pleiotropy was not observed in our MR analysis (Table 1), which verified the robustness and credibility of the IVW-derived causal estimates. After one-by-one removal of each individual SNP, the following causal estimates of the remaining SNPs on anxiety were tested by leave-one-out analysis, which was consistent with the results of MR analysis and demonstrated that the causal effects were unlikely to be caused by any individual SNP (Supplementary Figure 1). Overall, our MR analysis showed that genetic susceptibility to UC, but not CD, was associated with an increased risk of anxiety.

Causal estimations from anxiety to UC or CD

Both IVW and the supplementary methods showed no causal effects (all P > 0.05) of anxiety on UC or CD (Table 1). In addition, no heterogeneity or horizontal pleiotropy (all P > 0.05) was observed in the sensitivity analyses (Table 1), which indicated that these MR estimations were reliable and robust (Figure 3). The leave-one-out analysis also suggested that the MR analysis was reliable (Supplementary Figure 2). Taken together, our MR analysis suggested that genetic susceptibility to anxiety was not associated with UC or CD.

DISCUSSION

In this study, we estimated the bidirectional causal relationships between IBD and anxiety by MR analysis. Our results suggested that genetic susceptibility to UC, but not CD, was associated with anxiety; however, genetic susceptibility to anxiety was not associated with UC or CD.

Previous observational studies showed that IBD was a risk factor for anxiety. A recent meta-analysis showed that the pooled prevalence of anxiety in IBD patients was 12% (95%CI, 8%-18%)[26]. Another population-based cohort study in the United Kingdom demonstrated that young IBD patients had a significantly higher incidence and risk of anxiety (adjusted hazard ratio, 1.25; 95%CI, 1.06-1.48)[27]. In addition, two large nationwide cohort studies showed that anxiety was more commonly seen in both patients with adult-onset IBD and those with childhood-onset IBD[28,29]. However, the abovementioned results could not be used to clarify the causality and directionality of the relationship between IBD and anxiety. Our study is the first to estimate the causal associations between IBD and anxiety using MR analysis and provides evidence that UC has a causal effect on anxiety.

Some studies observed that CD patients had a higher OR value of anxiety symptoms than UC patients[30-32]. However, in our study, genetic susceptibility to UC but not CD was associated with an increased risk of anxiety. This result may be explained as follows: (1) UC and CD are two different diseases of the gut, with UC mainly restricted to the colonic mucosa, whereas CD involves the immune response of the entire gastrointestinal tract. Differences in the distribution of the enteric nervous system in the gastrointestinal tract may affect the function of different brain regions *via* the gut-brain axis[33,34]; and (2) discrepancies in gut microbiota and immune cell populations between UC and CD may have different influences on the brain through the microbiota-gut-brain axis[35-37]. These results reminded us that many factors other than genetic predisposition to IBD can also increase the risk of developing anxiety during the progression of IBD.

The biological route from UC or CD to anxiety has not yet been fully clarified. Increased evidence indicates that the gut-brain axis regulated by inflammation can affect neuronal development and subsequent behavioral phenotypes[5,38,39]. Circulating leukocytes and cytokines can reach the brain by crossing the blood-brain barrier, even leading to neuropsychiatric disorders[40]. For example, induced colitis in mice can result in increased levels of circulating cytokines, which influence certain brain regions, especially the hippocampus[41,42]. The hippocampus is related to memory and emotions, and damage to the hippocampus is closely associated with anxiety and depression[18,43-45]. Additionally, the gut microbiota plays a critical role in the interconnections between the gut and the brain[46,47]. The key routes or mediators between the gut microbiota and the brain are the enteric vagus nervous system, tryptophan metabolites, and microbial products[38,48]. Therefore, dysregulated inflammation and gut microbiota in patients with UC may lead to the

Table 1 Causal estimates between ulcerative colitis or Crohn's disease and anxiety by Mendelian randomization analysis

Exposure	Outcome	SNPs (*n*)	IVW			Weighted median		MR Egger		
			OR [95%CI]	*P* value	Cochran's Q *P* value	OR [95% CI]	*P* value	OR [95%CI]	*P* value	Intercept *P* value
UC	Anxiety	34	1.071 (1.009-1.135)	**0.023**	0.709	1.064 (0.981-1.154)	0.131	1.138 (0.945-1.371)	0.182	0.501
CD	Anxiety	46	1.005 (0.960-1.052)	0.825	0.713	1.027 (0.960-1.100)	0.435	1.023 (0.914-1.145)	0.689	0.734
Anxiety	UC	21	0.920 (0.779-1.086)	0.325	0.858	0.820 (0.654-1.027)	0.085	0.807 (0.594-1.096)	0.187	0.333
Anxiety	CD	21	1.012 (0.851-1.204)	0.892	0.808	0.998 (0.771-1.291)	0.989	1.016 (0.744-1.388)	0.919	0.974

MR: Mendelian randomization; UC: Ulcerative colitis; CD: Crohn's disease; IVW: Inverse-variance weighted; SNPs: Single-nucleotide polymorphisms; OR: Odds ratio; CI: Confidence intervals.

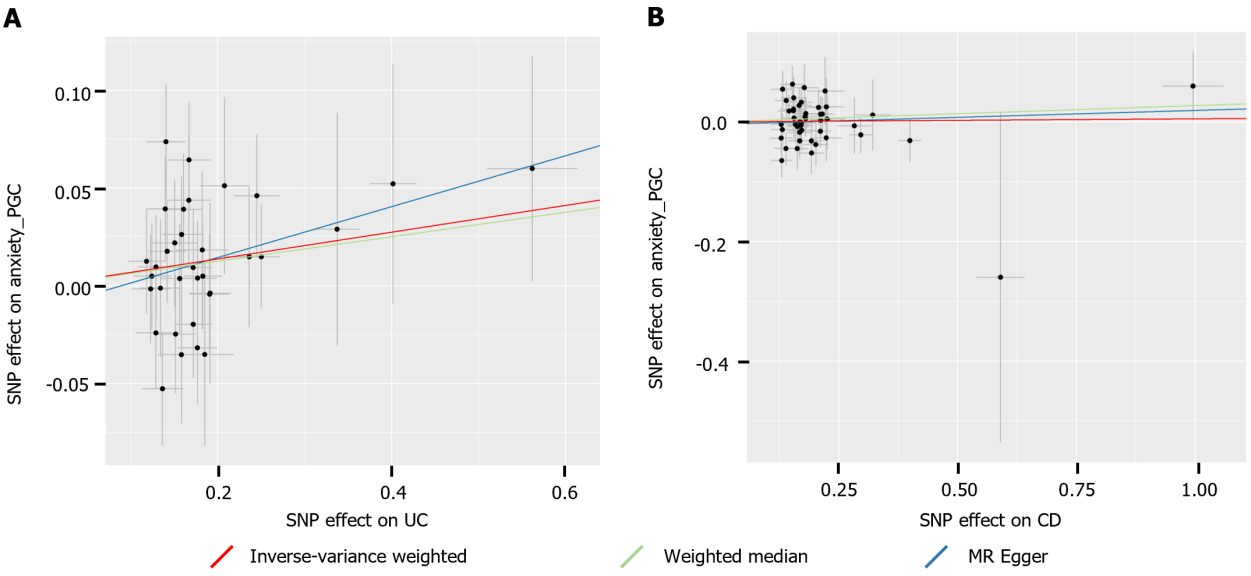

DOI: 10.3748/wjg.v29.i44.5872

Figure 2 Scatter plots of Mendelian randomization analysis showing the effect of ulcerative colitis and Crohn's disease on anxiety. A: Analysis of ulcerative colitis (UC) and anxiety; B: Analysis of Crohn's disease (CD) and anxiety. The x-axes represent the genetic instrument-UC or instrument-CD associations, and the y-axes represent genetic instrument-anxiety associations. Black dots denote the genetic instruments included in the primary Mendelian randomization (MR) analysis. Red: Inverse-variance weighted; Green: Weighted median; blue: MR Egger. CD: Crohn's disease; UC: Ulcerative colitis; PGC: Psychiatric Genomics Consortium; SNP: Single-nucleotide polymorphism.

progression of neuropsychiatric conditions, such as anxiety.

There are two main strengths in this study. First, this is the first study to assess the causal associations between IBD and anxiety using rigorous MR analysis. Second, the large-scale GWAS summary statistics for UC, CD and anxiety were all obtained from individuals of European descent, which would avoid the bias caused by a sample of individuals with different ethnicities. Meanwhile, some limitations should be considered. First, patients with CD or UC came from different medical units, and discrepancies in diagnostic approaches, data collection, and data processing may generate bias. Second, stratification analyses, especially those for sex, diverse severity, age, and drug use, are not viable due to using summary statistics for MR analysis. Third, all GWAS statistics included in the MR analysis came from European individuals; thus, the results of this study might not be generalizable to other ethnic groups.

Although this study investigated the causal relationship between IBD and anxiety, the precise biological mechanisms by which UC affects the development of anxiety remain unclear, such as whether and how the gut-brain axis plays a role. Hence, more basic and clinical studies regarding the identification of key regulators and pathways are needed to further uncover the biological mechanisms.

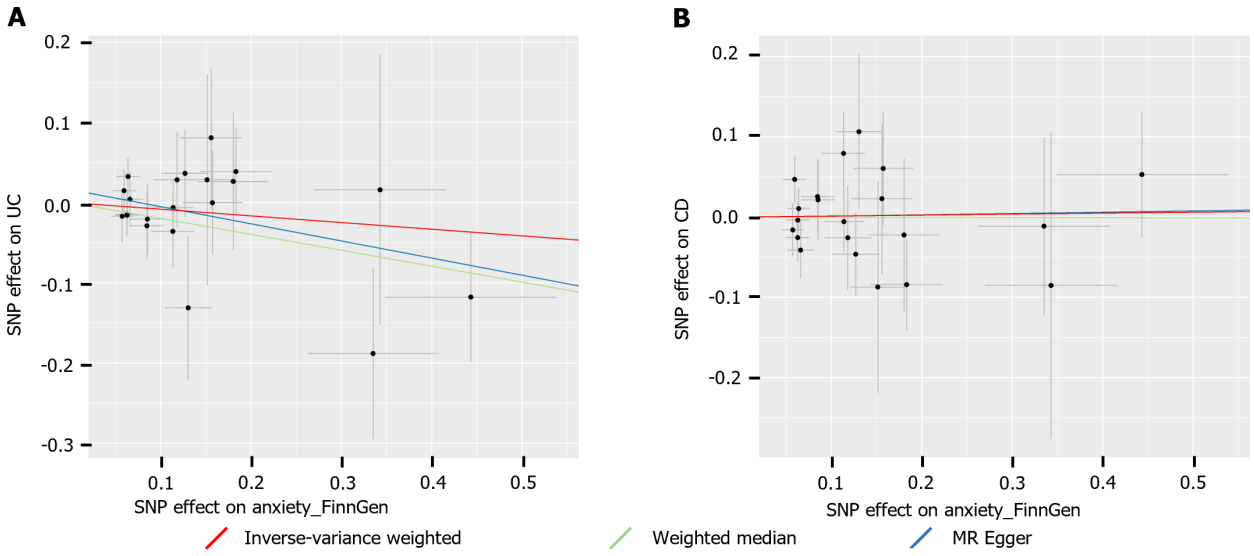

DOI: 10.3748/wjg.v29.i44.5872 **Copyright** ©The Author(s) 2023.

Figure 3 Scatter plots of Mendelian randomization analysis showing the effect of anxiety on ulcerative colitis and Crohn's disease. A: Analysis of anxiety and ulcerative colitis (UC); B: Analysis of anxiety and Crohn's disease (CD). The x-axes represent the genetic instrument-anxiety associations, and the y-axes represent genetic instrument-UC or instrument-CD associations. Black dots denote the genetic instruments included in the primary Mendelian randomization (MR) analysis. Red: inverse-variance weighted; green: weighted median; blue: MR Egger. Due to the same estimate from the weighted median and MR Egger methods in some analyses, those figures only contain two lines. However, the color of the overlapped lines is darker than that of the MR Egger. CD: Crohn's disease; UC: Ulcerative colitis; SNP: Single-nucleotide polymorphism.

CONCLUSION

This study revealed that genetic susceptibility to UC was significantly associated with anxiety and highlighted the importance of early screening for anxiety in patients with UC, which may be helpful to strengthen physicians' awareness of recognizing anxiety.

ARTICLE HIGHLIGHTS

Research background

Inflammatory bowel disease (IBD), mainly consisted of Crohn's disease (CD) and ulcerative colitis (UC), is a chronic inflammatory disease. Depression and anxiety are common co-occurrence in IBD. A recent Mendelian randomization (MR) study has inferred the causal effect of depression on IBD, while the causality between IBD and anxiety has not been investigated.

Research motivation

Previous observational studies showed that IBD patients had a significantly higher incidence and risk of anxiety. Despite the existing findings demonstrated the bidirectional relationship between IBD and anxiety, the causal association between them remain unclear. This study seeks to find out causal association between IBD and anxiety from the genetic perspective by using MR analysis, potentially offering new insights into the pathogenesis and clinical significance of anxiety in IBD.

Research objectives

The study aims to investigate the causal relationship between IBD and anxiety by performing bidirectional MR analysis, to better understand the gene susceptibility of anxiety in IBD.

Research methods

Single nucleotide polymorphisms retrieved from genome-wide association studies (GWAS) were identified as instrument variants. GWAS statistics for UC and CD were obtained from the International IBD Genetics Consortium. GWAS statistics for anxiety were obtained from the Psychiatric Genomics Consortium and FinnGen project. Inverse-variance weighted was applied to assess the causal relationship, and the results were strengthened by sensitivity analyses.

Research results

This study found that the genetic susceptibility to UC was associated with the increased risk of anxiety [odds ratio: 1.071 (95% confidence interval: 1.009, 1.135), P = 0.023]; while genetic susceptibility to CD was not associated with anxiety.

However, genetic susceptibility to anxiety was not associated with UC or CD. No heterogeneity and pleiotropy were found and leave-one-out analysis excluded the potential influence of a particular variant.

Research conclusions

This study identified that the genetic susceptibility to UC was significantly associated with anxiety, and provided the insight that early screening for the trait of anxiety is important for patients with UC.

Research perspectives

Although this study investigated the causal relationship between IBD and anxiety, the precise biological mechanisms by which UC affects the development of anxiety remain unclear, such as whether and how the gut-brain axis plays a role in this process. Hence, more basic and clinical studies are needed for the identification of key regulators and pathways to further uncover the biological mechanisms.

ACKNOWLEDGEMENTS

We want to acknowledge the participants and investigators of the International Inflammatory Bowel Disease Genetics Consortium, Psychiatric Genomics Consortium, FinnGen study, and IEU Open genome-wide association studies project.

FOOTNOTES

Co-first authors: Ying He and Chun-Lan Chen.

Author contributions: He Y, Chen CL and Liu SD proposed the study conception and designed the study methods; He Y, Chen CL and He J contributed to the data acquisition/analysis; He Y and He J contributed to the statistical analysis/interpretation; Liu SD supervised and managed the whole research process; He Y, Chen CL drafted the original manuscript; Liu SD reviewed and revised the original manuscript; all authors have read and approve the final manuscript. He Y and Chen CL contributed equally to this work; they were designated as co-first authors because they made equal and substantial contributions to the study conception, design, data analysis, and manuscript preparation and editing, each playing key roles in ensuring the integrity and quality of the manuscript.

Supported by China Postdoctoral Science Foundation, No. 2021M701614; Guangdong Basic and Applied Basic Research Foundation, No. 2022A1515111063 and No. 2022A1515111045; Foundation of Guangdong Provincial People's Hospital, No. 8200010545.

Institutional review board statement: The study used public GWAS statistics and did not collect new human data. Hence, ethical approval was not required by the ethics committee of Nanfang Hospital of Southern Medical University.

Clinical trial registration statement: As this study was not a clinical trial and did not involve any human studies, the clinical trial registration was not required for our research.

Informed consent statement: The study used public GWAS statistics and did not collect new human data. Hence, ethical approval was not required by the ethics committee of Nanfang Hospital of Southern Medical University.

Conflict-of-interest statement: The authors declare that they have no conflict of interest.

Data sharing statement: All GWAS summary data that support the findings of this study are openly available in the IIBDGC (https://www.ibdgenetics.org/), PGC (https://pgc.unc.edu/), and FinnGen project (https://www.finngen.fi/en).

Country/Territory of origin: China

ORCID number: Ying He 0000-0001-7295-0089; Chun-Lan Chen 0000-0001-6878-8461; Jian He 0000-0002-8644-2605; Si-De Liu 0000-0001-8192-988X.

S-Editor: QuXL
L-Editor: A
P-Editor: Chen YX

REFERENCES

1 **Baumgart DC**, Le Berre C. Newer Biologic and Small-Molecule Therapies for Inflammatory Bowel Disease. *N Engl J Med* 2021; **385**: 1302-1315 [PMID: 34587387 DOI: 10.1056/NEJMra1907607]

2 **Wehkamp J**, Götz M, Herrlinger K, Steurer W, Stange EF. Inflammatory Bowel Disease. *Dtsch Arztebl Int* 2016; **113**: 72-82 [PMID: 26900160 DOI: 10.3238/arztebl.2016.0072]

3 **Rogler G**, Singh A, Kavanaugh A, Rubin DT. Extraintestinal Manifestations of Inflammatory Bowel Disease: Current Concepts, Treatment, and Implications for Disease Management. *Gastroenterology* 2021; **161**: 1118-1132 [PMID: 34358489 DOI: 10.1053/j.gastro.2021.07.042]

4 **Bisgaard TH**, Allin KH, Keefer L, Ananthakrishnan AN, Jess T. Depression and anxiety in inflammatory bowel disease: epidemiology, mechanisms and treatment. *Nat Rev Gastroenterol Hepatol* 2022; **19**: 717-726 [PMID: 35732730 DOI: 10.1038/s41575-022-00634-6]

5 **Fairbrass KM**, Lovatt J, Barberio B, Yuan Y, Gracie DJ, Ford AC. Bidirectional brain-gut axis effects influence mood and prognosis in IBD: a systematic review and meta-analysis. *Gut* 2022; **71**: 1773-1780 [PMID: 34725197 DOI: 10.1136/gutjnl-2021-325985]

6 **Barberio B**, Zamani M, Black CJ, Savarino EV, Ford AC. Prevalence of symptoms of anxiety and depression in patients with inflammatory bowel disease: a systematic review and meta-analysis. *Lancet Gastroenterol Hepatol* 2021; **6**: 359-370 [PMID: 33721557 DOI: 10.1016/S2468-1253(21)00014-5]

7 **Bernstein CN**, Hitchon CA, Walld R, Bolton JM, Sareen J, Walker JR, Graff LA, Patten SB, Singer A, Lix LM, El-Gabalawy R, Katz A, Fisk JD, Marrie RA; CIHR Team in Defining the Burden and Managing the Effects of Psychiatric Comorbidity in Chronic Immunoinflammatory Disease. Increased Burden of Psychiatric Disorders in Inflammatory Bowel Disease. *Inflamm Bowel Dis* 2019; **25**: 360-368 [PMID: 29986021 DOI: 10.1093/ibd/izy235]

8 **Marrie RA**, Walld R, Bolton JM, Sareen J, Walker JR, Patten SB, Singer A, Lix LM, Hitchon CA, El-Gabalawy R, Katz A, Fisk JD, Bernstein CN; CIHR Team in Defining the Burden and Managing the Effects of Psychiatric Comorbidity in Chronic Immunoinflammatory Disease. Rising incidence of psychiatric disorders before diagnosis of immune-mediated inflammatory disease. *Epidemiol Psychiatr Sci* 2019; **28**: 333-342 [PMID: 29098977 DOI: 10.1017/S2045796017000579]

9 **Frolkis AD**, Vallerand IA, Shaheen AA, Lowerison MW, Swain MG, Barnabe C, Patten SB, Kaplan GG. Depression increases the risk of inflammatory bowel disease, which may be mitigated by the use of antidepressants in the treatment of depression. *Gut* 2019; **68**: 1606-1612 [PMID: 30337374 DOI: 10.1136/gutjnl-2018-317182]

10 **Luo J**, Xu Z, Noordam R, van Heemst D, Li-Gao R. Depression and Inflammatory Bowel Disease: A Bidirectional Two-sample Mendelian Randomization Study. *J Crohns Colitis* 2022; **16**: 633-642 [PMID: 34739073 DOI: 10.1093/ecco-jcc/jjab191]

11 **Emdin CA**, Khera AV, Kathiresan S. Mendelian Randomization. *JAMA* 2017; **318**: 1925-1926 [PMID: 29164242 DOI: 10.1001/jama.2017.17219]

12 **Liu JZ**, van Sommeren S, Huang H, Ng SC, Alberts R, Takahashi A, Ripke S, Lee JC, Jostins L, Shah T, Abedian S, Cheon JH, Cho J, Dayani NE, Franke L, Fuyuno Y, Hart A, Juyal RC, Juyal G, Kim WH, Morris AP, Poustchi H, Newman WG, Midha V, Orchard TR, Vahedi H, Sood A, Sung JY, Malekzadeh R, Westra HJ, Yamazaki K, Yang SK; International Multiple Sclerosis Genetics Consortium; International IBD Genetics Consortium, Barrett JC, Alizadeh BZ, Parkes M, Bk T, Daly MJ, Kubo M, Anderson CA, Weersma RK. Association analyses identify 38 susceptibility loci for inflammatory bowel disease and highlight shared genetic risk across populations. *Nat Genet* 2015; **47**: 979-986 [PMID: 26192919 DOI: 10.1038/ng.3359]

13 **Otowa T**, Hek K, Lee M, Byrne EM, Mirza SS, Nivard MG, Bigdeli T, Aggen SH, Adkins D, Wolen A, Fanous A, Keller MC, Castelao E, Kutalik Z, Van der Auwera S, Homuth G, Nauck M, Teumer A, Milaneschi Y, Hottenga JJ, Direk N, Hofman A, Uitterlinden A, Mulder CL, Henders AK, Medland SE, Gordon S, Heath AC, Madden PA, Pergadia ML, van der Most PJ, Nolte IM, van Oort FV, Hartman CA, Oldehinkel AJ, Preisig M, Grabe HJ, Middeldorp CM, Penninx BW, Boomsma D, Martin NG, Montgomery G, Maher BS, van den Oord EJ, Wray NR, Tiemeier H, Hettema JM. Meta-analysis of genome-wide association studies of anxiety disorders. *Mol Psychiatry* 2016; **21**: 1391-1399 [PMID: 26754954 DOI: 10.1038/mp.2015.197]

14 **Sullivan PF**, Agrawal A, Bulik CM, Andreassen OA, Børglum AD, Breen G, Cichon S, Edenberg HJ, Faraone SV, Gelernter J, Mathews CA, Nievergelt CM, Smoller JW, O'Donovan MC; Psychiatric Genomics Consortium. Psychiatric Genomics: An Update and an Agenda. *Am J Psychiatry* 2018; **175**: 15-27 [PMID: 28969442 DOI: 10.1176/appi.ajp.2017.17030283]

15 **Thompson S G**, Burgess S. Mendelian randomization: methods for using genetic variants in causal estimation. 1st ed. Chapman and Hall/CRC. 2015; 224 [DOI: 10.1201/b18084-7]

16 **Baurecht H**, Welker C, Baumeister SE, Weidnger S, Meisinger C, Leitzmann MF, Emmert H. Relationship between atopic dermatitis, depression and anxiety: a two-sample Mendelian randomization study. *Br J Dermatol* 2021; **185**: 781-786 [PMID: 33817779 DOI: 10.1111/bjd.20092]

17 **Freuer D**, Linseisen J, Meisinger C. Association Between Inflammatory Bowel Disease and Both Psoriasis and Psoriatic Arthritis: A Bidirectional 2-Sample Mendelian Randomization Study. *JAMA Dermatol* 2022; **158**: 1262-1268 [PMID: 36103169 DOI: 10.1001/jamadermatol.2022.3682]

18 **He J**, Luo X, Xin H, Lai Q, Zhou Y, Bai Y. The Effects of Fatty Acids on Inflammatory Bowel Disease: A Two-Sample Mendelian Randomization Study. *Nutrients* 2022; **14** [PMID: 35889840 DOI: 10.3390/nu14142883]

19 **Chen X**, Kong J, Pan J, Huang K, Zhou W, Diao X, Cai J, Zheng J, Yang X, Xie W, Yu H, Li J, Pei L, Dong W, Qin H, Huang J, Lin T. Kidney damage causally affects the brain cortical structure: A Mendelian randomization study. *EBioMedicine* 2021; **72**: 103592 [PMID: 34619639 DOI: 10.1016/j.ebiom.2021.103592]

20 **Rosoff DB**, Smith GD, Lohoff FW. Prescription Opioid Use and Risk for Major Depressive Disorder and Anxiety and Stress-Related Disorders: A Multivariable Mendelian Randomization Analysis. *JAMA Psychiatry* 2021; **78**: 151-160 [PMID: 33175090 DOI: 10.1001/jamapsychiatry.2020.3554]

21 **Verbanck M**, Chen CY, Neale B, Do R. Detection of widespread horizontal pleiotropy in causal relationships inferred from Mendelian randomization between complex traits and diseases. *Nat Genet* 2018; **50**: 693-698 [PMID: 29686387 DOI: 10.1038/s41588-018-0099-7]

22 **Borges MC**, Haycock PC, Zheng J, Hemani G, Holmes MV, Davey Smith G, Hingorani AD, Lawlor DA. Role of circulating polyunsaturated fatty acids on cardiovascular diseases risk: analysis using Mendelian randomization and fatty acid genetic association data from over 114,000 UK Biobank participants. *BMC Med* 2022; **20**: 210 [PMID: 35692035 DOI: 10.1186/s12916-022-02399-w]

23 **Bowden J**, Davey Smith G, Haycock PC, Burgess S. Consistent Estimation in Mendelian Randomization with Some Invalid Instruments Using a Weighted Median Estimator. *Genet Epidemiol* 2016; **40**: 304-314 [PMID: 27061298 DOI: 10.1002/gepi.21965]

24 **Burgess S**, Davey Smith G, Davies NM, Dudbridge F, Gill D, Glymour MM, Hartwig FP, Kutalik Z, Holmes MV, Minelli C, Morrison JV,

Pan W, Relton CL, Theodoratou E. Guidelines for performing Mendelian randomization investigations: update for summer 2023. *Wellcome Open Res* 2019; **4**: 186 [PMID: 32760811 DOI: 10.12688/wellcomeopenres.15555.3]

25 **Burgess S**, Thompson SG. Interpreting findings from Mendelian randomization using the MR-Egger method. *Eur J Epidemiol* 2017; **32**: 377-389 [PMID: 28527048 DOI: 10.1007/s10654-017-0255-x]

26 **Arp L**, Jansson S, Wewer V, Burisch J. Psychiatric Disorders in Adult and Paediatric Patients With Inflammatory Bowel Diseases - A Systematic Review and Meta-Analysis. *J Crohns Colitis* 2022; **16**: 1933-1945 [PMID: 35775920 DOI: 10.1093/ecco-jcc/jjac095]

27 **Cooney R**, Tang D, Barrett K, Russell RK. Children and Young Adults With Inflammatory Bowel Disease Have an Increased Incidence and Risk of Developing Mental Health Conditions: A UK Population-Based Cohort Study. *Inflamm Bowel Dis* 2023 [PMID: 37603846 DOI: 10.1093/ibd/izad169]

28 **Butwicka A**, Olén O, Larsson H, Halfvarson J, Almqvist C, Lichtenstein P, Serlachius E, Frisén L, Ludvigsson JF. Association of Childhood-Onset Inflammatory Bowel Disease With Risk of Psychiatric Disorders and Suicide Attempt. *JAMA Pediatr* 2019; **173**: 969-978 [PMID: 31424531 DOI: 10.1001/jamapediatrics.2019.2662]

29 **Ludvigsson JF**, Olén O, Larsson H, Halfvarson J, Almqvist C, Lichtenstein P, Butwicka A. Association Between Inflammatory Bowel Disease and Psychiatric Morbidity and Suicide: A Swedish Nationwide Population-Based Cohort Study With Sibling Comparisons. *J Crohns Colitis* 2021; **15**: 1824-1836 [PMID: 33640971 DOI: 10.1093/ecco-jcc/jjab039]

30 **Keefer L**. What can we do to tackle anxiety and depression in patients with inflammatory bowel disease? *Lancet Gastroenterol Hepatol* 2021; **6**: 337-338 [PMID: 33721556 DOI: 10.1016/S2468-1253(21)00066-2]

31 **Hu S**, Chen Y, Wang C. Depression and Anxiety Disorders in Patients With Inflammatory Bowel Disease. *Front Psychiatry* 2021; **12**: 714057 [PMID: 34690829 DOI: 10.3389/fpsyt.2021.714057]

32 **Neuendorf R**, Harding A, Stello N, Hanes D, Wahbeh H. Depression and anxiety in patients with Inflammatory Bowel Disease: A systematic review. *J Psychosom Res* 2016; **87**: 70-80 [PMID: 27411754 DOI: 10.1016/j.jpsychores.2016.06.001]

33 **Spencer NJ**, Hu H. Enteric nervous system: sensory transduction, neural circuits and gastrointestinal motility. *Nat Rev Gastroenterol Hepatol* 2020; **17**: 338-351 [PMID: 32152479 DOI: 10.1038/s41575-020-0271-2]

34 **Niesler B**, Kuerten S, Demir IE, Schäfer KH. Disorders of the enteric nervous system - a holistic view. *Nat Rev Gastroenterol Hepatol* 2021; **18**: 393-410 [PMID: 33514916 DOI: 10.1038/s41575-020-00385-2]

35 **Cryan JF**, O'Riordan KJ, Cowan CSM, Sandhu KV, Bastiaanssen TFS, Boehme M, Codagnone MG, Cussotto S, Fulling C, Golubeva AV, Guzzetta KE, Jaggar M, Long-Smith CM, Lyte JM, Martin JA, Molinero-Perez A, Moloney G, Morelli E, Morillas E, O'Connor R, Cruz-Pereira JS, Peterson VL, Rea K, Ritz NL, Sherwin E, Spichak S, Teichman EM, van de Wouw M, Ventura-Silva AP, Wallace-Fitzsimons SE, Hyland N, Clarke G, Dinan TG. The Microbiota-Gut-Brain Axis. *Physiol Rev* 2019; **99**: 1877-2013 [PMID: 31460832 DOI: 10.1152/physrev.00018.2018]

36 **Mayorga L**, Serrano-Gómez G, Xie Z, Borruel N, Manichanh C. Intercontinental Gut Microbiome Variances in IBD. *Int J Mol Sci* 2022; **23** [PMID: 36142786 DOI: 10.3390/ijms231810868]

37 **Mitsialis V**, Wall S, Liu P, Ordovas-Montanes J, Parmet T, Vukovic M, Spencer D, Field M, McCourt C, Toothaker J, Bousvaros A; Boston Children's Hospital Inflammatory Bowel Disease Center; Brigham and Women's Hospital Crohn's and Colitis Center, Shalek AK, Kean L, Horwitz B, Goldsmith J, Tseng G, Snapper SB, Konnikova L. Single-Cell Analyses of Colon and Blood Reveal Distinct Immune Cell Signatures of Ulcerative Colitis and Crohn's Disease. *Gastroenterology* 2020; **159**: 591-608.e10 [PMID: 32428507 DOI: 10.1053/j.gastro.2020.04.074]

38 **Agirman G**, Yu KB, Hsiao EY. Signaling inflammation across the gut-brain axis. *Science* 2021; **374**: 1087-1092 [PMID: 34822299 DOI: 10.1126/science.abi6087]

39 **Gracie DJ**, Hamlin PJ, Ford AC. The influence of the brain-gut axis in inflammatory bowel disease and possible implications for treatment. *Lancet Gastroenterol Hepatol* 2019; **4**: 632-642 [PMID: 31122802 DOI: 10.1016/S2468-1253(19)30089-5]

40 **D'Mello C**, Swain MG. Immune-to-Brain Communication Pathways in Inflammation-Associated Sickness and Depression. *Curr Top Behav Neurosci* 2017; **31**: 73-94 [PMID: 27677781 DOI: 10.1007/7854_2016_37]

41 **Haj-Mirzaian A**, Amiri S, Amini-Khoei H, Hosseini MJ, Haj-Mirzaian A, Momeny M, Rahimi-Balaei M, Dehpour AR. Anxiety- and Depressive-Like Behaviors are Associated with Altered Hippocampal Energy and Inflammatory Status in a Mouse Model of Crohn's Disease. *Neuroscience* 2017; **366**: 124-137 [PMID: 29080717 DOI: 10.1016/j.neuroscience.2017.10.023]

42 **Vitali R**, Prioreschi C, Lorenzo Rebenaque L, Colantoni E, Giovannini D, Frusciante S, Diretto G, Marco-Jiménez F, Mancuso M, Casciati A, Pazzaglia S. Gut-Brain Axis: Insights from Hippocampal Neurogenesis and Brain Tumor Development in a Mouse Model of Experimental Colitis Induced by Dextran Sodium Sulfate. *Int J Mol Sci* 2022; **23** [PMID: 36232813 DOI: 10.3390/ijms231911495]

43 **Ghasemi M**, Navidhamidi M, Rezaei F, Azizikia A, Mehranfard N. Anxiety and hippocampal neuronal activity: Relationship and potential mechanisms. *Cogn Affect Behav Neurosci* 2022; **22**: 431-449 [PMID: 34873665 DOI: 10.3758/s13415-021-00973-y]

44 **Tang M**, Huang H, Li S, Zhou M, Liu Z, Huang R, Liao W, Xie P, Zhou J. Hippocampal proteomic changes of susceptibility and resilience to depression or anxiety in a rat model of chronic mild stress. *Transl Psychiatry* 2019; **9**: 260 [PMID: 31624233 DOI: 10.1038/s41398-019-0605-4]

45 **Xu Y**, Sheng H, Bao Q, Wang Y, Lu J, Ni X. NLRP3 inflammasome activation mediates estrogen deficiency-induced depression- and anxiety-like behavior and hippocampal inflammation in mice. *Brain Behav Immun* 2016; **56**: 175-186 [PMID: 26928197 DOI: 10.1016/j.bbi.2016.02.022]

46 **Margolis KG**, Cryan JF, Mayer EA. The Microbiota-Gut-Brain Axis: From Motility to Mood. *Gastroenterology* 2021; **160**: 1486-1501 [PMID: 33493503 DOI: 10.1053/j.gastro.2020.10.066]

47 **Quigley EMM**. Microbiota-Brain-Gut Axis and Neurodegenerative Diseases. *Curr Neurol Neurosci Rep* 2017; **17**: 94 [PMID: 29039142 DOI: 10.1007/s11910-017-0802-6]

48 **Socała K**, Doboszewska U, Szopa A, Serefko A, Włodarczyk M, Zielińska A, Poleszak E, Fichna J, Wlaź P. The role of microbiota-gut-brain axis in neuropsychiatric and neurological disorders. *Pharmacol Res* 2021; **172**: 105840 [PMID: 34450312 DOI: 10.1016/j.phrs.2021.105840]

World Journal of Gastroenterology

Submit a Manuscript: https://www.f6publishing.com

World J Gastroenterol 2023 November 28; 29(44): 5882-5893

DOI: 10.3748/wjg.v29.i44.5882

ISSN 1007-9327 (print) ISSN 2219-2840 (online)

ORIGINAL ARTICLE

Retrospective Study

Changing trends and characteristics of peptic ulcer disease: A multicenter study from 2010 to 2019 in Korea

Yoon Jin Choi, Tae Jun Kim, Chang Seok Bang, Yong Kang Lee, Moon Won Lee, Su Youn Nam, Woon Geon Shin, Seung In Seo

Specialty type: Gastroenterology and hepatology

Provenance and peer review: Unsolicited article; Externally peer reviewed.

Peer-review model: Single blind

Peer-review report's scientific quality classification

Grade A (Excellent): A
Grade B (Very good): 0
Grade C (Good): C, C, C, C
Grade D (Fair): 0
Grade E (Poor): 0

P-Reviewer: Shelat VG, Singapore; Shiryajev YN, Russia; Skrypnyk I, Ukraine; Sugimoto M, Japan

Received: June 5, 2023
Peer-review started: June 5, 2023
First decision: August 26, 2023
Revised: September 30, 2023
Accepted: November 14, 2023
Article in press: November 14, 2023
Published online: November 28, 2023

Yoon Jin Choi, Department of Internal Medicine, National Cancer Center, Goyang-si 13620, South Korea

Tae Jun Kim, Department of Internal Medicine, Samsung Medical Center, Seoul 06351, South Korea

Chang Seok Bang, Department of Internal Medicine, Chuncheon Sacred Heart Hospital, Chuncheon 24253, South Korea

Yong Kang Lee, Department of Internal Medicine, National Health Insurance Service Ilsan Hospital, Goyang-si 10444, South Korea

Moon Won Lee, Department of Internal Medicine, Pusan National University School of Medicine, Busan 50463, South Korea

Su Youn Nam, Division of Gastroenterology and Hepatology, Department of Internal Medicine, Kyungpook National University Chilgok Hospital, Daegu 41404, South Korea

Woon Geon Shin, Department of Internal Medicine, Kangdong Sacred Heart Hospital, Hallym University College of Medicine, Seoul 05355, South Korea

Woon Geon Shin, Seung In Seo, Institute for Liver and Digestive Diseases, Hallym University, Chuncheon 24253, South Korea

Seung In Seo, Division of Gastroenterology, Department of Internal Medicine, Kangdong Sacred Heart Hospital, Seoul 05355, South Korea

Corresponding author: Seung In Seo, MD, PhD, Associate Professor, Division of Gastroenterology, Department of Internal Medicine, Kangdong Sacred Heart Hospital, 150, Seongan-ro, Gangdong-gu, Seoul 05355, South Korea. doctorssi@kdh.or.kr

Abstract

BACKGROUND

The clinical trend and characteristics of peptic ulcer disease (PUD) have not fully been investigated in the past decade.

AIM

To evaluate the changing trends and characteristics of PUD according to age and

etiology.

METHODS

We analyzed seven hospital databases converted into the Observational Medical Outcomes Partnership-Common Data Model between 2010 and 2019. We classified patients with PUD who underwent rapid urease tests or *Helicobacter pylori* (*H. pylori*) serology into three groups: *H. pylori*-related, drug [nonsteroidal anti-inflammatory drugs (NSAIDs) or aspirin]-related, and idiopathic (*H. pylori*/NSAID/aspirin-negative) PUD and compared the yearly trends and characteristics among the three groups.

RESULTS

We included 26785 patients in 7 databases, and the proportion of old age (≥ 65 years) was 38.8%. The overall number of PUD exhibited no decrease, whereas PUD in old age revealed an increasing trend (P = 0.01 for trend). Of the 19601 patients, 41.8% had *H. pylori*-related, 36.1% had drug-related, and 22.1% had idiopathic PUD. *H. pylori*-related PUD exhibited a decreasing trend after 2014 (P = 0.01), drug-related PUD demonstrated an increasing trend (P = 0.04), and idiopathic PUD showed an increasing trend in the old-age group (P = 0.01) during 10 years. Patients with drug-related PUD had significantly more comorbidities and concomitant ulcerogenic drugs. The idiopathic PUD group had a significantly higher number of patients with chronic liver disease.

CONCLUSION

With the aging population increase, the effects of concomitant ulcerogenic drugs and preventive strategies should be investigated in drug-induced PUD. Further studies are required to clarify the relationship between idiopathic PUD and chronic liver disease.

Key Words: Peptic ulcer disease; Drug; Idiopathic; Trend; Characteristics

Core Tip: In the multicenter study including 26785 peptic ulcer disease (PUD) patients from 7 databases, the overall number of PUD exhibited no decrease, whereas PUD in old age revealed an increasing trend from 2010 to 2019 in Korea. According to etiology, decreasing trend of *Helicobacter pylori*-related PUD after year 2014, and increasing trend of drug-related PUD were observed in the past decade. Drug-related PUD showed significantly more comorbidities and exposure to concomitant ulcerogenic drugs, and the idiopathic PUD group had a significantly higher proportion in the chronic liver disease. Further studies are required to clarify the relationship between idiopathic PUD and chronic liver disease.

Citation: Choi YJ, Kim TJ, Bang CS, Lee YK, Lee MW, Nam SY, Shin WG, Seo SI. Changing trends and characteristics of peptic ulcer disease: A multicenter study from 2010 to 2019 in Korea. *World J Gastroenterol* 2023; 29(44): 5882-5893
URL: https://www.wjgnet.com/1007-9327/full/v29/i44/5882.htm
DOI: https://dx.doi.org/10.3748/wjg.v29.i44.5882

INTRODUCTION

Peptic ulcer disease (PUD) remains a critical cause of hospitalization, particularly when complicated by hemorrhage, perforation, or obstruction[1]. The main etiologies of PUD include *Helicobacter pylori* (*H. pylori*) infection and the use of aspirin or nonsteroidal anti-inflammatory drugs (NSAIDs)[1]. The overall decline of *H. pylori* infection in the general population and advances in the management of *H. pylori* infection have led to a decline in the PUD incidence over the past two decades, however, prescriptions of aspirin and NSAIDs have increased over the same period owing to the rising number of older patients and patients with comorbidities[2]. Furthermore, direct oral anticoagulants (DOAC), newer NSAIDs, and antiplatelet agents continue to be used in chronic disease, and public awareness of *H. pylori* eradication has improved. Consequently, trends of PUD have demonstrated inconsistent results among regions[2-7]. A recent population-based study reported that morbidity and mortality due to PUD decreased significantly from 1990 to 2019, while a gradual upward trend has been observed in the recent 15 years, which might be associated with changes in risk factors [2]. Meanwhile, the incidence of non-*H. pylori*, non-NSAIDs/aspirin PUD, also termed idiopathic PUD, has increased in recent years, particularly in Asian countries[8]. The clinical outcomes of idiopathic PUD revealed recurrent ulcer bleeding and higher mortality in previous studies[9-14]; however, characteristics of idiopathic PUD remain poorly understood and warrant further investigation.

To date, few large-scale studies have comprehensively investigated the recent changing trends and clinical characteristics of PUD, including the multiple risk factors. Therefore, we investigated the trends and characteristics of PUD according to age and etiology in Korea between 2010 and 2019.

MATERIALS AND METHODS

Data source and study design

We analyzed seven hospital databases converted into the Observational Medical Outcomes Partnership-Common Data Model (OMOP-CDM) using the FEEDER-NET platform, which is a coordinating platform that enables data user and supplier connections and multi-institution analyses, with the anonymity of patients' personal information, as applied in previous studies[15-17]. The included institutions were Ajou University Medical Center (AUMC), Daegu Catholic Medical Center (DCMC), Ewha Womans University Medical Center (EUMC), Gyeongsang National University Hospital (GNUH), Kangdong Sacred Heart Hospital (KDH), Kangwon National University Hospital (KNUH), and Wonkwang University Hospital (WKUH). The detailed characteristics of each database are presented in Supplementary Table 1.

The characteristics of PUD were analyzed using the characterization tab on ATLAS, which is a web-based open platform developed by the Observational Health Data Sciences and Informatics community[18]. We analyzed basic demographic information, prescriptions, and comorbidities during the year before entering the cohort. We evaluated for exposure to aspirin and other antiplatelet agents, NSAIDs, anticoagulants, and potential ulcerogenic drugs (steroids, antidepressants, bisphosphonates, and immunosuppressive agents). Further, the mean Charlson Comorbidity Index (CCI) was calculated for each database. The same analytic codes were applied to seven hospital databases, and the results of each database were combined as proportions without extracting the raw data. The combined results were analyzed yearly for trend analysis and compared according to age group and etiology of PUD. This study was approved by the Institutional Review Board (IRB) of Kangdong Sacred Hospital (IRB number: 2021-11-001). The other six hospitals were affiliated with the Research Border Free Zone, which recognizes IRB approval of the research organizing center and waives individual IRB approval.

Definition of PUD

We defined a newly diagnosed PUD as having a 1-year observation period between January 1, 2010, and December 31, 2019, combining diagnostic codes for PUD, esophagogastroduodenoscopy, and exposure to proton pump inhibitors (PPIs). This operational definition was based on previous reports[3,19]. The index date was defined as the initial diagnosis of PUD. Exclusion criteria were as follows: (1) Age < 20 years; (2) Observation period < 1 year before the index date; (3) No exposure to PPIs 30 d before or after the index date; (4) No exposure to esophagogastroduodenoscopy 30 d before or after the index date; (5) Gastric cancer before the index date; and (6) Benign gastric neoplasm before the index date. Each concept name and identifier included in the OMOP-CDM databases matched to diagnostic codes or drugs are listed in Supplementary Table 2.

PUD classification according to etiology

We classified PUD patients who underwent rapid urease tests or *H. pylori* serology tests according to etiology into the following three groups: (1) *H. pylori*-related; (2) Drug-related (*H. pylori*-negative and NSAIDs/aspirin-related); and (3) Idiopathic (*H. pylori*/NSAID/aspirin-negative) PUD. *H. pylori*-related PUD included patients who were concomitantly prescribed *H. pylori* eradication therapy (PPI, amoxicillin, clarithromycin, bismuth, tetracycline, and metronidazole) for 7-14 d. Drug-related PUD included patients who were not exposed to *H. pylori* eradication therapy and were exposed to aspirin or NSAIDs before the index date. Idiopathic PUD included patients without exposure to aspirin, NSAIDs, or *H. pylori* eradication therapy. We further performed a subgroup analysis according to age and sex. We defined the old age group as ≥ 65 years, and the young age group as < 65 years.

Statistical analysis

Categorical variables were compared using the χ^2 or Fisher's exact test based on the results from the ATLAS version 2.7.6. Continuous variables were expressed as means with standard deviations. The yearly trend was analyzed with simple linear regression, and the yearly trend for each group was compared using the Cochran Armitage test for trends. Statistical significance was set at $P < 0.05$. Statistical analyses were performed using R version 4.2.1 (R Foundation for Statistical Computing).

RESULTS

Characteristics of PUD in total patients

The flowchart of the study is presented in Figure 1. A total of 26785 patients (AUMC, *n* = 4629; DCMC, *n* = 4690; EUMC, *n* = 3118; GNUH, *n* = 2998; KDH, *n* = 6320; KNUH, *n* = 1854; and WKUH, *n* = 3176) were included between 2010 and 2019. Finally, 15544 (58%) were men, and 11241 (42%) were women. The yearly trend of PUD exhibited no declining pattern in the total patients ($P = 0.69$ for trend) (Figure 2A). The yearly PUD trend in each database is presented in Supplementary Figure 1.

The baseline demographics are presented in Table 1. The proportion of gastric ulcers (69.2%) was over twofold that of duodenal ulcers (31.3%). The most prevalent comorbidity was hypertensive disorder, followed by diabetes mellitus. The proportions of exposure to NSAIDs, aspirin, and antiplatelet agents were 19.9%, 15.2%, and 11.4%, respectively. Regarding anticoagulants, warfarin and DOAC were prescribed in 2.2% and 1.1% of total patients, respectively. The proportion of exposure to steroids was 12.7%. Detailed information for each database is presented in Supplementary Table 3.

Table 1 Baseline characteristics of all patients with peptic ulcer disease, *n* (%)

	Total (*n* = 26785)
Age ≥ 65 yr	10392 (38.8)
Men	15544 (58.0)
RUT or serology	19601 (73.2)
Gastric ulcer	18527 (69.2)
Duodenal ulcer	8377 (31.3)
Diagnosis	
Hypertensive disorder	4773 (17.8)
Diabetes mellitus	2239 (8.4)
Hyperlipidemia	2038 (7.6)
Chronic kidney disease	1282 (4.8)
Ischemic heart disease	2221 (8.3)
Cerebrovascular disease	812 (3.0)
Chronic liver disease	1436 (5.4)
Osteoarthritis	425 (1.6)
Chronic obstructive lung disease	515 (1.9)
Medication	
Aspirin	4068 (15.2)
Other antiplatelet agent[1]	3065 (11.4)
Clopidogrel	2386 (8.9)
Cilostazole	691 (2.6)
NSAID	5342 (19.9)
Warfarin	579 (2.2)
DOAC	297 (1.1)
Steroid	3404 (12.7)
Antidepressant	6308 (23.6)
Bisphosphonate	488 (1.8)
Immunosuppressant	578 (2.2)

[1]Antiplatelet agents other than aspirin include clopidogrel, cilostazole, ticlopidine, triflusal, ticagrelor, and prasugrel.
RUT: Rapid urease test; NSAIDs: Nonsteroidal anti-inflammatory drugs; DOAC: Direct oral anticoagulant.

Characteristics of PUD in old age

The proportion of patients with old age (≥ 65 years) was 38.8% (10392/26785). The PUD with the old-age group demonstrated an increasing annual trend (P = 0.01 for trend), whereas the young age group (< 65 years) showed no specific trend overall (P = 0.47 for trend) (Figure 2A). The mean CCI in old age was higher than that in total patients (old-age group *vs* total group; 3.18 ± 2.6 *vs* 2.58 ± 2.4 in AUMC; 2.94 ± 2.2 *vs* 2.30 ± 1.9 in DCMC; 2.37 ± 1.9 *vs* 1.77 ± 1.5 in EUMC; 2.61 ± 2.0 *vs* 2.19 ± 1.8 in GNUH; 2.58 ± 2.0 *vs* 2.05 ± 1.7 in KDH; 2.78 ± 2.1 *vs* 2.36 ± 1.9 in KNUH; and 3.21 ± 2.4 *vs* 2.66 ± 2.2 in WKUH).

Characteristics of PUD according to etiology

Of the total patients, 19601 underwent rapid urease or *H. pylori* serology tests. The number of *H. pylori*-related, drug-related, and idiopathic PUD patients was 8202 (41.8%); 7066 (36.1%); and 4333 (22.1%), respectively. The proportions according to etiology in each hospital are presented in Supplementary Table 3. *H. pylori*-related PUD exhibited a decreasing trend after 2014 (P = 0.01 for trend), and drug-related PUD showed a slightly increasing trend in the past 10 years (P = 0.04 for trend). In contrast, idiopathic PUD revealed no statistically increasing trend in the past 10 years (P = 0.08 for trend) (Figure 2B).

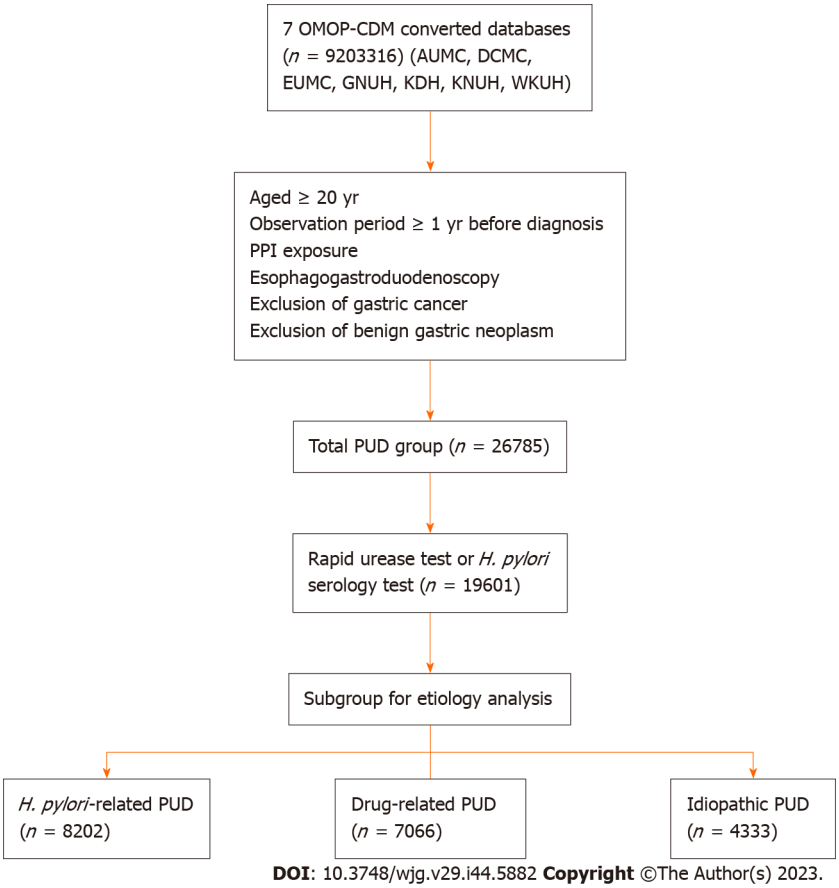

DOI: 10.3748/wjg.v29.i44.5882

Figure 1 Flow chart of the study. OMOP-CDM: Observational Medical Outcomes Partnership-Common Data Model; AUMC: Ajou University Medical Center; DCMC: Daegu Catholic Medical Center; EUMC: Ewha Womans University Medical Center; GNUH: Gyeongsang National University Hospital; KDH: Kangdong Sacred Heart Hospital; KNUH: Kangwon National University Hospital; WKUH: Wonkwang University Hospital; PPI: Proton pump inhibitor; PUD: Peptic ulcer disease; *H. pylori* : *Helicobacter pylori*.

The comparison of characteristics among the three groups is presented in Table 2. The *H. pylori*-related PUD group showed the lowest proportion of old age among the three groups. The proportion of duodenal ulcers was significantly higher in the *H. pylori*-related PUD than in the other groups. The drug-related PUD group had significantly more elderly patients, less predominance of men, more gastric ulcers, comorbidities except for chronic liver disease, exposure to concomitant potential ulcerogenic drugs than the other groups (Table 2). Notably, there were more patients with chronic liver disease in the idiopathic PUD group than in the other groups. In addition, there were significantly more patients with alcoholic liver damage and cirrhosis in the idiopathic PUD group (Table 2).

Subgroup analysis according to age and sex

Of 19601 patients, we conducted a subgroup analysis according to age group and sex. In the old-age (≥ 65 years) group (*n* = 7486), *H. pylori*-related PUD was 2043 (27.3%); drug-related was 3842 (51.3%); and idiopathic was 1601 (21.4%). In the young age (< 65 years) group (*n* = 12115), *H. pylori*-related PUD was 6159 (50.8%); drug-related was 3224 (26.6%); and idiopathic was 2732 (22.6%). In the old-age group, *H. pylori*-related PUD exhibited a decreasing trend after 2014 ($P < 0.01$ for trend), whereas drug-related and idiopathic PUD showed an overall increasing trend (drug-related, $P = 0.001$ for trend; idiopathic, $P = 0.01$ for trend) (Figure 2C). In the young age group, there was only a decreasing trend for *H. pylori*-related PUD after 2014 ($P = 0.01$ for trend) (Figure 2D). The yearly trend did not differ according to sex.

In the old-age group, more women had drug-related PUD than total patients (Table 3). The proportion of gastric ulcers was highest in drug-related PUD, regardless of age, whereas the proportion of duodenal ulcers showed different patterns according to age. In the old-age group, the proportion of duodenal ulcer was highest in the idiopathic PUD, and it was highest in *H. pylori*-related PUD in the young age group (Table 3). Other comorbidities or exposure to concomitant drugs did not differ according to age (Table 3). Supplementary Table 4 lists the subgroup analysis according to sex. No significant difference was found according to sex.

DISCUSSION

The findings of this multicenter OMOP-CDM-based study revealed that the total number of PUD patients demonstrated no decreasing trend, whereas newly diagnosed PUD in the old-age group showed an increasing trend in the past 10

Table 2 Comparison of characteristics according to the etiology of peptic ulcer disease

	H. pylori-related PUD (*n* = 8202)	Drug-related PUD (*n* = 7066)	Idiopathic PUD (*n* = 4333)	*P* value	All (*n* = 19601)
Age ≥ 65	2043 (24.9)	3842 (54.4)	1601 (36.9)	< 0.001	7486 (38.2)
Men, *n* (%)	5268 (64.2)	3774 (53.4)	2747 (63.4)	< 0.001	11789 (60.1)
Gastric ulcer	5062 (61.7)	5052 (71.5)	2758 (63.7)	< 0.001	12872 (65.7)
Duodenal ulcer	3272 (39.9)	2171 (30.7)	1574 (36.3)	< 0.001	7017 (35.8)
Diagnosis, *n* (%)					
Hypertensive disorder	928 (11.3)	2036 (28.8)	529 (12.2)	< 0.001	3493 (17.8)
Diabetes mellitus	438 (5.3)	954 (13.5)	256 (5.9)	< 0.001	1648 (8.4)
Hyperlipidemia	587 (7.2)	829 (11.7)	129 (3.0)	< 0.001	1545 (7.9)
Chronic kidney disease	173 (2.1)	604 (8.5)	123 (2.8)	< 0.001	900 (4.6)
Ischemic heart disease	483 (5.9)	1098 (15.5)	49 (1.1)	< 0.001	1630 (8.3)
Cerebrovascular disease	161 (2.0)	372 (5.3)	35 (0.8)	< 0.001	568 (2.9)
Chronic liver disease	224 (2.7)	447 (6.3)	349 (8.1)	< 0.001	1020 (5.2)
Alcoholic liver damage	164 (2.0)	253 (3.6)	234 (5.4)	< 0.001	651 (3.3)
Liver cirrhosis	175 (2.1)	381 (5.4)	325 (7.5)	< 0.001	881 (4.5)
Osteoarthritis	84 (1.0)	191 (2.7)	13 (0.4)	< 0.001	288 (1.5)
Chronic obstructive lung disease	76 (0.9)	209 (3.0)	74 (1.7)	< 0.001	359 (1.8)
Medication, *n* (%)					
Antiplatelet agent[1]	634 (7.7)	1514 (21.4)	77 (1.8)	< 0.001	2225 (11.4)
Warfarin	84 (1.0)	258 (3.7)	34 (0.8)	< 0.001	376 (1.9)
DOAC	33 (0.4)	129 (1.8)	20 (0.5)	< 0.001	182 (0.9)
Steroid	690 (8.4)	1423 (20.1)	227 (5.2)	< 0.001	2340 (11.9)
Antidepressant	1188 (14.5)	2408 (34.1)	868 (20.0)	< 0.001	4464 (22.8)
Bisphosphonate	94 (1.1)	223 (3.2)	18 (0.4)	< 0.001	335 (1.7)
Immunosuppressant	125 (1.5)	275 (3.9)	35 (0.8)	< 0.001	435 (2.2)

[1]Antiplatelet agents other than aspirin include clopidogrel, cilostazole, ticlopidine, triflusal, ticagrelor, and prasugrel.
PUD: Peptic ulcer disease; DOAC: Direct oral anticoagulant; *H. pylori*: *Helicobacter pylori*.

years. We classified PUD patients who underwent *H. pylori* serology or rapid urease tests into *H. pylori*-related, drug-related, and idiopathic PUD to clarify the characteristics and changing trends of PUD according to etiology. *H. pylori*-related PUD showed a decreasing trend after 2014; drug-related PUD, an increasing trend; and idiopathic PUD, an increasing trend only in the old-age group. Drug-related PUD revealed significantly more comorbidities and exposure to concomitant ulcerogenic drugs. Notably, the proportion of patients with chronic liver disease was significantly higher in idiopathic PUD.

Several studies have investigated the trends of PUD, and the overall prevalence has exhibited a decreasing trend in the past few decades; however, the trend differed according to region or sex owing to changes in the distribution of the etiologies of PUD[2,3]. A recent global study has reported that the age-standardized incidence rate exhibited an increasing annual trend with increasing age[2], and our results showed an increasing trend of PUD in the old-age group. A recent Korean nationwide cohort study conducted in 2006-2015 showed a decreasing trend in the *H. pylori* infection rate and no change in drug exposure that increases the risk of peptic ulcer bleeding (PUB)[3]. Furthermore, the *H. pylori* infection rate was 34.4% in that study when it was defined by including patients who received *H. pylori* eradication therapy out of the patients who underwent rapid urease tests, *H. pylori* cultures, urea breath tests, Warthin-Starry silver stains, and *H. pylori* stool antigen tests[3]. The lower *H. pylori* infection rate than that in our study may be attributed to the lack of *H. pylori* serology testing and false-negative results in the PUB setting in that study. *H. pylori*-related PUD was 41.8% in our study, which was consistent with a recent Korean nationwide multicenter study that reported 43.9% *H. pylori* seropositivity from 2016 to 2017[20]. Our proportion of *H. pylori*-related PUD also included patients who had *H. pylori* eradication therapy, which suggests that the knowledge and awareness of the public was improved in the past decade. A

Table 3 Subgroup analysis of characteristics of peptic ulcer disease according to age, *n* (%)

	Age (yr)	*H. pylori*-related PUD (*n* = 8202)	Drug-related PUD (*n* = 7066)	Idiopathic PUD (*n* = 4333)	*P* value
Men	≥ 65	1161/2043 (56.8)	1869/3842 (48.6)	934/1601 (58.3)	< 0.001
	< 65	4107/6159 (66.7)	1905/3224 (59.1)	1813/2732 (66.4)	< 0.001
Gastric ulcer	≥ 65	1481/2043 (72.5)	2855/3842 (74.3)	1093/1601 (68.3)	< 0.001
	< 65	3581/6159 (58.1)	2197/3224 (68.1)	1665/2732 (60.9)	< 0.001
Duodenal ulcer	≥ 65	612/2043 (30.0)	1117/3842 (29.1)	561/1601 (35.0)	< 0.001
	< 65	2660/6159 (43.2)	1054/3224 (32.7)	1013/2732 (37.1)	< 0.001
Diagnosis					
Hypertensive disorder	≥ 65	452/2043 (22.1)	1431/3842 (37.2)	321/1601 (20.0)	< 0.001
	< 65	476/6159 (7.7)	605/3224 (18.8)	208/2732 (7.6)	< 0.001
Diabetes mellitus	≥ 65	194/2043 (9.5)	610/3842 (15.9)	148/1601 (9.2)	< 0.001
	< 65	244/6159 (4.0)	344/3224 (10.7)	108/2732 (4.0)	< 0.001
Hyperlipidemia	≥ 65	201/2043 (9.8)	533/3842 (13.9)	53/1601 (3.3)	< 0.001
	< 65	386/6159 (6.3)	296/3224 (9.2)	76/2732 (2.8)	< 0.001
Chronic kidney disease	≥ 65	76/2043 (3.7)	382/3842 (9.9)	64/1601 (4.0)	< 0.001
	< 65	97/6159 (1.6)	222/3224 (6.9)	59/2732 (2.3)	< 0.001
Ischemic heart disease	≥ 65	247/2043 (12.1)	794/3842 (20.7)	35/1601 (2.6)	< 0.001
	< 65	236/6159 (3.8)	304/3224 (9.4)	14/2732 (0.6)	< 0.001
Cerebrovascular disease	≥ 65	92/2043 (4.5)	288/3842 (7.5)	25/1601 (1.6)	< 0.001
	< 65	69/6159 (1.1)	84/3224 (2.7)	10/2732 (0.5)	< 0.001
Chronic liver disease	≥ 65	42/2043 (2.3)	202/3842 (5.3)	120/1601 (7.5)	< 0.001
	< 65	182/6159 (3.0)	245/3224 (7.6)	229/2732 (8.4)	< 0.001
Alcoholic liver damage	≥ 65	20/2043 (1.1)	85/3842 (2.2)	64/1601 (4.0)	< 0.001
	< 65	144/6159 (2.3)	168/3224 (5.2)	170/2732 (6.2)	< 0.001
Liver cirrhosis	≥ 65	29/2043 (1.6)	161/3842 (4.2)	113/1601 (7.1)	< 0.001
	< 65	146/6159 (2.4)	220/3224 (6.8)	212/2732 (7.8)	< 0.001
Osteoarthritis	≥ 65	56/2043 (2.7)	145/3842 (3.8)	10/1601 (1.1)	< 0.001
	< 65	28/6159 (0.5)	46/3224 (1.6)	3/2732 (0.2)	< 0.001
Chronic obstructive lung disease	≥ 65	53/2043 (2.6)	176/3842 (4.6)	57/1601 (3.6)	0.001
	< 65	23/6159 (0.4)	33/3224 (1.0)	17/2732 (0.6)	0.001
Medication					
Antiplatelet agent	≥ 65	324/2043 (15.9)	1058/3842 (27.5)	51/1601 (3.2)	< 0.001
	< 65	310/6159 (5.0)	456/3224 (14.1)	26/2732 (1.0)	< 0.001
Warfarin	≥ 65	49/2043 (2.4)	190/3842 (4.9)	28/1601 (1.9)	< 0.001
	< 65	35/6159 (0.6)	68/3224 (2.1)	6/2732 (0.3)	< 0.001
DOAC	≥ 65	23/2043 (1.2)	112/3842 (2.9)	19/1601 (1.2)	< 0.001
	< 65	10/6159 (0.2)	17/3224 (0.6)	1/2732 (0.1)	0.015
Steroid	≥ 65	237/2043 (11.6)	807/3842 (21.0)	111/1601 (6.9)	< 0.001
	< 65	453/6159 (7.4)	616/3224 (19.1)	116/2732 (4.2)	< 0.001
Antidepressant	≥ 65	456/2043 (22.3)	1568/3842 (40.8)	435/1601 (27.2)	< 0.001
	< 65	732/6159 (11.9)	840/3224 (26.1)	433/2732 (15.8)	< 0.001

Bisphosphonate	≥ 65	54/2043 (2.6)	174/3842 (4.5)	11/1601 (0.7)	< 0.001
	< 65	40/6159 (0.6)	49/3224 (1.5)	7/2732 (0.4)	< 0.001
Immunosuppressant	≥ 65	49/2043 (2.4)	108/3842 (2.8)	13/1601 (0.9)	< 0.001
	< 65	76/6159 (1.2)	167/3224 (5.2)	22/2732 (1.0)	< 0.001

PUD: Peptic ulcer disease; DOAC: Direct oral anticoagulant; *H. pylori*: *Helicobacter pylori*.

recent meta-analysis also revealed that technology-enhanced communication initiatives effectively improve compliance to the *H. pylori* eradication regimen and increase the eradication rate[21].

The use of NSAIDs or aspirin has increased dramatically in recent decades, and the prevalence of NSAID use in patients aged ≥ 65 years is reported to be as high as 96%[22,23]. The proportion of drug-related PUD revealed an increasing trend, and it was prominent in the old-age group. The drug-related PUD group included more elderly patients and showed comorbidities and exposure to concomitant ulcerogenic drugs compared with the other groups, consistent with previous reports[24]. Drug-related PUD may cause serious complications, including bleeding or perforation[25]. Clinical practice guidelines for the appropriate treatment and prevention of drug-related PUD have been recently developed[26,27]. The guidelines recommend high-risk patients who are on long-term NSAID medications receive low-dose PPIs to prevent PUD and its complications; however, evidence in patients who take multiple ulcerogenic drugs remains lacking[26]. In a previous case series analysis from seven population-based healthcare databases, concomitant use of NSAIDs or aspirin with selective serotonin reuptake inhibitors, aldosterone antagonists, corticosteroids, or anticoagulants significantly increased the risk of upper gastrointestinal bleeding[28]. Our results suggest that drug-induced PUD may have more severe clinical outcomes; therefore, further strategies should be investigated to prevent complications in elderly patients.

The proportion of idiopathic PUD was 22.1% in our study, which is consistent with the proportion in the previous multicenter prospective study in 2008[9] and higher than that in the study by Chung *et al*[8] (8.6%) of patients with PUB in Korea[12]. Idiopathic PUD can be defined after excluding the missed diagnosis of *H. pylori* infection and undocumented use of NSAIDs or aspirin; therefore, the definition and diagnosis of *H. pylori* infection differed among the previous studies. Epidemiological studies have consistently reported an increasing proportion of *H. pylori*-negative PUD, particularly in Asian countries[8]; however, most of these studies were conducted before 2014, and few large-scale studies have investigated the changing trends or characteristics of idiopathic PUD in recent years. Our idiopathic PUD group included patients who had no exposure to aspirin, NSAIDs, or *H. pylori* eradication therapy before the index date. In our study, the exact results of the *H. pylori* tests could not be obtained, and patients with idiopathic PUD may overlap with those with drug-induced PUD. Despite these limitations, our study was the first to demonstrate the increasing trend of idiopathic PUD in old age in the past decade. In addition, we confirmed that the proportion of idiopathic PUD may differ regionally depending on the regional *H. pylori* prevalence.

The proportions of most of the comorbidities and drug exposures were higher in drug-induced PUD in our study, and only chronic liver disease was significantly higher in patients with idiopathic PUD among the three groups. Previous studies have compared the characteristics of idiopathic PUD with those of *H. pylori*-related PUD. The risks for idiopathic PUD included older age, smoking, alcohol, comorbid diseases, and higher psychological stress[8]. In our study, among three PUD groups, only the proportion of chronic liver disease was significantly higher in the idiopathic PUD; therefore, it may be a distinct characteristic compared with drug-induced PUD. The relationship between idiopathic PUD and liver disease has been suggested in several studies. Kim *et al*[29] have reported that despite the decreased *H. pylori* infection in patients with severe liver cirrhosis, PUD was increased in 288 patients with liver cirrhosis. Therefore, factors other than *H. pylori* infection may be involved in the pathogenesis of PUD in patients with cirrhosis[29,30]. A proposed pathophysiological mechanism is that portal hypertension induces splanchnic vascular congestion followed by gastrointestinal mucosal changes involving impaired mucosal secretion and microvascular flow, leading to peptic ulcer formation[31]. Moreover, we demonstrated that alcoholic liver disease was more prevalent in idiopathic PUD, suggesting that alcohol may be another risk factor for idiopathic PUD, although the causal relationship is uncertain.

Our study had several limitations. First, the proportion of idiopathic PUD may have been overestimated since we could not identify the exact *H. pylori* infection or confirmation after *H. pylori* eradication using an administrative database. However, this limitation may be overcome by converting text data to CDM in future studies. Second, our study was not conducted nationwide; therefore, we could not demonstrate the PUD trend as a proportion of the total patients. However, we observed that the pattern or severity of PUD may vary according to the scale of each hospital. Third, patients may overlap across hospital databases. Patients may be diagnosed with PUD in one hospital and treated in another. Fourth, the claims data-based research design may include misclassification bias or inaccurate data. Lastly, we could not include data on smoking or alcohol consumption; therefore, it could not be evaluated as a cause of idiopathic PUD.

Despite these limitations, our study had the following strengths. The main strength is that the analysis was performed using the OMOP-CDM database, which can be applied to other databases worldwide with the same analytic code. Second, our study used the operational definition of PUD based on a previous validation study, which showed high sensitivity and specificity[19]. Lastly, our study confirmed the changing trends and characteristics of PUD according to etiology and age group in the past 10 years using a large-scale multicenter design.

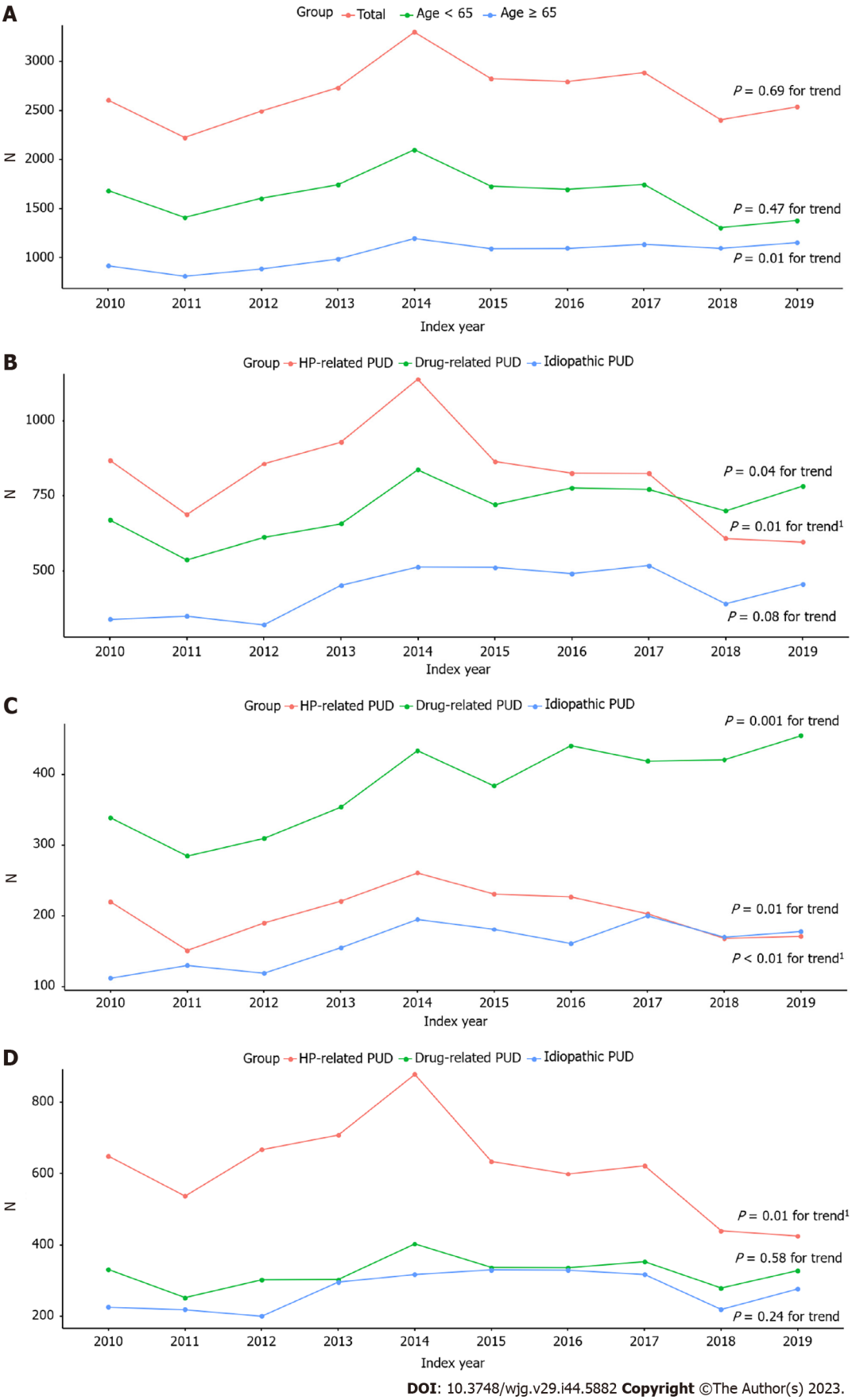

DOI: 10.3748/wjg.v29.i44.5882

Figure 2 Yearly trend of peptic ulcer disease according to age group, etiology in total, in the old age (≥ 65) group, and in the young age (< 65) group. A: Age group; B: Etiology in total group; C: Etiology in the old age (≥ 65) group; D: Etiology in the young age (< 65) group. PUD: Peptic ulcer disease; HP: *Helicobacter pylori*. [1]*P* for trend after 2014.

CONCLUSION

In conclusion, PUD exhibited an increasing trend in the old-age group in the past decade. Regarding etiology, *H. pylori*-related PUD decreased, whereas drug-related and idiopathic PUD increased, particularly in the old-age group. With the rising number of older patients, the effects of concomitant ulcerogenic drugs on PUD should be investigated, and preventive strategies for drug-induced PUD should be developed. Further studies are required to clarify the relationship between idiopathic PUD and chronic liver disease.

ARTICLE HIGHLIGHTS

Research background

To date, few large-scale studies have comprehensively investigated the recent changing trends and clinical characteristics of peptic ulcer disease (PUD), including the multiple risk factors.

Research motivation

The incidence of idiopathic PUD, has increased in recent years, particularly in Asian countries. The clinical outcomes of idiopathic PUD revealed recurrent ulcer bleeding and higher mortality in previous studies; however, characteristics of idiopathic PUD remain poorly understood and warrant further investigation.

Research objectives

We aimed to evaluate the changing trends and characteristics of PUD according to age and etiology.

Research methods

We analyzed seven hospital databases that were converted to a common data model between 2010 and 2019. We classified PUD patients who underwent rapid urease testing or *Helicobacter pylori* (*H. pylori*) serology testing into the following three groups according to etiology: (1) *H. pylori*-related; (2) drug-related [*H. pylori*-negative and nonsteroidal anti-inflammatory drugs (NSAIDs)/aspirin-related]; and (3) Idiopathic (*H. pylori*/NSAID/aspirin-negative) PUD.

Research results

The overall number of PUD exhibited no decrease, whereas PUD in old age revealed an increasing trend. *H. pylori*-related PUD exhibited a decreasing trend after 2014, drug-related PUD demonstrated an increasing trend, and idiopathic PUD showed an increasing trend in the old-age group during 10 years. The idiopathic PUD group had a significantly higher number of patients with chronic liver disease.

Research conclusions

There was an increase in the incidence of PUD in the older age group during the last decade. There was a decrease in *H. pylori*-related PUD and an increase in drug-related and idiopathic PUD, especially in the elderly group.

Research perspectives

Further preventive strategies for drug-induced PUD should be developed. Further studies are required to clarify the relationship between idiopathic PUD and chronic liver disease.

ACKNOWLEDGEMENTS

We acknowledge to Dr. Kee Myung Lee (Department of Gastroenterology, Ajou University School of Medicine, Suwon, Korea), Dr. Ji Min Han (Department of Internal Medicine, Daegu Catholic University Medical Center, Daegu, Korea), Dr. Ki-Nam Shim (Department of Internal Medicine, Ewha Womans University College of Medicine, Seoul, Korea), Dr. Chang Min Lee (Department of Internal Medicine, Gyeongsang National University Hospital, Gyeongsang National University, College of Medicine, Jinju, Korea), Dr. Sung Chul Park (Department of Internal Medicine, Kangwon National University School of Medicine, Chuncheon, Korea), and Dr. Suck Chei Choi (Department of Internal Medicine, Digestive Disease Research Institute, Wonkwang University College of Medicine, Iksan, Korea) for supplying the CDM data. We thank Jinseob Kim, MD (CEO, Zarathu), for his statistical advice.

FOOTNOTES

Author contributions: Choi YJ and Seo SI contributed to the acquisition of data, analysis and interpretation of data, drafting of the manuscript; Kim TJ, Bang CS, Lee YK, and Lee MW participated in the technical or material support of this study; Nam SY and Shin WG contributed to the critical revision of the manuscript for important intellectual content; Seo SI involved in the study concept and design, and study supervision.

Institutional review board statement: This study was approved by the Institutional Review Board (IRB) of Kangdong Sacred Hospital (IRB number: 2021-11-001). The other six hospitals were affiliated with the Research Border Free Zone, which recognizes IRB approval of the research organizing center and waives individual IRB approval.

Informed consent statement: As the study used anonymous and pre-existing data, the requirement for the informed consent from patients was waived.

Conflict-of-interest statement: All the authors report no relevant conflicts of interest for this article.

Data sharing statement: Dataset available from the corresponding author's e-mail doctorssi@kdh.or.kr.

Country/Territory of origin: South Korea

ORCID number: Yoon Jin Choi 0000-0002-1922-9388; Tae Jun Kim 0000-0001-8101-9034; Yong Kang Lee 0000-0003-2929-4447; Moon Won Lee 0000-0002-8411-6398; Su Youn Nam 0000-0002-5568-7714; Woon Geon Shin 0000-0002-9851-5576; Seung In Seo 0000-0003-4417-0135.

S-Editor: Wang JJ
L-Editor: A
P-Editor: Yu HG

REFERENCES

1 **Lanas A**, Chan FKL. Peptic ulcer disease. *Lancet* 2017; **390**: 613-624 [PMID: 28242110 DOI: 10.1016/S0140-6736(16)32404-7]
2 **Xie X**, Ren K, Zhou Z, Dang C, Zhang H. The global, regional and national burden of peptic ulcer disease from 1990 to 2019: a population-based study. *BMC Gastroenterol* 2022; **22**: 58 [PMID: 35144540 DOI: 10.1186/s12876-022-02130-2]
3 **Kim YS**, Lee J, Shin A, Lee JM, Park JH, Jung HY. A Nationwide Cohort Study Shows a Sex-Dependent Change in the Trend of Peptic Ulcer Bleeding Incidence in Korea between 2006 and 2015. *Gut Liver* 2021; **15**: 537-545 [PMID: 33071238 DOI: 10.5009/gnl20079]
4 **Sung JJ**, Kuipers EJ, El-Serag HB. Systematic review: the global incidence and prevalence of peptic ulcer disease. *Aliment Pharmacol Ther* 2009; **29**: 938-946 [PMID: 19220208 DOI: 10.1111/j.1365-2036.2009.03960.x]
5 **Lanas A**, García-Rodríguez LA, Polo-Tomás M, Ponce M, Quintero E, Perez-Aisa MA, Gisbert JP, Bujanda L, Castro M, Muñoz M, Del-Pino MD, Garcia S, Calvet X. The changing face of hospitalisation due to gastrointestinal bleeding and perforation. *Aliment Pharmacol Ther* 2011; **33**: 585-591 [PMID: 21205256 DOI: 10.1111/j.1365-2036.2010.04563.x]
6 **Malmi H**, Kautiainen H, Virta LJ, Färkkilä N, Koskenpato J, Färkkilä MA. Incidence and complications of peptic ulcer disease requiring hospitalisation have markedly decreased in Finland. *Aliment Pharmacol Ther* 2014; **39**: 496-506 [PMID: 24461085 DOI: 10.1111/apt.12620]
7 **Leow AH**, Lim YY, Liew WC, Goh KL. Time trends in upper gastrointestinal diseases and Helicobacter pylori infection in a multiracial Asian population--a 20-year experience over three time periods. *Aliment Pharmacol Ther* 2016; **43**: 831-837 [PMID: 26847417 DOI: 10.1111/apt.13550]
8 **Chung CS**, Chiang TH, Lee YC. A systematic approach for the diagnosis and treatment of idiopathic peptic ulcers. *Korean J Intern Med* 2015; **30**: 559-570 [PMID: 26354049 DOI: 10.3904/kjim.2015.30.5.559]
9 **Jang HJ**, Choi MH, Shin WG, Kim KH, Chung YW, Kim KO, Park CH, Baek IH, Baik KH, Kae SH, Kim HY. Has peptic ulcer disease changed during the past ten years in Korea? A prospective multi-center study. *Dig Dis Sci* 2008; **53**: 1527-1531 [PMID: 17932759 DOI: 10.1007/s10620-007-0028-6]
10 **McColl KE**. Helicobacter pylori-negative nonsteroidal anti-inflammatory drug-negative ulcer. *Gastroenterol Clin North Am* 2009; **38**: 353-361 [PMID: 19446263 DOI: 10.1016/j.gtc.2009.03.004]
11 **Wong GL**, Wong VW, Chan Y, Ching JY, Au K, Hui AJ, Lai LH, Chow DK, Siu DK, Lui YN, Wu JC, To KF, Hung LC, Chan HL, Sung JJ, Chan FK. High incidence of mortality and recurrent bleeding in patients with Helicobacter pylori-negative idiopathic bleeding ulcers. *Gastroenterology* 2009; **137**: 525-531 [PMID: 19445937 DOI: 10.1053/j.gastro.2009.05.006]
12 **Chung WC**, Jeon EJ, Kim DB, Sung HJ, Kim YJ, Lim ES, Kim MA, Oh JH. Clinical characteristics of Helicobacter pylori-negative drug-negative peptic ulcer bleeding. *World J Gastroenterol* 2015; **21**: 8636-8643 [PMID: 26229405 DOI: 10.3748/wjg.v21.i28.8636]
13 **Wong GLH**, Lau LHS, Ching JYL, Tse YK, Ling RHY, Wong VWS, Chiu PWY, Lau JYW, Chan FKL. Prevention of recurrent idiopathic gastroduodenal ulcer bleeding: a double-blind, randomised trial. *Gut* 2020; **69**: 652-657 [PMID: 31229990 DOI: 10.1136/gutjnl-2019-318715]
14 **Hung LC**, Ching JY, Sung JJ, To KF, Hui AJ, Wong VW, Leong RW, Chan HL, Wu JC, Leung WK, Lee YT, Chung SC, Chan FK. Long-term outcome of Helicobacter pylori-negative idiopathic bleeding ulcers: a prospective cohort study. *Gastroenterology* 2005; **128**: 1845-1850 [PMID: 15940620 DOI: 10.1053/j.gastro.2005.03.026]
15 **Kim Y**, Seo SI, Lee KJ, Kim J, Yoo JJ, Seo WW, Shin WG. Risks of long-term use of proton pump inhibitor on ischemic vascular events: A distributed network analysis of 5 real-world observational Korean databases using a common data model. *Int J Stroke* 2023; **18**: 590-598 [PMID: 36190338 DOI: 10.1177/17474930221133219]
16 **Park DH**, Seo SI, Lee KJ, Kim J, Kim Y, Seo WW, Lee HS, Shin WG, Yoo JJ. Long-term proton pump inhibitor use and risk of osteoporosis and hip fractures: A nationwide population-based and multicenter cohort study using a common data model. *J Gastroenterol Hepatol* 2022; **37**: 1534-1543 [PMID: 35501296 DOI: 10.1111/jgh.15879]

17 **Seo WW**, Seo SI, Kim Y, Yoo JJ, Shin WG, Kim J, You SC, Park RW, Park YM, Kim KJ, Rhee SY, Park M, Jin ES, Kim SE. Impact of pitavastatin on new-onset diabetes mellitus compared to atorvastatin and rosuvastatin: a distributed network analysis of 10 real-world databases. *Cardiovasc Diabetol* 2022; **21**: 82 [PMID: 35606846 DOI: 10.1186/s12933-022-01524-6]

18 **Hripcsak G**, Duke JD, Shah NH, Reich CG, Huser V, Schuemie MJ, Suchard MA, Park RW, Wong IC, Rijnbeek PR, van der Lei J, Pratt N, Norén GN, Li YC, Stang PE, Madigan D, Ryan PB. Observational Health Data Sciences and Informatics (OHDSI): Opportunities for Observational Researchers. *Stud Health Technol Inform* 2015; **216**: 574-578 [PMID: 26262116]

19 **Lee JW**, Kim HK, Woo YS, Jahng J, Jin YR, Park JH, Kim YS, Jung HY. [Optimal Operational Definition of Patient with Peptic Ulcer Bleeding for Big Data Analysis Using Combination of Clinical Characteristics in a Secondary General Hospital]. *Korean J Gastroenterol* 2016; **68**: 77-86 [PMID: 27554214 DOI: 10.4166/kjg.2016.68.2.77]

20 **Lim SH**, Kim N, Kwon JW, Kim SE, Baik GH, Lee JY, Park KS, Shin JE, Song HJ, Myung DS, Choi SC, Kim HJ, Yim JY, Kim JS. Trends in the seroprevalence of Helicobacter pylori infection and its putative eradication rate over 18 years in Korea: A cross-sectional nationwide multicenter study. *PLoS One* 2018; **13**: e0204762 [PMID: 30332428 DOI: 10.1371/journal.pone.0204762]

21 **Chua BQY**, Chong VWS, Teng TZJ, Chia CTW, Aung MO, Shelat VG. Does technology-enhanced communication improve Helicobacter pylori eradication outcomes?-A meta-analysis. *Helicobacter* 2022; **27**: e12890 [PMID: 35363943 DOI: 10.1111/hel.12890]

22 **Pilotto A**, Franceschi M, Leandro G, Di Mario F; Geriatric Gastroenterology Study Group (Societè Italiana Gerontologie Geriatria). NSAID and aspirin use by the elderly in general practice: effect on gastrointestinal symptoms and therapies. *Drugs Aging* 2003; **20**: 701-710 [PMID: 12831293 DOI: 10.2165/00002512-200320090-00006]

23 **Wongrakpanich S**, Wongrakpanich A, Melhado K, Rangaswami J. A Comprehensive Review of Non-Steroidal Anti-Inflammatory Drug Use in The Elderly. *Aging Dis* 2018; **9**: 143-150 [PMID: 29392089 DOI: 10.14336/AD.2017.0306]

24 **Zullo A**, Hassan C, Campo SM, Morini S. Bleeding peptic ulcer in the elderly: risk factors and prevention strategies. *Drugs Aging* 2007; **24**: 815-828 [PMID: 17896831 DOI: 10.2165/00002512-200724100-00003]

25 **Yang YJ**, Bang CS, Shin SP, Park TY, Suk KT, Baik GH, Kim DJ. Clinical characteristics of peptic ulcer perforation in Korea. *World J Gastroenterol* 2017; **23**: 2566-2574 [PMID: 28465641 DOI: 10.3748/wjg.v23.i14.2566]

26 **Joo MK**, Park CH, Kim JS, Park JM, Ahn JY, Lee BE, Lee JH, Yang HJ, Cho YK, Bang CS, Kim BJ, Jung HK, Kim BW, Lee YC; Korean College of Helicobacter Upper Gastrointestinal Research. Clinical Guidelines for Drug-Related Peptic Ulcer, 2020 Revised Edition. *Gut Liver* 2020; **14**: 707-726 [PMID: 33191311 DOI: 10.5009/gnl20246]

27 **Kamada T**, Satoh K, Itoh T, Ito M, Iwamoto J, Okimoto T, Kanno T, Sugimoto M, Chiba T, Nomura S, Mieda M, Hiraishi H, Yoshino J, Takagi A, Watanabe S, Koike K. Evidence-based clinical practice guidelines for peptic ulcer disease 2020. *J Gastroenterol* 2021; **56**: 303-322 [PMID: 33620586 DOI: 10.1007/s00535-021-01769-0]

28 **Masclee GM**, Valkhoff VE, Coloma PM, de Ridder M, Romio S, Schuemie MJ, Herings R, Gini R, Mazzaglia G, Picelli G, Scotti L, Pedersen L, Kuipers EJ, van der Lei J, Sturkenboom MC. Risk of upper gastrointestinal bleeding from different drug combinations. *Gastroenterology* 2014; **147**: 784-792.e9; quiz e13 [PMID: 24937265 DOI: 10.1053/j.gastro.2014.06.007]

29 **Kim DJ**, Kim HY, Kim SJ, Hahn TH, Jang MK, Baik GH, Kim JB, Park SH, Lee MS, Park CK. Helicobacter pylori infection and peptic ulcer disease in patients with liver cirrhosis. *Korean J Intern Med* 2008; **23**: 16-21 [PMID: 18363275 DOI: 10.3904/kjim.2008.23.1.16]

30 **Kirk AP**, Dooley JS, Hunt RH. Peptic ulceration in patients with chronic liver disease. *Dig Dis Sci* 1980; **25**: 756-760 [PMID: 7428583 DOI: 10.1007/BF01345294]

31 **Bang CS**, Baik GH, Kim JH, Kim JB, Suk KT, Yoon JH, Kim YS, Kim DJ. Peptic ulcer disease in liver cirrhosis and chronic hepatitis: impact of portal hypertension. *Scand J Gastroenterol* 2014; **49**: 1051-1057 [PMID: 24902119 DOI: 10.3109/00365521.2014.923501]

World Journal of Gastroenterology

Submit a Manuscript: https://www.f6publishing.com

World J Gastroenterol 2023 November 28; 29(44): 5894-5906

DOI: 10.3748/wjg.v29.i44.5894

ISSN 1007-9327 (print) ISSN 2219-2840 (online)

ORIGINAL ARTICLE

Retrospective Study

Role of intelligent/interactive qualitative and quantitative analysis-three-dimensional estimated model in donor-recipient size mismatch following deceased donor liver transplantation

Han Ding, Zhi-Guo Ding, Wen-Jing Xiao, Xu-Nan Mao, Qi Wang, Yi-Chi Zhang, Hao Cai, Wei Gong

Specialty type: Gastroenterology and hepatology

Provenance and peer review: Unsolicited article; Externally peer reviewed.

Peer-review model: Single blind

Peer-review report's scientific quality classification

Grade A (Excellent): 0
Grade B (Very good): B, B
Grade C (Good): 0
Grade D (Fair): 0
Grade E (Poor): 0

P-Reviewer: Abbas Z, Pakistan; Ferreira GSA, Brazil

Received: August 18, 2023
Peer-review started: August 18, 2023
First decision: November 3, 2023
Revised: November 10, 2023
Accepted: November 14, 2023
Article in press: November 14, 2023
Published online: November 28, 2023

Han Ding, Yi-Chi Zhang, Hao Cai, Department of Transplantation, Xinhua Hospital, Affiliated to Shanghai Jiaotong University School of Medicine, Shanghai 200092, China

Zhi-Guo Ding, Department of General Surgery, The Third People's Hospital of Yangzhou, Yangzhou 225126, Jiangsu Province, China

Wen-Jing Xiao, Department of Tuberculosis Control, Shanghai Municipal Center for Disease Control and Prevention, Shanghai 200336, China

Xu-Nan Mao, Department of Biliary-Pancreatic Surgery, Shanghai Changzheng Hospital, Second Military Medical University, Shanghai 200003, China

Qi Wang, Department of Pathology, First Affiliated Hospital of Nanjing Medical University, Nanjing 210029, Jiangsu, China

Wei Gong, Department of General Surgery, Xinhua Hospital, Affiliated to Shanghai Jiaotong University School of Medicine, Shanghai 200092, China

Wei Gong, Shanghai Key Laboratory of Biliary Tract Disease Research, Shanghai, 200092, China

Corresponding author: Wei Gong, Doctor, MD, PhD, Doctor, Professor, Surgeon, Department of General Surgery, Xinhua Hospital, Affiliated to Shanghai Jiaotong University School of Medicine, No.1665 Kongjiang Road, Shanghai 200092, China. gongwei@xinhuamed.com.cn

Abstract

BACKGROUND

Donor-recipient size mismatch (DRSM) is considered a crucial factor for poor outcomes in liver transplantation (LT) because of complications, such as massive intraoperative blood loss (IBL) and early allograft dysfunction (EAD). Liver volumetry is performed routinely in living donor LT, but rarely in deceased donor LT (DDLT), which amplifies the adverse effects of DRSM in DDLT. Due to the various shortcomings of traditional manual liver volumetry and formula methods, a feasible model based on intelligent/interactive qualitative and quantitative analysis-three-dimensional (IQQA-3D) for estimating the degree of DRSM is needed.

AIM
To identify benefits of IQQA-3D liver volumetry in DDLT and establish an estimation model to guide perioperative management.

METHODS
We retrospectively determined the accuracy of IQQA-3D liver volumetry for standard total liver volume (TLV) (sTLV) and established an estimation TLV (eTLV) index (eTLVi) model. Receiver operating characteristic (ROC) curves were drawn to detect the optimal cut-off values for predicting massive IBL and EAD in DDLT using donor sTLV to recipient sTLV (called sTLVi). The factors influencing the occurrence of massive IBL and EAD were explored through logistic regression analysis. Finally, the eTLVi model was compared with the sTLVi model through the ROC curve for verification.

RESULTS
A total of 133 patients were included in the analysis. The Changzheng formula was accurate for calculating donor sTLV (P = 0.083) but not for recipient sTLV (P = 0.036). Recipient eTLV calculated using IQQA-3D highly matched with recipient sTLV (P = 0.221). Alcoholic liver disease, gastrointestinal bleeding, and sTLVi > 1.24 were independent risk factors for massive IBL, and drug-induced liver failure was an independent protective factor for massive IBL. Male donor-female recipient combination, model for end-stage liver disease score, sTLVi ≤ 0.85, and sTLVi ≥ 1.32 were independent risk factors for EAD, and viral hepatitis was an independent protective factor for EAD. The overall survival of patients in the 0.85 < sTLVi < 1.32 group was better compared to the sTLVi ≤ 0.85 group and sTLVi ≥ 1.32 group (P < 0.001). There was no statistically significant difference in the area under the curve of the sTLVi model and IQQA-3D eTLVi model in the detection of massive IBL and EAD (all P > 0.05).

CONCLUSION
IQQA-3D eTLVi model has high accuracy in predicting massive IBL and EAD in DDLT. We should follow the guidance of the IQQA-3D eTLVi model in perioperative management.

Key Words: Intelligent/interactive qualitative and quantitative analysis-three-dimensional; Donor-recipient size mismatch; Intraoperative blood loss; Early allograft dysfunction

Core Tip: This is a retrospective study to identify benefits of intelligent/interactive qualitative and quantitative analysis-three-dimensional (IQQA-3D) liver volumetry in deceased donor liver transplantation and establish an estimation model to guide perioperative management. Patients with estimation total liver volume index (eTLVi) ≥ 1.24 have an increased risk of massive intraoperative blood loss and patients with eTLVi ≤ 0.85 or eTLVi ≥ 1.32 have an increased risk of early allograft dysfunction. To improve the overall survival of patients, we should follow the guidance of the IQQA-3D eTLVi model either for organ allocation or perioperative management.

Citation: Ding H, Ding ZG, Xiao WJ, Mao XN, Wang Q, Zhang YC, Cai H, Gong W. Role of intelligent/interactive qualitative and quantitative analysis-three-dimensional estimated model in donor-recipient size mismatch following deceased donor liver transplantation. *World J Gastroenterol* 2023; 29(44): 5894-5906
URL: https://www.wjgnet.com/1007-9327/full/v29/i44/5894.htm
DOI: https://dx.doi.org/10.3748/wjg.v29.i44.5894

INTRODUCTION

An understanding of the interaction between donors and recipients is crucial to ensure optimum outcomes in liver transplantation (LT)[1]. Studies have investigated the effects of mismatch in age, gender[2,3] and ethnicity[4] on the outcomes of LT, with donor-recipient size mismatch (DRSM) being the most important factor[5,6]. Nowadays, with most organ allocation systems worldwide relying on the 'sickest first' policy. However, they do not consider the mismatch of the mismatch of the morphological parameters in the abdominal cavity between donors and recipients[7]. Liver volumetry is rarely undertaken in deceased donor LT (DDLT), which amplifies the adverse effects of DRSM. Massive intraoperative blood loss (IBL), early allograft dysfunction (EAD)[8-10], and other complications caused by small-for-size syndrome (SFSS) or large-for-size syndrome (LFSS) have been found to lead to lower allograft survival and higher patient mortality[11,12]. Therefore, experienced centers have focused more on liver volumetry for total liver volume (TLV) and are committed to establishing a model to estimate the degree of DRSM.

The use of the Archimedes drainage method, the gold standard for liver volumetry, is restricted due to the disadvantage of measuring only for liver *in vitro*[13]. Whether TLV is calculated by height/weight or by body surface

area (BSA), the results are subject to differences in race, gender, and various clinical factors[14]. Estimations by simple empirical formulas are handy and suitable for donor TLV but not for recipient TLV (mostly accompanied by ascites, hepatic carcinomas, cirrhosis, or post-hepatectomy status). Over the years, imaging equipment and visualization techniques have improved significantly and become increasingly refined. Consequently, liver volumetry, based on Doppler ultrasound (DUS), contrast-enhanced computed tomography (CT), or magnetic resonance imaging (MRI) scans, has shown a close correlation with TLV when highly trained operators spend considerable time in postprocessing analysis[15-17]. However, the expensive and time-consuming post process may impede the widespread application of non-automatic liver volumetry, particularly in some emerging transplantation centers.

With advanced technology, the trend towards automated interactive volumetry-assist software replacing manual liver volumetry in the future is anecdotally known. Intelligent/interactive qualitative and quantitative analysis-three-dimensional (IQQA-3D), one of the automated computerized liver volumetry calculators, is characterized by real accuracy, high intelligence, and robust applicability. Scattered reports[18] indicated that the advantages of high repeatability, stability, and reliability of IQQA-3D in measuring standard liver volume can reduce IBL, operative duration, and postoperative complications in precise hepatectomy and living donor LT (LDLT). However, few results have been reported on the role of IQQA-3D in liver volumetry in DDLT. Thus, we conducted this study to identify the benefits of IQQA-3D-based liver volumetry in DDLT and establish a convenient, feasible, and accurate estimation model to guide perioperative management, especially for DRSM-induced massive IBL and EAD.

MATERIALS AND METHODS

Patient selection

We retrospectively analyzed patients who underwent DDLT by a single experienced surgeon between November 2017 and February 2022 in our center and ensured that all surviving patients had been followed up for more than 1 year. All liver allografts were allocated by China Organ Transplant Response System which follows the sickest first policy. Recipients with extreme marginal allografts were excluded according to the following criteria: (1) Donors over 70 years old; (2) Severe allografts steatosis with more than 60% macrosteatosis confirmed by wedge biopsy 1 h after reperfusion; (3) The warm ischemia time of allografts of > 20 min or cold ischemia time of allografts of > 12 h; (4) Prolonged hypotension of the donors (diastolic blood pressure < 60 mmHg, maintenance time > 2 h); (5) Continuous serum total bilirubin and transaminase higher than normal by more than 3 times (maintenance time > 7 d); and (6) ABO-incompatible LT. The recipients of multiorgan transplants or liver re-transplants and recipients with missing demographic characteristics or LT-related information were also excluded.

The study was conducted in accordance with the Helsinki Declaration, and the protocol was approved by the Ethics Committee of Xinhua Hospital Affiliated to Shanghai Jiao Tong University School of Medicine (No. XHEC-D-2023-076).

Procedures

IQQA-3D was applied to calculate estimated TLV (eTLV) for all recipients by analyzing the imported contrast-enhanced CT/MRI scan and automatically outlining the liver parenchyma contour in each layer according to the liver anatomy and density. To improve the accuracy of eTLV, further amendments were carried out by experienced surgeons if necessary.

Donors included in this study were free of liver disease and hence the donor eTLV was similar to that of the normal population. Therefore, due to the extensive practicability for the Chinese population among existing studies, we chose the formula[19] derived by the Shanghai Changzheng Hospital to calculate donor eTLV: TLV (cm^3) = 758.259 × BSA (m^2) - 124.272. Standard TLV (sTLV) was preferably determined using the Archimedes method and secondly deduced from liver weight and density[20] (1.00 ± 0.06 kg/L). To estimate the degree of DRSM, the sTLV index (sTLVi), which was calculated as the ratio of donor TLV to recipient TLV, became a crucial parameter and a gold standard model in this study.

All enrolled patients underwent classic orthotopic LT without the piggyback technique, portocaval shunt, or veno-venous bypass. Anesthesiologists ensured that hypotension and hypothermia did not occur during the operation. An autotransfusion machine was used for all patients to not only maintain the concentration of blood hemoglobin but also to determine IBL. Liver allografts were weighed or volume was measured using the Archimedes method immediately after back-table procedures. Native diseased livers were subjected to the same measurement after removing the gallbladder and accessory ligaments. The donor risk index (DRI) for liver allografts was calculated using the formula described formula[21].

Outcomes

The primary outcomes were massive IBL and EAD caused by DRSM during the perioperative period. Massive IBL was defined as 2000 mL as the baseline. EAD was determined based on the presence of 1 or more of the following most widely accepted criteria[22]: (1) Bilirubin ≥ 10 mg/dL on post operative day 7; (2) International normalized ratio ≥ 1.6 on post operative day 7; and (3) Alanine or aspartate aminotransferase ≥ 2000 IU/L within the first 7 d.

Secondary outcomes included: (1) Procedure-related outcomes including tracheal extubation time, intensive care unit (ICU) stay, postoperative hospital stay, and complications, such as infection and incision nonunion; and (2) perioperative mortality and overall survival (OS) at the end of follow-up.

Statistical analysis

Continuous variables were expressed as mean ± SD or median (interquartile range) and categorical variables as numbers and percentages. Statistical methods used in this study included the Student's *t*-test (or Mann-Whitney U test), Fisher's exact test (or Pearson's chi-square test), Kaplan-Meier method for survival analysis, and Cox regression analyses. All tests were two-sided and differences were considered statistically significant when the *P*-value was < 0.05. Receiver operating characteristic (ROC) curves were drawn to not only detect the optimal cut-off values for the index but also confirm the equivalence of the sTLVi model and the eTLV index (eTLVi) model in predicting massive IBL and EAD. Univariate and multivariable logistic regression analyses were performed successively to predict how sTLVi affected the development of massive IBL and EAD.

RESULTS

Demographics of recipients and donors

A total of 133 patients were enrolled in this study. Patients with chronic hepatitis B virus/hepatitis C virus (HBV/HCV) infection accounted for the majority (63.9%) of the patients, followed by those with chronic alcoholic liver disease (ALD) (18.0%) and drug-induced liver failure (DILF) (9.0%; Table 1). Gastrointestinal bleeding (64.7%), ascites (51.9%), and hepatic encephalopathy (23.3%) were the most common clinical symptoms in the included patients. Pathologically confirmed hepatic carcinomas were found in 42 removed livers (31.6%). Twenty-eight patients (21.1%) used to undergo open upper abdominal surgery and 29 patients (21.8%) had a history of one or more artificial liver support system (ALSS) use.

Donors were younger (mean age, 48.1 ± 13.1 years *vs* 49.4 ± 12.8 years, *P* = 0.388) than recipients and had a higher proportion of males (83.5% *vs* 76.7%, *P* = 0.002). Although the body shape of recipients was generally smaller than that of donors, which was reflected in mean height (168.1 ± 10.2 cm *vs* 170.6 ± 11.2 cm, *P* = 0.032) and mean weight (67.5 ± 18.0 kg *vs* 73.7 ± 17.5 kg, *P* = 0.003), there was no statistical difference in sTLV of recipients and donors (1299 ± 482 mL *vs* 1311 ± 267 mL, *P* = 0.799). Notably, considering the shortage of donor pool in China, 23 liver allografts with HBV or HCV infection (17.3%) and 43 allografts with mild or moderate steatosis (32.3%) were transplanted after exclusion of extreme marginal allografts through a rapid biopsy. The mean DRI of liver allografts was 2.28 ± 0.42. Male donor-female recipient (MD-FR) combination and female donor-male recipient (FD-MR) combination were observed in 26 cases (19.5%) and 17 cases (12.8%), respectively, which were also considered for our analyses.

Operational parameters and outcomes

The mean cold ischemia time was 5.9 ± 1.8 h, and the mean anhepatic phase time was 50.7 ± 9.0 min. Massive IBL developed in 71.4% of recipients with a mean IBL of 3117 ± 1725 mL and a mean intraoperative blood transfusion (IBT) of 1949 ± 1749 mL. The median tracheal extubation time, ICU stay, and postoperative hospital stay were 1 (1-3) d, 2 (1-6) d, and 15 (11-23) d, respectively. EAD developed in 42.1% of recipients, of which SFSS was the cause in 36 recipients (27.1%) and LFSS was the cause in 20 recipients (15.0%). Infection occurred in 36.8% of recipients, and incision nonunion occurred in 21.8%. In terms of perioperative adverse events, there were 29 perioperative deaths (21.8%), including 7 blood loss-specific deaths (5.3%), and 17 EAD-specific deaths (12.8%).

Accuracy of IQQA-3D and the formula method for calculating donor and recipient eTLV

Compared with donor sTLV, there was no statistical difference in donor eTLV calculated using the Changzheng formula (1287 ± 207 mL *vs* 1311 ± 267 mL, *P* = 0.083). However, compared with recipient sTLV, the Changzheng formula for calculating recipient eTLV was not accurate (1213 ± 212 mL *vs* 1299 ± 482 mL, *P* = 0.036), while recipient eTLV calculated using IQQA-3D was highly matched up with recipient sTLV (1311 ± 522 mL *vs* 1299 ± 482 mL, *P* = 0.221). Therefore, the IQQA-3D eTLVi model was defined as the ratio of donor eTLV to IQQA-3D recipient eTLV and selected as an estimation model in the study.

Association between sTLVi and massive IBL

Univariate logistic regression revealed that sTLVi was a risk factor for massive IBL [odds ratio (OR) = 2.968, *P* = 0.037]. The optimal cut-off value of sTLVi in predicting massive IBL calculated using the ROC curve was 1.24, with a sensitivity of 46.3% and a specificity of 94.7% (Figure 1A). Except for a higher proportion of males (82.8% *vs* 65.2%, *P* = 0.023) in the sTLVi < 1.24 group, there was no significant statistical difference in other recipient characteristics (all *P* > 0.05). The distribution of donor characteristics was similar, except for the MD-FR combination (11.5% *vs* 34.8%, *P* = 0.001) and allograft steatosis (25.3% *vs* 45.7%, *P* = 0.017). In addition, the sTLVi < 1.24 group showed advantages in terms of the anhepatic phase time (49.3 ± 7.2 min *vs* 53.6 ± 11.4 min, *P* = 0.024), IBL (2430 ± 1203 mL *vs* 4417 ± 1821 mL, *P* < 0.001), and IBT (1366 ± 1235 mL *vs* 3052 ± 2039 mL, *P* < 0.001). In terms of recovery course, the sTLVi < 1.24 group had a longer survival time (45.6 ± 2.8 mo *vs* 37.0 ± 4.1 mo, *P* = 0.132), and shorter tracheal extubation time (median, 1 d *vs* 2 d, *P* = 0.089), ICU stay (median, 2 d *vs* 3 d, *P* = 0.082) and postoperative hospital stay (median, 15 d *vs* 16 d, *P* = 0.239) than the sTLVi ≥ 1.24 group. These data were not statistically significant except for blood loss-specific mortality (1.1% *vs* 13.0%, *P* = 0.007).

The results of multivariate logistic regression analysis revealed that sTLVi ≥ 1.24 (OR = 18.43, *P* < 0.001), ALD (OR = 9.371, *P* = 0.040) and gastrointestinal bleeding (OR = 3.954, *P* = 0.005) were associated with massive IBL, while DILF (OR = 0.226, *P* = 0.047) was protective against massive IBL (Table 2).

Table 1 Demographics, operational parameters and outcomes of recipients and donors

	Recipient	Donor
Demographics		
Age (yr)	49.4 ± 12.8	48.1 ± 13.1
Male	102 (76.7)	111 (83.5)
Height (cm)	168.1 ± 10.2	170.6 ± 11.2
Weight (kg)	67.5 ± 18.0	73.7 ± 17.5
sTLV (mL)	1299 ± 482	1311 ± 267
eTLV by formula (mL)	1213 ± 212	1287 ± 207
eTLV by IQQA-3D (mL)	1311 ± 522	-
DRI	-	2.28 ± 0.42
Cold ischemia time (h)	-	5.9 ± 1.8
Liver disease		
HBV/HCV	85 (63.9)	23 (17.3)
ALD	24 (18.0)	0
DILF	12 (9.0)	0
Steatosis	8 (6.0)	43 (32.3)
Hepatic carcinoma	42 (31.6)	0
Signs and symptoms		
Moderate or severe ascites	69 (51.9)	-
Gastrointestinal bleeding	86 (64.7)	-
Hepatic encephalopathy	31 (23.3)	-
Operational parameters		
Anhepatic phase time (min)	50.7 ± 9.0	-
IBL (mL)	3117 ± 1725	-
IBT (mL)	1949 ± 1749	-
Hospitalization Information		
Tracheal extubation time (d)	1 (1-3)	-
ICU stay (d)	2 (1-6)	-
Postoperative hospital stay (d)	15 (11-23)	-
Complications		
Massive intraoperative blood loss	95 (71.4)	-
EAD caused by SFSS	36 (27.1)	-
EAD caused by LFSS	20 (15.0)	-
Infection	49 (36.8)	-
Incision nonunion	29 (21.8)	-
Outcomes and follow-up		
Perioperative mortality	29 (21.8)	-
Blood loss-specific mortality	7 (5.3)	-
EAD-specific mortality	17 (12.8)	-
All-cause mortality	46 (34.6)	-
Follow-up time (mo)	27 (9-44)	-

Values are mean ± SD, *n* (%), or median (interquartile range). sTLV: Standard total liver volume; eTLV: estimated total liver volume; DRI: Donor risk index; HBV: Hepatitis B virus; HCV: Hepatitis C virus; ALD: Alcoholic liver disease; DILF: Drug-induced liver failure; IBL: Intraoperative blood loss; IBT: Intraoperative blood transfusion; ICU: Intensive care unit; EAD: Early allograft dysfunction; SFSS: Small-for-size syndrome; LFSS: Large-for-size syndrome; IQQA-3D: Intelligent/interactive qualitative and quantitative analysis-three-dimensional.

Table 2 Univariate and multivariate logistic regression to predict massive intraoperative blood loss

	Univariate			Multivariate		
	OR	95% CI	*P* value	OR	95% CI	*P* value
Recipient age	1.038	1.007-1.070	0.017			0.106
Male	0.835	0.336-2.074	0.697			0.815
sTLVi ≥ 1.24	22.00	4.804-100.8	< 0.001	18.43	3.809-89.15	< 0.001
Donor age	1.014	0.986-1.042	0.340			
MD-FR combination	1.873	0.650-5.396	0.245			
FD-MR combination	0.698	0.238-2.046	0.513			
Graft steatosis (< 60%)	2.187	0.903-5.297	0.083			
Cold ischemia time	1.005	0.815-1.239	0.963			
DRI	1.074	0.437-2.644	0.876			
HBV/HCV	1.225	0.564-2.661	0.608			
ALD	11.82	1.535-90.99	0.018	9.371	1.112-78.98	0.040
DILF	0.165	0.406-0.586	0.005	0.226	0.052-0.983	0.047
Hepatic carcinoma	1.422	0.615-3.288	0.410			
Gastrointestinal bleeding	2.393	1.104-5.188	0.027	3.954	1.502-10.41	0.005
Moderate or severe ascites	1.065	0.502-2.261	0.869			
History of open upper abdominal surgery	2.108	0.737-6.032	0.164			
Platelet count	1.000	0.955-1.005	0.914			
PT	1.011	0.976-1.045	0.577			
Child-Pugh grade C	2.347	0.961-5.731	0.061			
MELD score	1.012	0.975-1.052	0.526			
Anhepatic phase time	1.020	0.975-1.067	0.396			

OR: Odds ratio; 95%CI: 95% confidence interval; sTLVi: Standard total liver volume index; MD-FR: Male donor-female recipient; FD-MR: Female donor-male recipient; DRI: Donor risk index; HBV: Hepatitis B virus; HCV: Hepatitis C virus; ALD: Alcoholic liver disease; DILF: Drug-induced liver failure; PT: Prothrombin time; MELD: Model for end-stage liver disease.

Association between sTLVi with EAD

Unconventional sTLVi was found to be related to an increased risk of EAD ($P < 0.001$). The optimal cut-off values of sTLVi calculated using the ROC curve for predicting EAD caused by SFSS and LFSS were 0.85 (sensitivity 96.0%, specificity 88.0%) and 1.32 (sensitivity 95.0%, specificity 85.0%), respectively (Figure 1B and C). In the sTLVi ≥ 1.32 group, there were significant differences in the proportion of males (61.1% *vs* 83.8% and 81.7%, $P = 0.034$), MD-FR combination (41.7% *vs* 8.1% and 13.3%, $P < 0.001$), and allograft steatosis (50.0% *vs* 13.5% and 33.3%, $P = 0.004$) compared to the 0.85< sTLVi <1.32 group and the sTLVi ≤ 0.85 group. The mean Child-Pugh score for patients in the 0.85 < sTLVi < 1.32 group was the lowest among the 3 groups (8.2 ± 2.8 *vs* 9.6 ± 2.8 and 9.4 ± 2.7, $P = 0.033$). The distribution of other characteristics was similar between the 3 groups, except for the prolonged anhepatic phase time with the increase of sTLVi ($P = 0.002$).

An sTLVi of ≤ 0.85 (OR = 21234, $P < 0.001$) and model for end-stage liver disease (MELD) score (OR = 1.333, $P = 0.002$) were associated with EAD caused by SFSS, whereas HBV/HCV (OR = 0.095, $P = 0.042$) infection was protective against EAD on multivariate logistic regression (Table 3). An sTLVi of ≥ 1.32 (OR = 78.56, $P < 0.001$) and MD-FR combination (OR = 6.540, $P = 0.008$) were associated with EAD caused by LFSS on multivariate logistic regression.

In general, patients with sTLVi between 0.85 and 1.32 had a longer survival time (52.5 ± 2.6 mo *vs* 37.3 ± 4.4 mo and 25.0 ± 4.3 mo, $P < 0.001$), shorter tracheal extubation time (median, 1 d *vs* 1 d and 2 d, $P = 0.002$), lower EAD-associated

Table 3 Univariate and multivariate logistic regression to predict early allograft dysfunction

	EAD caused by SFSS						EAD caused by LFSS					
	Univariate			Multivariate			Univariate			Multivariate		
	OR	95%CI	*P* value	OR	95%CI	*P* value	OR	95%CI	*P* value	OR	95%CI	*P* value
Recipient age	0.980	0.948-1.013	0.235			0.992	1.062	1.014-1.113	0.012			0.069
Male	1.268	0.433-3.715	0.665			0.357	0.295	0.109-0.800	0.016			0.134
sTLVi ≤ 0.85/≥ 1.32	175.4	21.85-1407	< 0.001	21234	126-3585713	< 0.001	100.3	16.06-970.4	< 0.001	78.56	9.529-648.0	< 0.001
Donor age	0.992	0.961-1.025	0.645				1.003	0.967-1.040	0.887			
MD-FR combination	0.504	0.139-1.833	0.298				10.61	3.693-30.47	< 0.001	6.540	1.617-26.45	0.008
FD-MR combination	0.916	0.242-3.464	0.897				1.923	0.557-6.637	0.301			
Graft steatosis (< 60%)	0.065	0.009-0.502	0.009			0.444	2.424	0.923-6.368	0.072			
Cold ischemia time	0.923	0.725-1.174	0.512				1.006	0.772-1.312	0.962			
DRI	2.376	0.859-6.573	0.095			0.086	1.069	0.346-3.305	0.908			
HBV/HCV positive graft	0.163	0.021-1.271	0.083				2.420	0.817-7.174	0.111			
HBV/HCV	0.361	0.149-0.877	0.025	0.095	0.010-0.919	0.042	1.058	0.391-2.862	0.912			
ALD	0.838	0.259-2.712	0.768				1.649	0.535-5.084	0.384			
DILF	3.607	1.040-12.51	0.043			0.979	0.488	0.059-4.005	0.504			
Hepatic carcinoma	0.480	0.167-1.381	0.173				0.493	0.154-1.579	0.234			
Hepatic encephalopathy	1.739	0.667-4.534	0.258				3.384	1.249-9.167	0.016			0.186
History of ALSS	2.475	0.957-6.400	0.062				1.677	0.581-4.842	0.339			
Child-Pugh grade C	18.85	2.408-147.5	0.005			0.319	2.200	0.563-8.598	0.257			
MELD score	1.082	1.035-1.133	0.001	1.333	1.109-1.602	0.002	1.024	0.978-1.073	0.305			
Anhepatic phase time	0.949	0.893-1.009	0.097				1.049	1.000-1.100	0.050			0.808

OR: Odds ratio; 95%CI: 95% confidence interval; sTLVi: Standard total liver volume index; MD-FR: Male donor-female recipient; FD-MR: Female donor-male recipient; DRI: Donor risk index; HBV: Hepatitis B virus; HCV: Hepatitis C virus; ALD: Alcoholic liver disease; DILF: Drug-induced liver failure; PT: Prothrombin time; MELD: Model for end-stage liver disease.

morbidity (3.4% *vs* 64.9% and 52.8%, $P < 0.001$) and lower EAD-specific mortality (1.7% *vs* 13.5% and 30.6%, $P < 0.001$) compared to the sTLVi ≥ 1.32 group and the sTLVi ≤ 0.85 group. However, the sTLVi did not influence ICU stay ($P = 0.383$) and postoperative hospital stay ($P = 0.101$). There were significant differences in terms of median survival time between the 3 groups (median, 57 mo *vs* 60 mo *vs* 24 mo, $P < 0.001$). Figure 2 shows that the OS of patients with sTLVi between 0.85 and 1.32 was significantly superior to those with sTLVi ≤ 0.85 ($P = 0.006$) and sTLVi ≥ 1.32 ($P < 0.001$).

Equivalence between the sTLVi model and IQQA-3D eTLVi model

The area under the curve (AUC) of the sTLVi and IQQA-3D eTLVi models for the detection of massive IBL were 0.618 and 0.598 ($Z = 0.889$, $P = 0.374$; Figure 3A), respectively. The AUC of the sTLVi model and IQQA-3D eTLVi model for predicting EAD caused by SFSS and LFSS were 0.932 and 0.889 ($Z = 1.501$, $P = 0.133$), 0.933 and 0.922 ($Z = 0.710$, $P =$

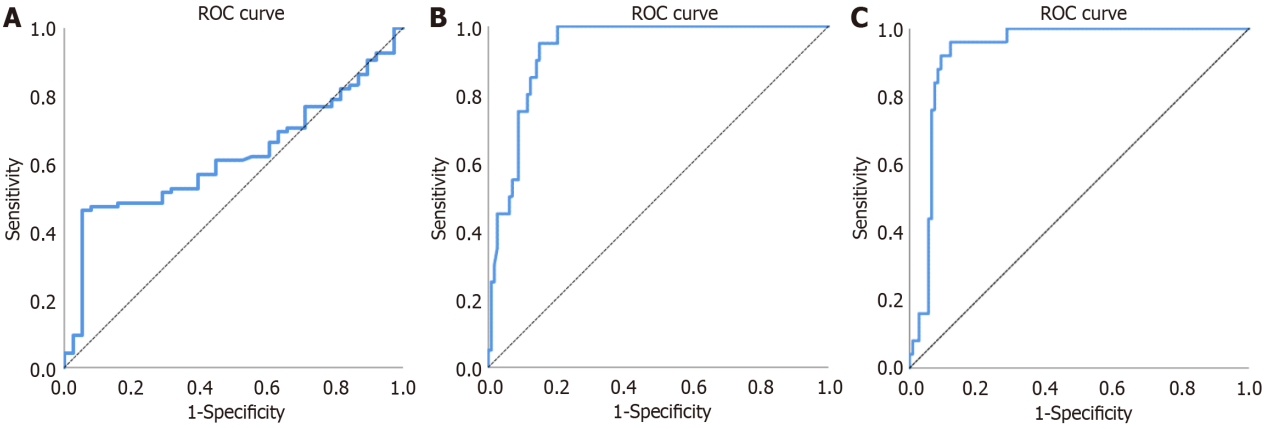

DOI: 10.3748/wjg.v29.i44.5894 **Copyright** ©The Author(s) 2023.

Figure 1 Optimal cut-off values of the index in predicting massive intraoperative blood loss and early allograft dysfunction. A: The standard total liver volume index (sTLVi) value of 1.24 was the optimal cutoff value for predicting massive intraoperative blood loss, with a sensitivity of 46.3% and a specificity of 94.7%; B: The sTLVi value of 0.85 was the optimal cutoff value for predicting early allograft dysfunction (EAD) caused by small-for-size syndrome, with a sensitivity of 96.0% and a specificity of 88.0%; C: The sTLVi value of 1.32 was the optimal cutoff value for predicting EAD caused by large-for-size syndrome, with a sensitivity of 95.0% and a specificity of 85.0%. ROC: Receiver operating characteristic.

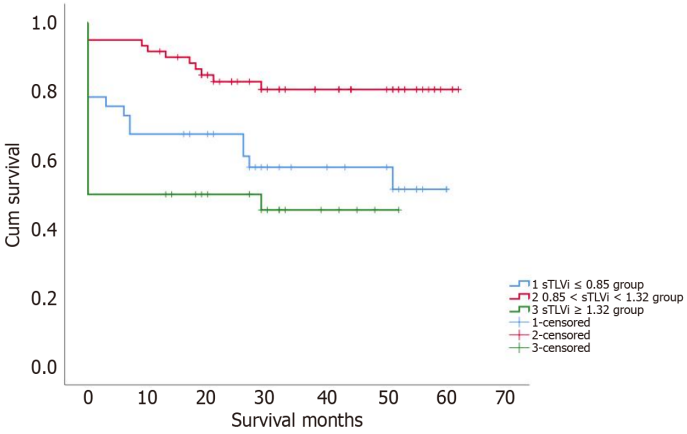

DOI: 10.3748/wjg.v29.i44.5894 **Copyright** ©The Author(s) 2023.

Figure 2 Overall survival of patients in 0.85 < standard total liver volume index < 1.32 group was significantly superior to those in standard total liver volume index ≤ 0.85 group (P = 0.006) and sTLVi ≥ 1.32 group (P < 0.001). sTLVi: Standard total liver volume index.

0.478), respectively (Figure 3B and C). There were no statistically significant differences in the AUC of the sTLVi model and IQQA-3D eTLVi model for predicting massive IBL and EAD. Finally, we found that the IQQA-3D eTLVi model was also applicable to all optimal cut-off values and was equivalent to the sTLVi model in predicting massive IBL and EAD after verification.

DISCUSSION

Postoperative complications associated with DRSM have been reported in an increasing number of DDLT studies[8-12, 23]. Conclusions drawn from LDLT-related studies are that sTLVi < 0.5 is associated with poor outcomes[24] and cannot be used for DRSM in DDLT because additional risk factors, such as brain death and longer preservation injury, result in the need for a larger allograft in DDLT. Therefore, this study aimed to establish an easy, feasible, and accurate estimation model using IQQA-3D to predict massive IBL and EAD associated with DRSM and guide perioperative management in DDLT.

Massive IBT has been reported to possibly increase the risk of acute renal failure, surgical site infections, and recurrence of hepatic carcinomas in patients[25-27]. McCluskey *et al*[28] and Cywinski *et al*[29] attempt to create a model to predict the demand for IBT based on preoperative variables was not successful. The influence of preoperative risk factors and surgical factors on massive IBL have been widely studied[30], but donor factors were rarely mentioned. We have concluded that sTLVi ≥ 1.24 is an independent risk factor for massive IBL, which has not been reported in existing literatures. This may be attributed to the greater surgical difficulty and longer anhepatic phase time. In addition, the

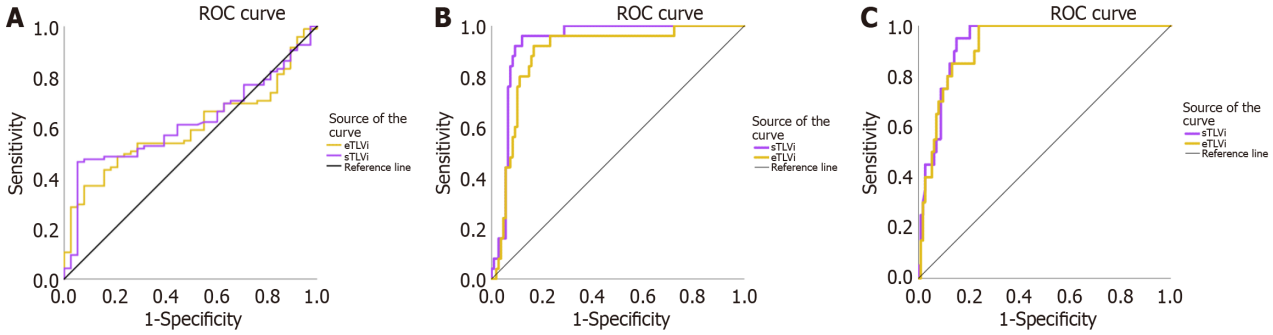

DOI: 10.3748/wjg.v29.i44.5894

Figure 3 The equivalence of the standard total liver volume index model and the estimation total liver volume index model in predicting massive intraoperative blood loss and early allograft dysfunction. A: The area under the curve (AUC) of standard total liver volume index (sTLVi) model and intelligent/interactive qualitative and quantitative analysis-three-dimensional (IQQA-3D) estimation total liver volume index (eTLVi) model in detection of massive IBL were 0.618 and 0.598 (Z = 0.889, P = 0.374), demonstrating equivalence; B: The AUC of sTLVi model and IQQA-3D eTLVi model in detection of early allograft dysfunction (EAD) caused by small-for-size syndrome were 0.932 and 0.889 (Z = 1.501, P = 0.133), demonstrating equivalence; C: The AUC of sTLVi model and IQQA-3D eTLVi model in detection of EAD caused by large-for-size syndrome were 0.933 and 0.922 (Z = 0.710, P = 0.478), demonstrating equivalence. eTLVi: estimation total liver volume index; sTLVi: Standard total liver volume index; ROC: Receiver operating characteristic.

probability of large allografts accompanied by steatosis is higher than that of small allografts, which was seen in our analysis. Theoretically, a large allograft can fill the abdominal space to tamponade of bleeding, but allograft steatosis can have a greater effect on massive IBL due to the delayed recovery of coagulation function after reperfusion.

Besides DRSM, we observed that ALD and gastrointestinal bleeding were independent risk factors for massive IBL. Patients with ALD always experience a long course of liver disease and usually experience portal hypertension, plentiful collateral circulation, and cavernous transformation of the portal vein. Gastrointestinal bleeding can serve as a significant marker of portal hypertension, indicating a greater likelihood of multiple thin and varicose blood vessels being transected during surgical dissection. Animal experiments have shown that replacing the exact IBL volume results in an increase in portal pressure by 20%[31], higher rates of massive IBL, and worse outcome[32] in portal hypertensive rats subjected to a period of gastrointestinal bleeding. This has subsequently been demonstrated in our study, as adequate IBT was usually given to recipients with gastrointestinal bleeding before transplantation to correct hypovolemia. Surprisingly, we observed that DILF, a severe liver disease characterized by rapid onset and progression, has become an independent protective factor for massive IBL. Since patients with DILF rarely show anatomic changes in the native liver, the incidence of massive IBL can be reduced with a shorter hepatectomy duration, which is consistent with other reports[33].

Studies have reported factors related to EAD, with the most important being ischemia-reperfusion injury (IRI), which is difficult to regulate. We found that improper sTLVi is associated with an increased risk of EAD and this effect is 'U' shaped. Due to the unavailability of an index to quantify the magnitude of the DRSM effect and of a statistical methodology to formulate the model for describing its nonlinear effect, scattered studies[5,10] only reported the impact of SFSS or LFSS on EAD separately. To overcome the statistical difficulty, we divided recipients into 3 groups and found that the effect on EAD becomes stronger toward both ends of sTLVi values.

MELD score and sTLVi ≤ 0.85 were independent risk factors for EAD caused by SFSS. SFSS occurs when the functional liver volume is too small to provide enough activated hepatocytes for hepatic metabolism. Moreover, the small allograft will withstand the entire blood flow of the original liver, leading to severe congestion of the hepatic sinuses and portal hypertension after reperfusion. MELD score has been reported by various authors as an independent risk factor for the occurrence of EAD in DDLT recipients[34,35], which is consistent with our conclusion.

The MD-FR combination and sTLVi ≥ 1.32 were independent risk factors for EAD caused by LFSS. Patients with sTLVi ≥ 1.32 underwent a higher number of challenging surgeries, had longer anhepatic phase time, and had a higher probability of allograft steatosis, which aggravated IRI. Other anatomical causes of LFSS-related EAD included external compression affecting allograft perfusion and outflow tract obstruction, which were also potential factors with the lowest median survival time in the sTLVi ≥ 1.32 group. In terms of secondary outcomes, the tracheal extubation time in the sTLVi ≥ 1.32 group was longer than that in the other 2 groups, indicating the potential impact of large volume allograft on respiratory complications, consistent with Levesque *et al* report[6]. Gender mismatch, especially the FD-MR combination, has been reported in most studies as an independent risk factor for EAD[2,36,37]. Hormonal factors and differences in IRI and SFSS are the main hypotheses currently[38]. It is speculated that female allografts face a greater risk of IRI due to the sudden loss of protection from estrogen during implantation[2]. However, in our study, the MD-FR combination rather than the FD-MR combination played a significant role in EAD, size which could be related to the differences among males and females.

Because of time constraints with organ allocation and limited services at the donor hospital, donor eTLV measured using cross-sectional imaging is usually not feasible. We confirmed the accuracy of the Changzheng formula method in calculating donor eTLV rather than recipient eTLV. Therefore, we focused on IQQA-3D because of its high accuracy, shorter time, and not having to rely on experienced operators[39,40]. Foreign studies[41] have reported the application of IQQA-3D in precise hepatectomy and LDLT, which not only shortens the operation time but also reduces IBL and other complications. The application of IQQA-3D was rarely reported in DDLT. However, our study has innovatively used

IQQA-3D into the eTLVi model after demonstrating its accuracy in measuring recipient eTLV and confirmed its equivalence with the sTLVi model in predicting massive IBL and EAD. For patients with stable liver diseases, the IQQA-3D eTLVi model can be used to exclude extremely sized mismatched allografts. For patients with critical diseases having minimal choice but to receive unsuitable allografts, timely and sufficient perioperative management can suppress adverse outcomes. For patients with eTLVi ≥ 1.24, sufficient blood products, antifibrinolytics, terlipressin, autotransfusion machine, and liver resection time should be prepared for and reserved before DDLT to reduce IBL. For patients with eTLVi ≤ 0.85, the intraoperative ligation of the splenic artery or resection of the spleen should be considered to control the velocity of the portal vein. Also, if necessary, ALSS therapy should be performed promptly to reduce the burden of the allografts. For patients with eTLVi ≥ 1.32, in addition to sufficient preoperative treatments to reduce the Child-Pugh score and MELD score, strict respiratory management and frequent DUS monitoring to prevent vascular complications, reduced-size LT should be considered.

To improve the accuracy of the results of this impact, we first used sTLVi calculated using the Archimedes method as the gold standard instead of the formula method based on BSA[9,42,43] or graft-to-recipient weight ratio[6,44]. If a simpler or more accurate liver volumetry tool other than IQQA-3D is developed in the future, researchers can still create a new eTLVi model to compare with the sTLVi model in our study. However, like the shortcomings of other studies on DRSM, we only compared TLV between donors and recipients, but failed to compare the abdominal parameters in detail. Due to the limitations of a single-center retrospective study without numerous patients and sufficient follow-up time, future prospective studies are warranted to carried out.

CONCLUSION

We established the IQQA-3D eTLVi model to estimate the degree of DRSM and predict massive IBL and EAD in DDLT. Patients with eTLVi ≥ 1.24 have an increased risk of massive IBL and patients with eTLVi ≤ 0.85 or eTLVi ≥ 1.32 have an increased risk of EAD. To improve the OS of patients, we should follow the guidance of the IQQA-3D eTLVi model either for organ allocation or perioperative management.

ARTICLE HIGHLIGHTS

Research background

Donor-recipient size mismatch (DRSM) is considered a crucial factor for poor outcomes in deceased donor liver transplantation (DDLT).

Research motivation

A feasible model for estimating the degree of DRSM is needed.

Research objectives

To identify benefits of intelligent/interactive qualitative and quantitative analysis-three-dimensional (IQQA-3D) liver volumetry in DDLT and establish an estimation model to guide perioperative management.

Research methods

A retrospective study was conducted to determine the accuracy of IQQA-3D liver volumetry and to establish an estimation total liver volume (TLV) index (eTLVi) model. Receiver operating characteristic curves and logistic regression analysis were used to detect the influencing factors for the occurrence of massive intraoperative blood loss (IBL) and early allograft dysfunction (EAD) in DDLT.

Research results

Recipient estimation TLV calculated using IQQA-3D highly matched with recipient standard TLV (P = 0.221). Alcoholic liver disease, gastrointestinal bleeding, and standard TLV index (sTLVi) > 1.24 were independent risk factors for massive IBL, and drug-induced liver failure was an independent protective factor for massive IBL. Male donor-female recipient combination, model for end-stage liver disease score, sTLVi ≤ 0.85, and sTLVi ≥ 1.32 were independent risk factors for EAD, and viral hepatitis was an independent protective factor for EAD. The overall survival of patients in the 0.85 < sTLVi < 1.32 group was better compared to the sTLVi ≤ 0.85 group and sTLVi ≥ 1.32 group (P < 0.001). There was no statistically significant difference in the area under the curve of the sTLVi model and IQQA-3D eTLVi model in the detection of massive IBL and EAD (all P > 0.05).

Research conclusions

IQQA-3D eTLVi model has high accuracy in predicting massive IBL and EAD in DDLT. We should follow the guidance of the IQQA-3D eTLVi model in perioperative management.

Research perspectives

By establishing the eTLVi model, the degree of DRSM was estimated and IQQA-3D proved to be of guiding value in

perioperative management in DDLT.

ACKNOWLEDGEMENTS

The authors gratefully acknowledge all the doctors who collaborated on this project by collecting data.

FOOTNOTES

Co-first authors: Zhi-Guo Ding and Wen-Jing Xiao.

Co-corresponding authors: Hao Cai and Yi-Chi Zhang.

Author contributions: Gong W, Cai H and Zhang YC contributed to the study conception and design; Material preparation and data collection were performed by Ding H, Ding ZG and Wang Q; Data analysis was performed by Xiao WJ and Mao XN; The first draft of the manuscript was written by Ding H and all authors commented on previous versions of the manuscript; All authors read and approved the final manuscript. Ding ZG and Xiao WJ contributed equally to this work as co-first authors. The follow-up and data collection of 133 patients included in this study were all completed by Ding ZG, which is a time-consuming and difficult task. Therefore, it is reasonable to list him as a co-first author. The data analysis and figure drawing involved in this article were mostly completed by Xiao WJ. She maintained the rigorous principle and ensured data authenticity in the process of data analysis, which justifies her as a qualified co-first author. Cai H and Zhang YC contributed equally to this work as co-corresponding authors. Cai H consulted a large amount of relevant literature and designed this study together with Gong Wei and Zhang YC. The details of the study (such as primary outcomes, secondary outcomes, influencing factors, *etc*.) were determined by Cai H, which makes it reasonable for him to become a co-corresponding author. Zhang YC also participated in the design of the study, and as an experienced surgeon, he was mainly responsible for calculating eTLV using IQQA-3D and carrying out further amendments if necessary. In addition, he was mainly committed to revising the manuscript, which makes it reasonable for him to become a co-corresponding author.

Supported by National Natural Science Foundation of China, No. 82172628.

Institutional review board statement: The study was reviewed and approved by the Ethics Committee of Xinhua Hospital Affifiliated to Shanghai Jiao Tong University School of Medicine (No. XHEC-D-2023-076).

Informed consent statement: All study participants or their legal guardian provided informed written consent about personal and medical data collection prior to study enrolment.

Conflict-of-interest statement: The authors have no relevant financial or non-financial interests to disclose.

Data sharing statement: Technical appendix, statistical code, and dataset available from the corresponding author at gongwei@xinhuamed.com.cn.

Country/Territory of origin: China

ORCID number: Han Ding 0000-0002-7914-1193; Zhi-Guo Ding 0009-0005-0091-662X; Wen-Jing Xiao 0000-0003-2371-7920; Xu-Nan Mao 0009-0004-1436-6684; Qi Wang 0009-0009-0676-3037; Yi-Chi Zhang 0000-0002-9332-4316; Hao Cai 0000-0002-1492-4701; Wei Gong 0000-0002-9949-6207.

S-Editor: Lin C
L-Editor: A
P-Editor: Zhao S

REFERENCES

1 **Reddy MS**, Varghese J, Venkataraman J, Rela M. Matching donor to recipient in liver transplantation: Relevance in clinical practice. *World J Hepatol* 2013; **5**: 603-611 [PMID: 24303088 DOI: 10.4254/wjh.v5.i11.603]

2 **Lai Q**, Giovanardi F, Melandro F, Larghi Laureiro Z, Merli M, Lattanzi B, Hassan R, Rossi M, Mennini G. Donor-to-recipient gender match in liver transplantation: A systematic review and meta-analysis. *World J Gastroenterol* 2018; **24**: 2203-2210 [PMID: 29853738 DOI: 10.3748/wjg.v24.i20.2203]

3 **Germani G**, Zeni N, Zanetto A, Adam R, Karam V, Belli LS, O'Grady J, Mirza D, Klempnauer J, Cherqui D, Pratschke J, Jamieson N, Salizzoni M, Hidalgo E, Lerut J, Paul A, Garcia-Valdecasas JC, Rodríguez FSJ, Villa E, Burra P; European Liver, Intestine Transplant Association (ELITA). Influence of donor and recipient gender on liver transplantation outcomes in Europe. *Liver Int* 2020; **40**: 1961-1971

[PMID: 32418358 DOI: 10.1111/liv.14510]

4 **Zhang Y**. Impact of Donor Recipient Gender and Race Mismatch on Graft Outcomes in Patients With End-Stage Liver Disease Undergoing Liver Transplantation. *Prog Transplant* 2017; **27**: 39-47 [PMID: 27895103 DOI: 10.1177/1526924816679839]

5 **Tanaka K**, Ogura Y. "Small-for-size graft" and "small-for-size syndrome" in living donor liver transplantation. *Yonsei Med J* 2004; **45**: 1089-1094 [PMID: 15627301 DOI: 10.3349/ymj.2004.45.6.1089]

6 **Levesque E**, Duclos J, Ciacio O, Adam R, Castaing D, Vibert E. Influence of larger graft weight to recipient weight on the post-liver transplantation course. *Clin Transplant* 2013; **27**: 239-247 [PMID: 23293941 DOI: 10.1111/ctr.12059]

7 **Tschuor C**, Ferrarese A, Kuemmerli C, Dutkowski P, Burra P, Clavien PA; Liver Allocation Study Group. Allocation of liver grafts worldwide - Is there a best system? *J Hepatol* 2019; **71**: 707-718 [PMID: 31199941 DOI: 10.1016/j.jhep.2019.05.025]

8 **Fukazawa K**, Nishida S, Volsky A, Tzakis AG, Pretto EA Jr. Body surface area index predicts outcome in orthotopic liver transplantation. *J Hepatobiliary Pancreat Sci* 2011; **18**: 216-225 [PMID: 20936303 DOI: 10.1007/s00534-010-0334-9]

9 **Croome KP**, Lee DD, Saucedo-Crespo H, Burns JM, Nguyen JH, Perry DK, Taner CB. A novel objective method for deceased donor and recipient size matching in liver transplantation. *Liver Transpl* 2015; **21**: 1471-1477 [PMID: 26358746 DOI: 10.1002/lt.24333]

10 **Shen Z**, Wang Z, Jiang Y, Wu T, Zheng S. Early outcomes of implanting larger-sized grafts in deceased donor liver transplantation. *ANZ J Surg* 2020; **90**: 1352-1357 [PMID: 32691510 DOI: 10.1111/ans.16132]

11 **Reyes J**, Perkins J, Kling C, Montenovo M. Size mismatch in deceased donor liver transplantation and its impact on graft survival. *Clin Transplant* 2019; **33**: e13662 [PMID: 31283049 DOI: 10.1111/ctr.13662]

12 **Allard MA**, Lopes F, Frosio F, Golse N, Sa Cunha A, Cherqui D, Castaing D, Adam R, Vibert E. Extreme large-for-size syndrome after adult liver transplantation: A model for predicting a potentially lethal complication. *Liver Transpl* 2017; **23**: 1294-1304 [PMID: 28779555 DOI: 10.1002/lt.24835]

13 **Yu HC**, You H, Lee H, Jin ZW, Moon JI, Cho BH. Estimation of standard liver volume for liver transplantation in the Korean population. *Liver Transpl* 2004; **10**: 779-783 [PMID: 15162473 DOI: 10.1002/Lt.20188]

14 **Pomposelli JJ**, Tongyoo A, Wald C, Pomfret EA. Variability of standard liver volume estimation *vs* software-assisted total liver volume measurement. *Liver Transpl* 2012; **18**: 1083-1092 [PMID: 22532341 DOI: 10.1002/lt.23461]

15 **Choi SH**, Kwon JH, Kim KW, Jang HY, Kim JH, Kwon HJ, Lee J, Song GW, Lee SG. Measurement of liver volumes by portal vein flow by Doppler ultrasound in living donor liver transplantation. *Clin Transplant* 2017; **31** [PMID: 28681460 DOI: 10.1111/ctr.13050]

16 **Schroeder T**, Malagó M, Debatin JF, Goyen M, Nadalin S, Ruehm SG. "All-in-one" imaging protocols for the evaluation of potential living liver donors: comparison of magnetic resonance imaging and multidetector computed tomography. *Liver Transpl* 2005; **11**: 776-787 [PMID: 15973711 DOI: 10.1002/lt.20429]

17 **Haimerl M**, Schlabeck M, Verloh N, Zeman F, Fellner C, Nickel D, Barreiros AP, Loss M, Stroszczynski C, Wiggermann P. Volume-assisted estimation of liver function based on Gd-EOB-DTPA-enhanced MR relaxometry. *Eur Radiol* 2016; **26**: 1125-1133 [PMID: 26186960 DOI: 10.1007/s00330-015-3919-5]

18 **Mise Y**, Tani K, Aoki T, Sakamoto Y, Hasegawa K, Sugawara Y, Kokudo N. Virtual liver resection: computer-assisted operation planning using a three-dimensional liver representation. *J Hepatobiliary Pancreat Sci* 2013; **20**: 157-164 [PMID: 23135735 DOI: 10.1007/s00534-012-0574-y]

19 **Feng LM**, Wang PQ, Yu H, Chen RT, Wang J, Sheng X, Yuan ZL, Shi PM, Xie WF, Zeng X. New formula for predicting standard liver volume in Chinese adults. *World J Gastroenterol* 2017; **23**: 4968-4977 [PMID: 28785151 DOI: 10.3748/wjg.v23.i27.4968]

20 **Yuan D**, Lu T, Wei YG, Li B, Yan LN, Zeng Y, Wen TF, Zhao JC. Estimation of standard liver volume for liver transplantation in the Chinese population. *Transplant Proc* 2008; **40**: 3536-3540 [PMID: 19100432 DOI: 10.1016/j.transproceed.2008.07.135]

21 **Feng S**, Goodrich NP, Bragg-Gresham JL, Dykstra DM, Punch JD, DebRoy MA, Greenstein SM, Merion RM. Characteristics associated with liver graft failure: the concept of a donor risk index. *Am J Transplant* 2006; **6**: 783-790 [PMID: 16539636 DOI: 10.1111/j.1600-6143.2006.01242.x]

22 **Olthoff KM**, Kulik L, Samstein B, Kaminski M, Abecassis M, Emond J, Shaked A, Christie JD. Validation of a current definition of early allograft dysfunction in liver transplant recipients and analysis of risk factors. *Liver Transpl* 2010; **16**: 943-949 [PMID: 20677285 DOI: 10.1002/lt.22091]

23 **Fukazawa K**, Nishida S. Size mismatch in liver transplantation. *J Hepatobiliary Pancreat Sci* 2016; **23**: 457-466 [PMID: 27474079 DOI: 10.1002/jhbp.371]

24 **Kiuchi T**, Kasahara M, Uryuhara K, Inomata Y, Uemoto S, Asonuma K, Egawa H, Fujita S, Hayashi M, Tanaka K. Impact of graft size mismatching on graft prognosis in liver transplantation from living donors. *Transplantation* 1999; **67**: 321-327 [PMID: 10075602 DOI: 10.1097/00007890-199901270-00024]

25 **Reichert B**, Kaltenborn A, Becker T, Schiffer M, Klempnauer J, Schrem H. Massive blood transfusion after the first cut in liver transplantation predicts renal outcome and survival. *Langenbecks Arch Surg* 2014; **399**: 429-440 [PMID: 24682384 DOI: 10.1007/s00423-014-1181-y]

26 **Freire MP**, Soares Oshiro IC, Bonazzi PR, Guimarães T, Ramos Figueira ER, Bacchella T, Costa SF, Carneiro D'Albuquerque LA, Abdala E. Surgical site infections in liver transplant recipients in the model for end-stage liver disease era: an analysis of the epidemiology, risk factors, and outcomes. *Liver Transpl* 2013; **19**: 1011-1019 [PMID: 23744748 DOI: 10.1002/lt.23682]

27 **Kornberg A**, Witt U, Kornberg J, Ceyhan GO, Mueller K, Friess H, Thrum K. Prognostic Impact of Intraoperative Blood Loss in Liver Transplant Patients with Advanced Hepatocellular Carcinoma. *Anticancer Res* 2016; **36**: 5355-5364 [PMID: 27798899 DOI: 10.21873/anticanres.11109]

28 **McCluskey SA**, Karkouti K, Wijeysundera DN, Kakizawa K, Ghannam M, Hamdy A, Grant D, Levy G. Derivation of a risk index for the prediction of massive blood transfusion in liver transplantation. *Liver Transpl* 2006; **12**: 1584-1593 [PMID: 16952177 DOI: 10.1002/Lt.20868]

29 **Cywinski JB**, Alster JM, Miller C, Vogt DP, Parker BM. Prediction of intraoperative transfusion requirements during orthotopic liver transplantation and the influence on postoperative patient survival. *Anesth Analg* 2014; **118**: 428-437 [PMID: 24445640 DOI: 10.1213/ANE.0b013e3182a76f19]

30 **Cleland S**, Corredor C, Ye JJ, Srinivas C, McCluskey SA. Massive haemorrhage in liver transplantation: Consequences, prediction and management. *World J Transplant* 2016; **6**: 291-305 [PMID: 27358774 DOI: 10.5500/wjt.v6.i2.291]

31 **Kravetz D**, Sikuler E, Groszmann RJ. Splanchnic and systemic hemodynamics in portal hypertensive rats during hemorrhage and blood volume restitution. *Gastroenterology* 1986; **90**: 1232-1240 [PMID: 3956942 DOI: 10.1016/0016-5085(86)90390-2]

32 **Castañeda B**, Morales J, Lionetti R, Moitinho E, Andreu V, Pérez-Del-Pulgar S, Pizcueta P, Rodés J, Bosch J. Effects of blood volume restitution following a portal hypertensive-related bleeding in anesthetized cirrhotic rats. *Hepatology* 2001; **33**: 821-825 [PMID: 11283845

DOI: 10.1053/jhep.2001.23437]

33 **Rana A**, Petrowsky H, Hong JC, Agopian VG, Kaldas FM, Farmer D, Yersiz H, Hiatt JR, Busuttil RW. Blood transfusion requirement during liver transplantation is an important risk factor for mortality. *J Am Coll Surg* 2013; **216**: 902-907 [PMID: 23478547 DOI: 10.1016/j.jamcollsurg.2012.12.047]

34 **Ito T**, Naini BV, Markovic D, Aziz A, Younan S, Lu M, Hirao H, Kadono K, Kojima H, DiNorcia J 3rd, Agopian VG, Yersiz H, Farmer DG, Busuttil RW, Kupiec-Weglinski JW, Kaldas FM. Ischemia-reperfusion injury and its relationship with early allograft dysfunction in liver transplant patients. *Am J Transplant* 2021; **21**: 614-625 [PMID: 32713098 DOI: 10.1111/ajt.16219]

35 **Grąt M**, Wronka KM, Patkowski W, Stypułkowski J, Grąt K, Krasnodębski M, Masior Ł, Lewandowski Z, Krawczyk M. Effects of Donor Age and Cold Ischemia on Liver Transplantation Outcomes According to the Severity of Recipient Status. *Dig Dis Sci* 2016; **61**: 626-635 [PMID: 26499986 DOI: 10.1007/s10620-015-3910-7]

36 **Rustgi VK**, Marino G, Halpern MT, Johnson LB, Umana WO, Tolleris C. Role of gender and race mismatch and graft failure in patients undergoing liver transplantation. *Liver Transpl* 2002; **8**: 514-518 [PMID: 12037781 DOI: 10.1053/jlts.2002.33457]

37 **Uemura T**, Randall HB, Sanchez EQ, Ikegami T, Narasimhan G, McKenna GJ, Chinnakotla S, Levy MF, Goldstein RM, Klintmalm GB. Liver retransplantation for primary nonfunction: analysis of a 20-year single-center experience. *Liver Transpl* 2007; **13**: 227-233 [PMID: 17256780 DOI: 10.1002/Lt.20992]

38 **Francavilla A**, di Leo A, Eagon PK, Wu SQ, Ove P, van Thiel DH, Starzl TE. Regenerating rat liver: correlations between estrogen receptor localization and deoxyribonucleic acid synthesis. *Gastroenterology* 1984; **86**: 552-557 [PMID: 6693017]

39 **Suzuki K**, Epstein ML, Kohlbrenner R, Garg S, Hori M, Oto A, Baron RL. Quantitative radiology: automated CT liver volumetry compared with interactive volumetry and manual volumetry. *AJR Am J Roentgenol* 2011; **197**: W706-W712 [PMID: 21940543 DOI: 10.2214/AJR.10.5958]

40 **Bozkurt B**, Emek E, Arikan T, Ceyhan O, Yazici P, Sahin T, Mammadov E, Serin A, Gurcan NI, Yuzer Y, Tokat Y. Liver Graft Volume Estimation by Manual Volumetry and Software-Aided Interactive Volumetry: Which is Better? *Transplant Proc* 2019; **51**: 2387-2390 [PMID: 31324483 DOI: 10.1016/j.transproceed.2019.01.152]

41 **Müller SA**, Bläuer K, Kremer M, Thorn M, Mehrabi A, Meinzer HP, Hinz U, Metzger J, Büchler MW, Schmied BM. Exact CT-based liver volume calculation including nonmetabolic liver tissue in three-dimensional liver reconstruction. *J Surg Res* 2010; **160**: 236-243 [PMID: 19765736 DOI: 10.1016/j.jss.2009.04.050]

42 **Fukazawa K**, Yamada Y, Nishida S, Hibi T, Arheart KL, Pretto EA Jr. Determination of the safe range of graft size mismatch using body surface area index in deceased liver transplantation. *Transpl Int* 2013; **26**: 724-733 [PMID: 23647566 DOI: 10.1111/tri.12111]

43 **Vauthey JN**, Chaoui A, Do KA, Bilimoria MM, Fenstermacher MJ, Charnsangavej C, Hicks M, Alsfasser G, Lauwers G, Hawkins IF, Caridi J. Standardized measurement of the future liver remnant prior to extended liver resection: methodology and clinical associations. *Surgery* 2000; **127**: 512-519 [PMID: 10819059 DOI: 10.1067/msy.2000.105294]

44 **Lo CM**, Fan ST, Liu CL, Chan JK, Lam BK, Lau GK, Wei WI, Wong J. Minimum graft size for successful living donor liver transplantation. *Transplantation* 1999; **68**: 1112-1116 [PMID: 10551638 DOI: 10.1097/00007890-199910270-00009]

World Journal of Gastroenterology

Submit a Manuscript: https://www.f6publishing.com

World J Gastroenterol 2023 November 28; 29(44): 5907-5918

DOI: 10.3748/wjg.v29.i44.5907

ISSN 1007-9327 (print) ISSN 2219-2840 (online)

ORIGINAL ARTICLE

Retrospective Study

Tenofovir amibufenamide *vs* tenofovir alafenamide for treating chronic hepatitis B: A real-world study

Wen-Ting Peng, Chuan Jiang, Fei-Lan Yang, Nian-Qi Zhou, Ke-Yu Chen, Jin-Qing Liu, Shi-Fang Peng, Lei Fu

Specialty type: Gastroenterology and hepatology

Provenance and peer review: Unsolicited article; Externally peer reviewed.

Peer-review model: Single blind

Peer-review report's scientific quality classification

Grade A (Excellent): 0
Grade B (Very good): 0
Grade C (Good): C, C
Grade D (Fair): 0
Grade E (Poor): 0

P-Reviewer: Martinez-Camacho A, United States; Mucenic M, Brazil

Received: September 2, 2023
Peer-review started: September 2, 2023
First decision: October 16, 2023
Revised: October 29, 2023
Accepted: November 14, 2023
Article in press: November 14, 2023
Published online: November 28, 2023

Wen-Ting Peng, Chuan Jiang, Fei-Lan Yang, Nian-Qi Zhou, Ke-Yu Chen, Jin-Qing Liu, Shi-Fang Peng, Lei Fu, Department of Infectious Diseases, Xiangya Hospital Central South University, Changsha 410008, Hunan Province, China

Corresponding author: Lei Fu, MD, PhD, Professor, Department of Infectious Diseases, Xiangya Hospital Central South University, No. 87 Xiangya Road, Changsha 410008, Hunan Province, China. fulei92@126.com

Abstract

BACKGROUND

The efficacy and safety profile of tenofovir amibufenamide (TMF) in chronic hepatitis B (CHB) patients is not well-established.

AIM

To compare the efficacy and safety of TMF and tenofovir alafenamide (TAF) over a 48-wk period in patients with CHB.

METHODS

A total of 215 subjects meeting the inclusion criteria were enrolled and divided into two groups: TMF group (n = 106) and the TAF group (n = 109). The study included a comparison of virological response (VR): Undetectable hepatitis B virus DNA levels, alanine transaminase (ALT) normalization rates, renal function parameters, and blood lipid profiles.

RESULTS

At 24 and 48 wk, VR rates for the TMF group were 53.57% and 78.57%, respectively, compared with 48.31% and 78.65% for the TAF group (P > 0.05). The VR rates were also similar in both groups among patients with low-level viremia, both hepatitis B e antigen (HBeAg)-positive and HBeAg-negative subgroups. The TMF cohort showed ALT normalization and renal safety profiles similar to the TAF group. There was a notable increase in total cholesterol levels in the TAF group (P = 0.045), which was not observed in the TMF group (P > 0.05). In patients with liver cirrhosis, both groups exhibited comparable VR and ALT normalization rates and renal safety profiles. However, the fibrosis 4 score at 48 wk showed a significant reduction in the TAF group as compared to the TMF group within the liver cirrhosis subgroup.

CONCLUSION

Our study found TMF is as effective as TAF in treating CHB and has a comparable safety profile. However, TAF may be associated with worsening lipid profiles.

Key Words: Alanine transaminase normalization; Chronic hepatitis B; Renal safety; Virological response; Blood lipid; Tenofovir

Core Tip: This is a retrospective study to compare the efficacy and safety of tenofovir amibufenamide (TMF) and tenofovir alafenamide (TAF) for 48 wk in patients with chronic hepatitis B (CHB). Our study found that TMF is as effective as TAF in treating CHB and has comparable safety profiles. In addition, TAF may cause deterioration of lipid profiles. These results suggest that TMF may be a viable alternative to TAF for CHB treatment.

Citation: Peng WT, Jiang C, Yang FL, Zhou NQ, Chen KY, Liu JQ, Peng SF, Fu L. Tenofovir amibufenamide *vs* tenofovir alafenamide for treating chronic hepatitis B: A real-world study. *World J Gastroenterol* 2023; 29(44): 5907-5918
URL: https://www.wjgnet.com/1007-9327/full/v29/i44/5907.htm
DOI: https://dx.doi.org/10.3748/wjg.v29.i44.5907

INTRODUCTION

Hepatitis B virus (HBV) infection represents a significant economic and health burden worldwide. As of 2019, over 1.5 million preventable new infections continue to occur annually, and there are approximately 296 million people living with chronic HBV infection, resulting in over 820,000 deaths annually due to liver cirrhosis and hepatocellular carcinoma (HCC)[1]. Achieving complete suppression of HBV in a safe and effective manner is crucial for preventing HBV-related adverse health events[2]. Consequently, efforts in this regard have primarily focused on antiviral treatment over the past decades. Current international guidelines recommend as first-line treatments newer antiviral agents with a high genetic barrier to HBV mutation, such as entecavir, tenofovir (TFV) disoproxil fumarate (TDF) and tenofovir alafenamide (TAF) [3-5]. Previous studies have shown that these drugs are safe and effective in treating chronic hepatitis B (CHB). However, long-term use of TDF leads to high levels of circulating TFV, resulting in kidney and bone toxicity, particularly in aging populations[6]. TAF, a TFV prodrug, is converted into the active form of TFV diphosphate *in vivo*, similar to TDF. At a dose of ≤ 25 mg, TAF reduces the total body exposure of TFV by more than 90%[7]. The correlativity study demonstrated that TAF, with its low concentration of TFV in the circulation, reduces the drug load on the kidneys and bones, thereby improving their safety[8].

Currently, tenofovir amibufenamide (TMF) is recommended as the fourth nucleoside analog for first-line treatment of CHB in mainland China[9]. TMF, another prodrug of TFV, is produced by ProTide technology and features an additional methyl group compared to TAF. This extra methyl group may enhance TMF's stability in peripheral blood and facilitate intracellular conversion[10]. *In vitro* studies have shown that TMF has a lower EC_{50} in HepG2.2.15 cells than TAF and TDF [11]. In randomized clinical trials and prospective clinical studies with treatment durations of 48 and 96 wk, TMF was found to be similarly effective in viral suppression to TDF, but with significantly less bone and renal toxicity[12,13]. TMF was approved in June 2021 and was included in the 2021 China National Reimbursement Drug List for CHB treatment.

Due to the recent introduction of TMF in the Chinese market and the limited real-world research data for the Chinese population, there is currently a knowledge gap regarding the drug's safety and efficacy. Therefore, we conducted this clinical study to assess the safety and effectiveness of TMF in treating patients with CHB in China.

MATERIALS AND METHODS

Study design and patient selection

In this retrospective study, we enrolled a total of 587 patients aged 18 and above who had been HBsAg positive for more than 6 mo. These patients were treated at Xiangya Hospital of Central South University between July 2021 and April 2022. Patients were excluded if they met any of the following criteria: (1) Concomitant with other liver diseases, such as alcoholic liver disease, nonalcoholic fatty liver disease, autoimmune liver disease, drug-induced liver injury, hepatolenticular degeneration, or other viral infections [hepatitis A, C, and E virus or human immunodeficiency virus (HIV)]; (2) pregnant or lactating women; (3) concomitant with malignant tumors or other serious diseases affecting survival time; (4) added or changed to other antiviral drugs during treatment; and (5) patients with missing data. Of the enrolled patients, 215 were included in the final analysis and were divided into two groups based on their drug selection: The TMF group and the TAF group.

The study protocol was approved by the Medical Ethics Committee of Xiangya Hospital Central South University (approval No. 202303047).

Treatment and follow-up

During the study period, all patients received anti-HBV treatment with 25 mg of TMF (Hansoh Pharmaceuticals Co., Ltd, Jiangsu, China) or 25 mg of TAF (Gilead Sciences, Inc.) once daily immediately after diagnosis of CHB. Additionally, liver protection drugs were used according to the needs of the disease as prescribed by clinicians. Clinical results and related indicators were collected for each participant during the 48-week follow-up period. These parameters were recorded at baseline, approximately at week 24, and again at week 48.

The efficacy endpoint at week 48 was defined as the proportion of patients achieving a virological response (VR), which is characterized by a reduction in serum HBV DNA levels to less than 10 IU/mL, as measured by the real-time polymerase chain reaction method. Additionally, a pre-specified safety outcome included the percentage change in renal function markers and lipid profiles at weeks 24 and 48 in comparison with the baseline values.

Data collection

Clinical and laboratory data were collected during hospitalization, including clinical characteristics, routine blood test results [including white blood cells (WBC) and platelets (PLT)], liver function tests [including albumin, globulin, total bilirubin (TBIL), direct bilirubin (DBIL), alanine aminotransferase (ALT), and aspartate aminotransferase (AST)], renal function tests [including serum creatinine (Cr), blood urea nitrogen (BUN), and estimated glomerular filtration rate (eGFR)], HBV DNA quantification, serological biomarkers, blood lipids [including triglycerides, total cholesterol (TC), high-density lipoprotein (HDL), and low-density lipoprotein (LDL)], serum phosphorus, alpha-fetoprotein (AFP), and liver stiffness measurement (LSM). The model for fibrosis 4 (FIB-4) score was calculated using the following formula[14]: FIB-4 = age [(year) × AST (U/L)] /[(PLT (10(9)/L) × [ALT (U/L) (1/2)]. In our study, ultrasound examinations were employed to diagnose liver cirrhosis in patients. Low-level viremia (LLV) was characterized as either persistent or intermittent detection of HBV DNA at levels below 2000 IU/mL, with a detection threshold of 10 IU/mL, following 48 wk of antiviral therapy.

Statistical analyses

The sample size for this study was calculated using G Power version 3.1.9.2 (Heinrich-Heine-Universität Düsseldorf). We predetermined the effect size f to range between 0.1 (small) and 0.4 (large), with a type I error rate (alpha) of 0.05 and a power of 0.8, considering two independent groups: TMF and TAF. Employing a one-way ANOVA model, the estimated sample size necessary varied from 84 for a large effect size to 788 for a small effect size. We ultimately recruited 215 participants for the study.

Statistical analyses were performed using SPSS for Windows, version 25.0. Continuous variables were reported as mean ± SD or median (interquartile range), while categorical variables were reported as percentages. The Student *t*-test and rank sum test were used to compare continuous variables, while the chi-squared test was used for categorical variables. All statistical tests were two-sided, and a P-value < 0.05 was considered statistically significant.

RESULTS

Baseline characteristics of the study population

A total of 587 patients with CHB were identified at our hospital between April 2022 and December 2021, of which 372 patients were excluded for various reasons (Figure 1). The final study population consisted of 215 patients, with 106 patients receiving TMF treatment and 109 patients receiving TAF treatment. The mean age of the study population was 40.57 ± 10.54 years, with 145 (67.74%) male patients. The mean LSM using FibroScan was 10.43 ± 3.99, and 42 (19.53%) of patients were diagnosed with cirrhosis. As shown in Table 1, there were no significant differences in baseline characteristics between the two treatment groups, including age, gender proportion, underlying disease, serum Cr, eGFR, BUN, albumin, globulin, AST, ALT, TBIL, DBIL, AFP, blood phosphorus, WBC, PLT, LSM, and FIB-4 score (all P > 0.05). These findings suggest that the two treatment groups were comparable.

Safety

During the 48-wk follow-up period, no significant drug-related adverse reactions were observed with either oral antiviral drug.

VRs

At week 48, the rate of undetectable HBV DNA (HBV DNA < 10 IU/mL) was slightly higher in the TMF treatment group (78.57%), compared to the TAF group (78.65%), although the difference was not statistically significant (Figure 2A). Similarly, the VR rates were similar in both treatment groups for patients with LLV (P > 0.05) (Figure 2B). Among the hepatitis B e antigen (HBeAg)-positive population, 74.36% of patients receiving TMF and 76.09% receiving TAF achieved HBV DNA less than 10 IU/mL (Figure 2C). In the HBeAg-negative population, 82.22% and 81.40% of patients in the TMF and TAF groups, respectively, achieved HBV DNA less than 10 IU/mL (Figure 2D).

The carrying capacity of HBV DNA decreased from 3.96 ± 2.18 to 2.13 ± 0.84 Log10 (IU/mL) in the TMF group and from 4.55 ± 2.31 to 2.35 ± 1.33 Log10 (IU/mL) in the TAF group (Figure 3A). While the TMF group showed a similar VR

Table 1 Baseline characteristics of the study population, *n* (%)

Variable	TMF group 25 mg (*n* = 106)	TAF group 25 mg (*n* = 109)	*P* value
Male	71 (66.98)	74 (67.89)	0.887
Age (yr)	40.96 ± 11.25	40.19 ± 9.84	0.707
Routine blood test			
WBC (× 10^9/L)	5.59 ± 1.64	5.59 ± 1.49	0.792
PLT (× 10^9/L)	193.97 ± 67.44	181.98 ± 68.63	0.218
Liver function			
Albumin (g/L)	45.57 ± 3.64	45.46 ± 3.59	0.746
Globulin (g/L)	29.32 ± 3.66	29.49 ± 3.70	0.617
TBIL (μmol/L)	4.55 (3.70, 5.90)	4.75 (2.20, 18.78)	0.070
DBIL (μmol/L)	2.50 (1.50, 3.90)	5.85 (4.10, 8.33)	0.152
ALT (U/L)	28.30 (20.10, 46.70)	32.40 (22.35, 49.60)	0.203
AST (U/L)	30.50 (24.90, 39.00)	30.00 (24.83, 40.80)	0.740
Kidney function			
BUN (mmol/L)	4.75 (3.99, 6.11)	4.88 (4.22, 5.70)	0.856
Creatinine (μmol/L)	79.50 (66.05, 91.00)	83.30 (73.00, 93.90)	0.177
eGFR (ml/min/1.73 m^2)	90.58 (79.84, 103.80)	97.19 (87.335, 106.38)	0.180
Viral load			
HBV DNA < 10 IU/mL	34 (32.08)	44 (40.37)	0.206
HBeAg positive	39 (36.79)	46 (42.20)	0.417
Blood lipid			
Triglycerides (mmol/L)	1.57 ± 0.82	1.65 ± 1.19	0.719
Total cholesterol (mg/dl)	4.83 ± 1.09	4.30 ± 1.54	0.173
HDL	1.18 ± 0.21	1.10 ± 0.14	0.341
LDL	3.19 ± 0.91	3.20 ± 0.94	0.877
Phosphorus (mmol/L)	1.64 ± 3.84	1.05 ± 0.44	0.958
AFP (ng/mL)	5.19 ± 8.90	5.24 ± 7.89	0.167
LSM (Kpa)	10.17 ± 4.41	10.94 ± 3.37	0.108
FIB-4 score	1.15 (0.75, 1.77)	1.27 (0.87, 2.03)	0.552
Underlying diseases			
Diabetes	5 (4.72)	6 (5.50)	0.793
Cirrhosis	23 (21.70)	19 (17.43)	0.430
Decompensated cirrhosis	4 (3.77)	4 (3.67)	0.968
Hepatocellular carcinoma	2 (1.89)	3 (2.75)	0.674
NAFLD	26 (24.53)	28 (25.69)	0.845
Treatment naïve	63 (59.43)	61 (55.96)	0.607

Data are frequency (%), median M (P25, P75), or mean ± SD deviation. TMF: Tenofovir amibufenamide; TAF: Tenofovir alafenamide; WBCs: White blood cells; PLTs: Platelets; ALT: Alanine aminotransferase; AST: Aspartate aminotransferase; TBIL: Total bilirubin; DBIL: Direct bilirubin; BUN: Blood urea nitrogen; eGFR: Estimated glomerular filtration rate; P: Phosphorus; HDL: High-density lipoprotein; LDL: Low-density lipoprotein; AFP: Alpha fetoprotein; LSM: Liver stiffness measurement; HBV: Hepatitis B virus; HBeAg: Hepatitis B e antigen; NAFLD: Nonalcoholic fatty liver disease; FIB-4: Fibrosis-4.

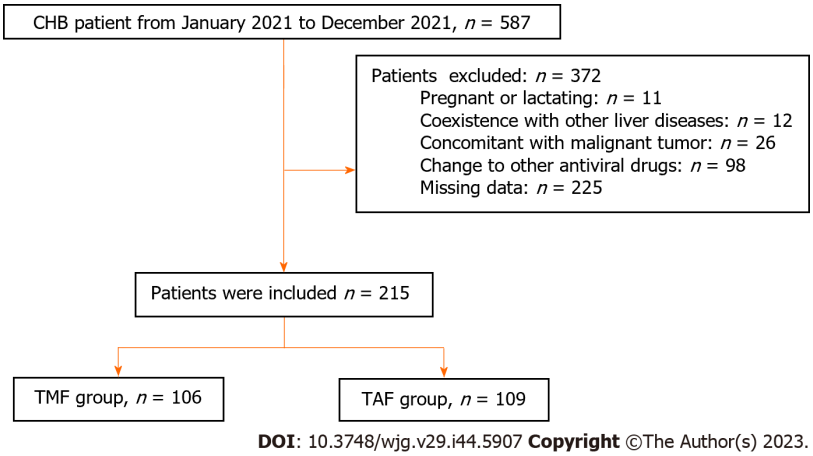

DOI: 10.3748/wjg.v29.i44.5907 **Copyright** ©The Author(s) 2023.

Figure 1 Flow chart of the patient inclusion process. CHB: Chronic hepatitis B; TMF: Tenofovir amibufenamide; TAF: Tenofovir alafenamide.

within 48 wk compared with the TAF group, there was no statistical difference between the two groups (Figure 3B).

On-treatment ALT normalization

The ALT normalization rate in the TMF group was 66.04% and 78.30% at 24 and 48 wk, respectively. In the TAF group, the ALT normalization rate was 55.96% and 74.31% at 24 and 48 wk, respectively. Although the ALT normalization rate in the TAF group showed a higher trend compared to the TMF group from baseline to 48 wk, this difference did not reach statistical significance (Figure 3C). As shown in Figure 3D, both TMF and TAF groups had similar trends in ALT changes during the 48-wk period.

Changes in renal function in TMF and TAF groups

After 48 wk of treatment, Cr levels in the TMF group decreased from 79.50 (66.05, 91.00) μmol/L to 72.00 (63.00, 83.00) μmol/L, and that in the TAF group decreased from 83.30 (73.00, 93.90) μmol/L to 78.10 (61.00, 90.70) μmol/L. Meanwhile, eGFR in both groups increased slightly. However, there was no significant difference in the changes of Cr and eGFR between the two groups within 48 wk (Table 2).

Changes in blood lipids

In this study, plasma lipids consisted primarily included triglycerides, TC, LDL, and HDL. There was no significant change observed in the triglycerides, HDL, and LDL levels at 48 wk. Specifically, in the TMF group, the TC levels demonstrated a mean change of -0.23 ± 0.71 mg/dL at the 48-wk mark (P = 0.822) (Table 3). Conversely, in the TAF group, TC values exhibited a continuous rise from 4.30 ± 1.54 mg/dL at baseline to 5.2 ± 0.99 mg/dL at week 48 (P = 0.045) (Table 3).

Antiviral therapy in patients with liver cirrhosis

In our study, 23 patients in the TMF group and 19 patients in the TAF group had liver cirrhosis. The complete VR rates after 48 wk of treatment were 78.26% in the TMF group and 73.68% in the TAF group, with no significant difference between the two groups (Figure 4A). The normalization rate of ALT was similar in the two groups after 48 wk of treatment (Figure 4B). Renal safety profiles for TMF were similar to those observed for TAF at the 48-wk mark (Supplementary Table 1).

The regression of liver fibrosis was evaluated using FIB-4 scores and LSM in this study (Supplementary Table 2). Liver stiffness was measured using FibroScan. The LSM of cirrhotic patients in the TAF group decreased from baseline to the 48th week (P > 0.05). For the TMF cohort, both LSM and FIB-4 scores demonstrated a marginal increase after 48 wk of treatment; however, these differences did not reach statistical significance. In patients with liver cirrhosis, there was no significant difference between the two groups in the reduction of LSM from baseline level at the 48th week. However, the decrease in FIB-4 in patients with TAF was significantly greater than in patients with TMF [0.29 (0.06, 0.77) *vs*. -0.43 (1.16, -0.08); P = 0.001].

DISCUSSION

TFV ester prodrugs, a class of nucleotide analogs (NAs), are the first-line clinical anti-HBV drugs with potent antiviral efficacy, low resistance rates, and high safety. Various types of ester prodrugs of TFV have been designed in recent decades to improve its antiviral activity and reduce its adverse reactions[15,16].

TMF, the third commercially available TFV ester prodrug, was developed by modifying TAF through the addition of a single methyl group. It received approval from China's National Medical Products Administration for the treatment of HBV infection in 2021. Clinical trials have demonstrated that TMF possesses superior plasma stability compared to TDF

Table 2 Comparison of changes in serum creatinine and estimated glomerular filtration rate between the tenofovir amibufenamide and tenofovir alafenamide groups.

	TMF group (*n* = 106)	TAF group (*n* = 109)	*P* value
Creatinine (μmol/L)			
Before treatment	79.50 (66.05, 91.00)	83.30 (73.00, 93.90)	0.856
After 48 wk	72.00 (63.00, 83.00)	78.10 (61.00, 90.70)	0.194
Reduction	4.00 (-19.65, 19.50)	3.37 (-7.96, 26.13)	0.728
P (baseline *vs*. 48 wk)	0.053	0.105	
eGFR (mL/min/1.73 m^2)			
Before treatment	90.58 (79.84, 103.80)	97.19 (87.35, 106.38)	0.180
After 48 wk	106.37 (94.58, 113.15)	105.17 (88.15,129.56)	0.617
Reduction	-2.22 (-9.72, 16.75)	-4.17 (-227.89, 7.67)	0.093
P (baseline *vs*. 48 wk)	0.301	0.108	

Data are median M (P25, P75). TMF: Tenofovir amibufenamide; TAF: Tenofovir alafenamide; eGFR: Estimated glomerular filtration rate.

Table 3 Changes in blood lipid profiles between the tenofovir amibufenamide and tenofovir alafenamide groups

	TMF group (*n* = 106)	TAF group (*n* = 109)	*P* value
Triglycerides (mmol/L)			
Before treatment	1.57 ± 0.82	1.65 ± 1.19	0.719
After 48 wk	2.16 ± 1.34	1.81 ± 0.87	0.931
Reduction	-0.64 ± 1.02	0.19 ± 0.31	0.103
P (baseline *vs*. 48 wk)	0.099	0.359	
Total cholesterol (mg/dl)			
Before treatment	4.83 ± 1.09	4.30 ± 1.54	0.173
After 48 wk	4.82 ± 1.52	5.20 ± 0.99	0.581
Reduction	-0.23 ± 0.95	-1.02 ± 1.18	0.182
P (baseline *vs*. 48 wk)	0.822	0.045	
HDL (mmol/L)			
Before treatment	1.18 ± 0.21	1.10 ± 0.14	0.341
After 48 wk	1.43 ± 0.74	1.23 ± 0.31	0.977
Reduction	-0.23 ± 0.71	-0.09 ± 0.16	0.672
P (baseline *vs*. 48 wk)	0.430	0.225	
LDL (mmol/L)			
Before treatment	3.19 ± 0.91	3.20 ± 0.94	0.877
After 48 wk	3.15 ± 1.18	3.40 ± 0.71	0.428
Reduction	0.10 ± 0.94	-0.04 ± 0.9	0.791
P (baseline *vs*. 48 wk)	0.807	0.332	

Data are median M (P25, P75). TMF: Tenofovir amibufenamide; TAF: Tenofovir alafenamide; HDL: High-density lipoprotein; LDL: Low-density lipoprotein.

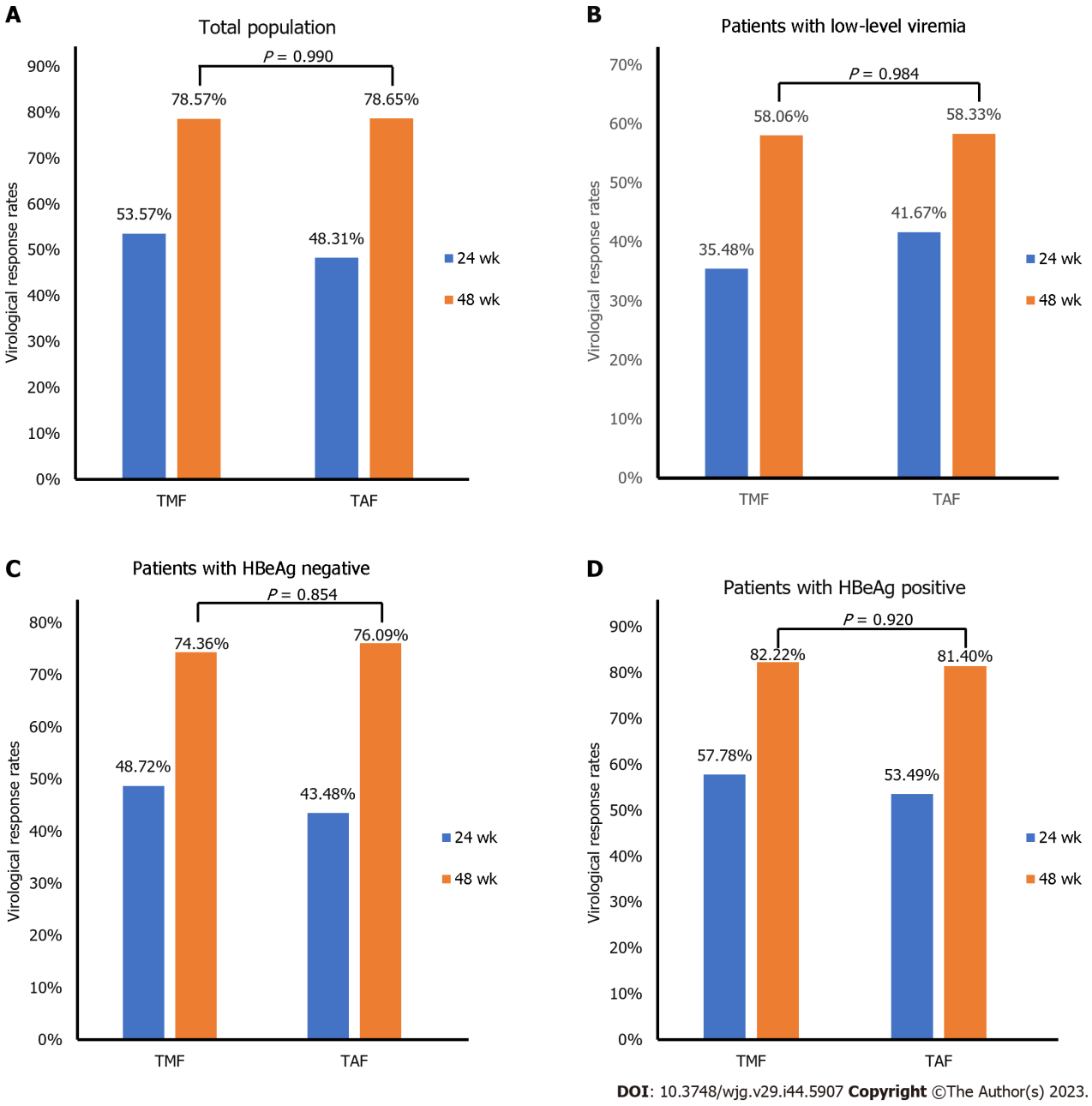

DOI: 10.3748/wjg.v29.i44.5907 **Copyright** ©The Author(s) 2023.

Figure 2 Comparison of virological response rates between tenofovir amibufenamide and tenofovir alafenamide. A: Virological response (VR) rates of tenofovir amibufenamide (TMF) and tenofovir alafenamide (TAF) groups at 24 and 48 wk; B: VR rates of TMF and TAF groups at 24 and 48 wk with low-level viremia; C: VR rates of TMF and TAF groups at 24 and 48 wk with hepatitis B e antigen (HBeAg) negative; D: VR rates of TMF and TAF groups at 24 and 48 wk with HBeAg positive. TMF: Tenofovir amibufenamide; TAF: Tenofovir alafenamide; VR: Virological response; HBeAg: Hepatitis B e antigen.

and exhibits a similar potency in inhibiting HBV, even when administered at a mere 1/30 of TDF's dosage[17]. Another study, however, revealed that both TMF and TAF displayed enhanced anti-HBV activity and corrective effects on liver biochemical metabolism disturbances relative to TDF *in vitro* and *in vivo*, with TMF exhibiting marginally superior performance to TAF[11]. Given the relatively recent introduction of TMF to the Chinese market and the scarcity of real-world research data for the Chinese population, limited information exists regarding its safety and efficacy.

Consequently, we conducted a real-world investigation to assess the safety and effectiveness of TMF in treating patients with CHB in Southern China. Our findings indicated that, apart from a few mild side effects, TMF did not induce any serious reactions, thus establishing its safety for the treatment of CHB.

In our present study, we observed that the antiviral effectiveness of the TMF and TAF treatment groups was comparable across various patient subpopulations, including the general population, those with LLV, and HBeAg-positive and HBeAg-negative individuals. Throughout the 48-wk TMF treatment duration, no instances of virological breakthrough were encountered. In the 48th week, prior research demonstrated the sustained non-inferiority of VR rates between TMF and TDF treatments, regardless of HBeAg status[13]. Another study corroborated that TAF maintained its efficacy in inhibiting HBV replication relative to TDF, with no emergence of virologic resistance[18]. These findings align with our results, substantiating the equivalent antiviral potency of TMF and TAF in patients with CHB following 48 wk of

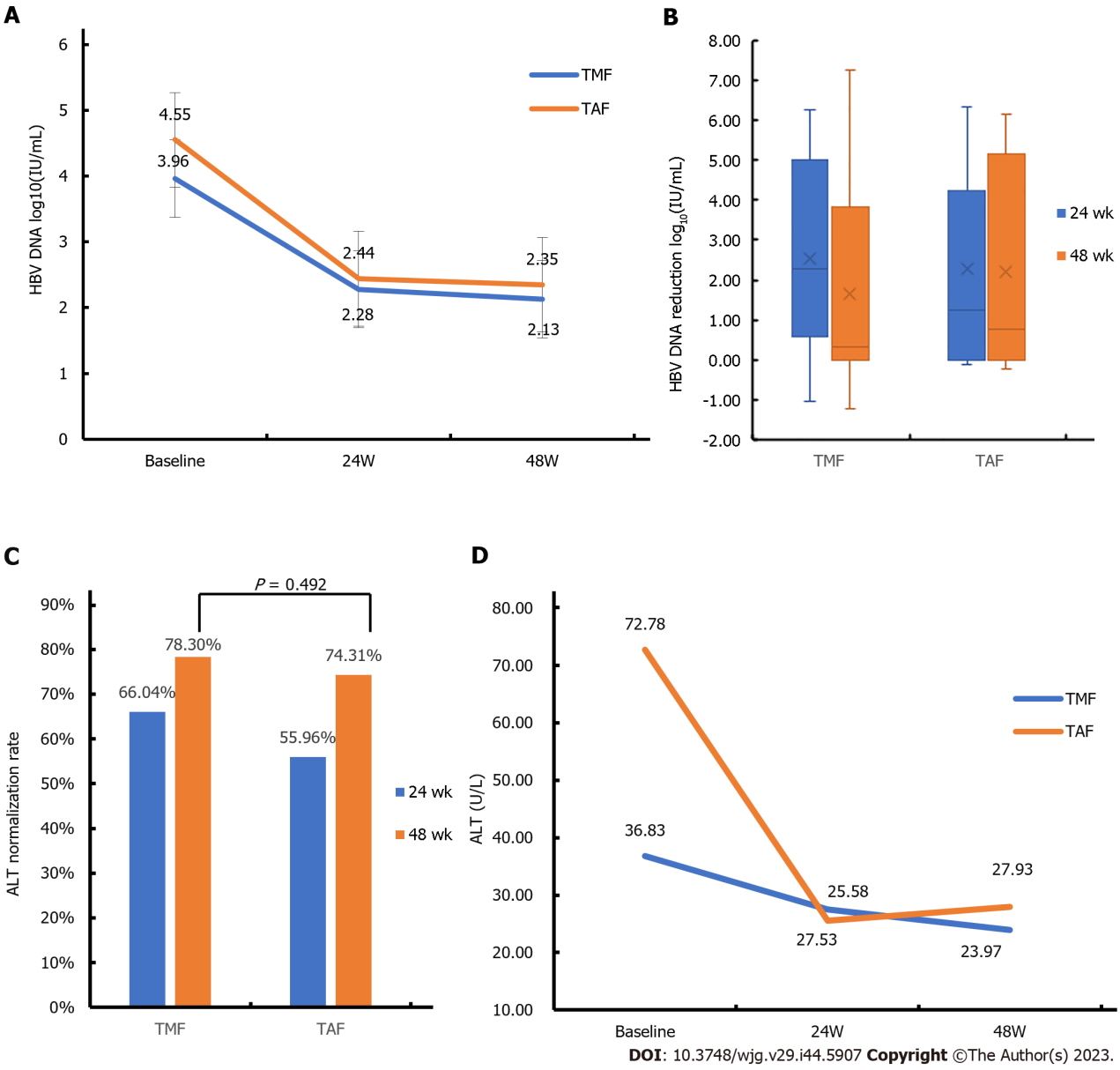

DOI: 10.3748/wjg.v29.i44.5907

Figure 3 Comparison of changes in hepatitis B virus DNA level, the ratios of alanine aminotransferase normalization and alanine aminotransferase level between the tenofovir amibufenamide and tenofovir alafenamide groups. A: Hepatitis B virus (HBV) DNA levels at baseline week, 24 wk and 48 wk in the tenofovir amibufenamide (TMF) and tenofovir alafenamide (TAF) groups; B: HBV-DNA reduction from 24 wk to 48 wk in the TMF and TAF groups; C: Alanine aminotransferase (ALT) normalization rate of TMF and TAF groups at 24 and 48 wk; D: ALT levels at baseline week, 24 wk and 48 wk in the TMF and TAF groups. TMF: Tenofovir amibufenamide; TAF: Tenofovir alafenamide; ALT: Alanine aminotransferase; HBV: Hepatitis B virus.

therapy.

The significance of achieving on-treatment ALT normalization in CHB patients has been emphasized in recent literature. A large-scale observational study revealed that patients who attained normal on-treatment ALT in the first 48 wk of antiviral treatment exhibited a reduced risk of hepatic events[19]. Liu *et al*[13] reported a notably higher ALT normalization rate for TMF-treated patients compared to those receiving TDF. Concurrently, Agarwal *et al*[18] observed a significantly greater ALT normalization rate among CHB patients treated with TAF relative to TDF recipients. In contrast, our study established that, at week 48, the rate of ALT normalization in the TMF group was comparable to that in the TAF group. These findings, taken together with the virological inhibition rate and biochemical response, confirm the equivalent efficacy of TMF and TAF in the treatment of CHB patients over a 48-wk period.

Prior research has demonstrated the nephrotoxic and osteotoxic effects of TFV[20], emphasizing the need to consider nephrotoxicity when developing TFV prodrugs. Renal impairment associated with TDF primarily arises from proximal tubulopathy[21], with the ensuing tubular dysfunction evidenced by increased serum Cr and reduced serum phosphate levels. The superior renal safety profile of TAF, compared to TDF, is attributable to the primary elimination of TAF through fecal excretion, with less than 1% excreted renally[22].

Since all NAs are eliminated *via* the kidneys, it is crucial for clinicians to monitor for progression of renal dysfunction [23]. The ability of TAF to reduce the risk of renal damage renders it a favorable option for CHB patients who have potential or associated risk factors for renal damage. Studies have confirmed that TAF can continuously enhance renal

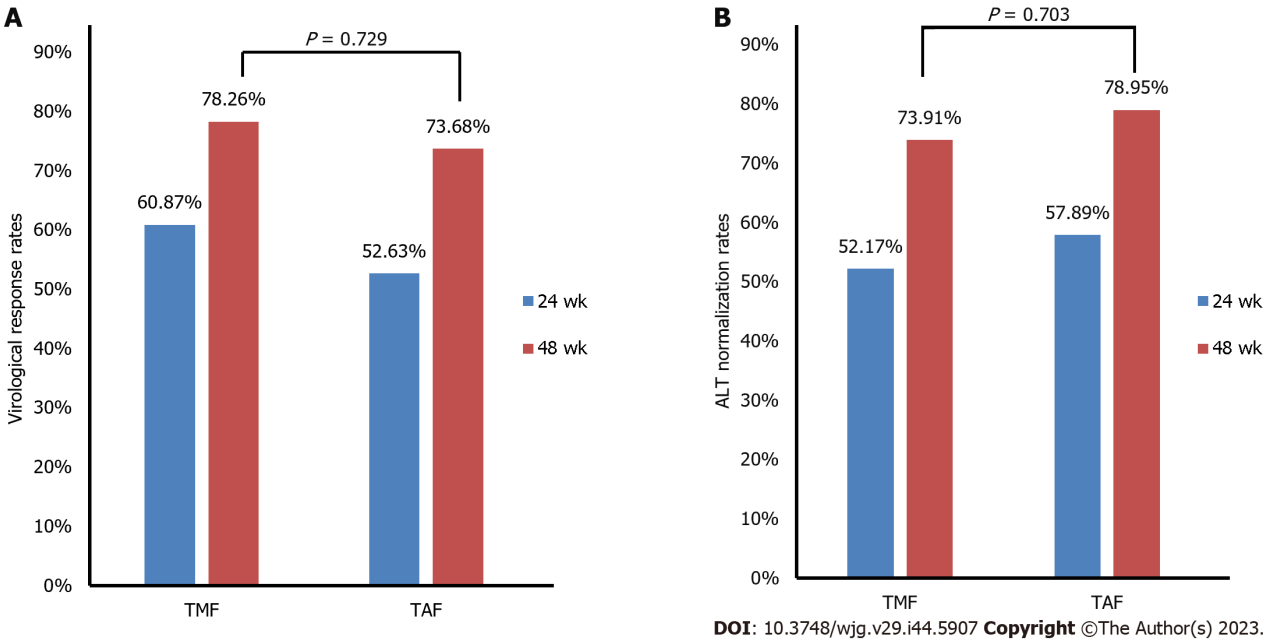

DOI: 10.3748/wjg.v29.i44.5907

Figure 4 Comparison of the virological response rate and the alanine aminotransferase normalization rate between tenofovir amibufenamide and tenofovir alafenamide groups in patients with cirrhosis. A: Virological response rates of tenofovir amibufenamide (TMF) and tenofovir alafenamide (TAF) groups at 24 and 48 wk; B: Alanine aminotransferase normalization rate of TMF and TAF groups at 24 and 48 wk. TMF: Tenofovir amibufenamide; TAF: Tenofovir alafenamide; ALT: Alanine aminotransferase.

function and maintain bone safety in patients with CHB[7,24]. Our findings indicate that the renal safety profile of the TMF group is comparable to that of the TAF group, suggesting that TMF could emerge as a novel therapeutic option for CHB patients, particularly those with an elevated risk of renal damage.

TDF and TAF are both efficacious nucleoside analogs, with TAF being preferred over TDF due to its lower incidence of renal and bone toxicities. However, there is evidence indicating a worsening of the lipid profile following the transition from TDF- to TAF-containing antiretroviral regimens in patients with HIV, as documented in clinical trials and observational studies[25,26]. Given the association between dyslipidemia, cardiovascular disease, and metabolic/non-alcoholic fatty liver disease-which may elevate the risk of HCC-it becomes imperative to determine whether TAF monotherapy alone adversely affects lipid profiles in CHB patients. This study compared lipid profile alterations in a cohort of CHB patients managed with either TMF or TAF over a 48-wk observation period. The findings indicated a significant increase in serum TC levels in the TAF group (4.3 ± 1.54 *vs*. 5.2 ± 0.99, mg/dL, $P < 0.05$) compared to the TMF cohort (4.83 ± 1.09 *vs* . 4.82 ± 1.52 mg/dL, $P > 0.05$). Therefore, this study suggests that TAF might contribute to the worsening of lipid profiles, whereas TMF appears to have a negligible impact on serum lipids. These conclusions are in contrast with the findings presented by Li *et al*[27] Despite these insights, the underlying mechanism by which TFV affects serum lipids remains to be elucidated. Further research is essential to fully understand this aspect. Nevertheless, physicians should monitor lipid levels vigilantly in patients at the higher end of the normal range when prescribing TAF.

Chronic HBV infection constitutes the primary cause of liver cirrhosis in China and may progress to decompensated liver cirrhosis and primary liver cancer, severely impacting the quality of life of patients. An increasing body of evidence indicates that sustained and effective antiviral therapy can reverse liver fibrosis and cirrhosis[4,28]. Therefore, our study evaluated the efficacy and safety of treatment in patients with cirrhosis.

In cirrhotic patients, the FIB-4 score reduction observed in the TAF cohort was significantly more pronounced than that in the TMF cohort. This could be partly attributed to the marginally higher ALT normalization rate associated with TAF treatment and the limited sample size of both groups. In contrast, no significant difference was discerned in the LSM values between the TMF and TAF groups. However, implications of these findings are not entirely clear, as it remains uncertain if the changes reflect true fibrosis regression or merely a biochemical variation. The observed decline in FIB-4 scores is noteworthy, warranting further research to ascertain if such biochemical alterations correspond to actual histological improvements. Where appropriate, liver tissue biopsies should be considered for conclusive evidence.

Our study is not without limitations. Firstly, the follow-up period of 48 wk may be insufficient to fully capture the antiviral effect, and a more extended timeframe would provide a clearer representation. Secondly, serum Cr and eGFR were employed as markers of renal function in this study, but incorporating indicators reflecting renal tubular function could bolster the study's reliability based on established clinical pharmacological research. Thirdly, the applicability of our findings is restricted, as TMF is not available worldwide. Fourthly, our study did not include data on bone health, such as that obtained *via* DEXA scans, and relied on serum Cr as a surrogate marker for renal function. Lastly, as a single-center retrospective study, future multi-center investigations with larger cohort and longer follow-up durations for CHB patients are essential to corroborate our findings.

CONCLUSION

In summary, our results indicate that TMF demonstrates comparable efficacy to TAF in terms of VR, ALT normalization rate, and renal safety among CHB patients in China. Nevertheless, TMF has an advantage over TAF in patients with hyperlipidemia. Additionally, TMF exhibits effectiveness and safety in cirrhotic patients. Collectively, these results suggest that TMF presents a viable therapeutic alternative for patients with CHB.

ARTICLE HIGHLIGHTS

Research background

Hepatitis B virus (HBV) infection may lead to cirrhosis and hepatocellular carcinoma, and the exploration of optimal antiviral drugs can improve patient prognosis.

Research motivation

Tenofovir amibufenamide (TMF) is a new antiviral drug with limited research on its safety and efficacy. Our research may provide new evidence for the treatment of patients with HBV infection.

Research objectives

To compare the efficacy and safety of TMF and tenofovir alafenamide (TAF) for 48 wk in patients with chronic hepatitis B (CHB). The primary outcome was the proportion of virological responses (VR) at 48 wk. Additional outcomes included the changes of renal function and lipid characteristic markers at weeks 24 and 48 compared to baseline.

Research methods

In this retrospective study, we enrolled a total of 587 patients who had been HBsAg positive for more than 6 mo. Of the enrolled patients, 215 were included in the final analysis and were divided into two groups based on their drug selection: The TMF group and the TAF group.

Research results

The VR rates of the TMF group and TAF group were comparable at 24 and 48 wk of treatment ($P > 0.05$). In patients with low-level viremia, hepatitis B e antigen (HBeAg) positive, and HBeAg negative, their VR rates are also similar. The alanine transaminase (ALT) normalization rate and renal safety of TMF are also comparable to those of TAF. However, total cholesterol levels increased in the TAF group ($P = 0.045$). In patients with liver cirrhosis, the renal safety, VR, and ALT normalization rate were comparable between the TMF group and the TAF group.

Research conclusions

TMF is as effective as TAF in treating CHB and has considerable safety. Moreover, TMF may have more advantages in lipid profile compared to TAF.

Research perspectives

The design and research of new nucleotide analogs should continue in the hope of achieving clinical cure of hepatitis B infection as soon as possible.

FOOTNOTES

Author contributions: Fu L designed the research and supervised the study; Peng WT, Chen KY, Zhou NQ, and Yang FL collected the clinical data; Peng WT, Liu JQ, and Jiang C performed the experiments and wrote the manuscript; Peng SF assisted in experiments; all authors critically reviewed the final manuscript.

Supported by National Natural Science Foundation of China, No. 82170640, and No. 81974080; Natural Science Foundation of Hunan Province, No. 2022JJ30954.

Institutional review board statement: This study was reviewed and approved by the Ethics Committee of the Xiangya Hospital Central South University.

Informed consent statement: The study is a retrospective study that will maximize the protection of the rights and privacy of the study participants, and the content of the study and the results of the study do not involve personal privacy and commercial interests, exempt from informed consent.

Conflict-of-interest statement: We have no financial relationships to disclose.

Data sharing statement: No additional data are available.

Country/Territory of origin: China

ORCID number: Wen-Ting Peng 0000-0002-9072-1332; Chuan Jiang 0000-0003-2022-5242; Shi-Fang Peng 0000-0003-4229-0299; Lei Fu 0000-0001-7550-1254.

S-Editor: Qu XL
L-Editor: A
P-Editor: Chen YX

REFERENCES

1 Hepatitis B Fact Sheet. World Health Organization. 2021. Available from: https://www.who.int/en/news-room/fact-sheets/detail/hepatitis-b
2 **Liaw YF**, Sung JJ, Chow WC, Farrell G, Lee CZ, Yuen H, Tanwandee T, Tao QM, Shue K, Keene ON, Dixon JS, Gray DF, Sabbat J; Cirrhosis Asian Lamivudine Multicentre Study Group. Lamivudine for patients with chronic hepatitis B and advanced liver disease. *N Engl J Med* 2004; **351**: 1521-1531 [PMID: 15470215 DOI: 10.1056/NEJMoa033364]
3 **European Association for the Study of the Liver**. EASL 2017 Clinical Practice Guidelines on the management of hepatitis B virus infection. *J Hepatol* 2017; **67**: 370-398 [PMID: 28427875 DOI: 10.1016/j.jhep.2017.03.021]
4 **Sarin SK**, Kumar M, Lau GK, Abbas Z, Chan HL, Chen CJ, Chen DS, Chen HL, Chen PJ, Chien RN, Dokmeci AK, Gane E, Hou JL, Jafri W, Jia J, Kim JH, Lai CL, Lee HC, Lim SG, Liu CJ, Locarnini S, Al Mahtab M, Mohamed R, Omata M, Park J, Piratvisuth T, Sharma BC, Sollano J, Wang FS, Wei L, Yuen MF, Zheng SS, Kao JH. Asian-Pacific clinical practice guidelines on the management of hepatitis B: a 2015 update. *Hepatol Int* 2016; **10**: 1-98 [PMID: 26563120 DOI: 10.1007/s12072-015-9675-4]
5 **Terrault NA**, Lok ASF, McMahon BJ, Chang KM, Hwang JP, Jonas MM, Brown RS Jr, Bzowej NH, Wong JB. Update on prevention, diagnosis, and treatment of chronic hepatitis B: AASLD 2018 hepatitis B guidance. *Hepatology* 2018; **67**: 1560-1599 [PMID: 29405329 DOI: 10.1002/hep.29800]
6 **Jung CY**, Kim HW, Ahn SH, Kim SU, Kim BS. Tenofovir is Associated With Higher Risk of Kidney Function Decline Than Entecavir in Patients With Chronic Hepatitis B. *Clin Gastroenterol Hepatol* 2022; **20**: 956-958.e2 [PMID: 34029751 DOI: 10.1016/j.cgh.2021.05.032]
7 **Chan HL**, Fung S, Seto WK, Chuang WL, Chen CY, Kim HJ, Hui AJ, Janssen HL, Chowdhury A, Tsang TY, Mehta R, Gane E, Flaherty JF, Massetto B, Gaggar A, Kitrinos KM, Lin L, Subramanian GM, McHutchison JG, Lim YS, Acharya SK, Agarwal K; GS-US-320-0110 Investigators. Tenofovir alafenamide versus tenofovir disoproxil fumarate for the treatment of HBeAg-positive chronic hepatitis B virus infection: a randomised, double-blind, phase 3, non-inferiority trial. *Lancet Gastroenterol Hepatol* 2016; **1**: 185-195 [PMID: 28404091 DOI: 10.1016/S2468-1253(16)30024-3]
8 **Murakami E**, Wang T, Park Y, Hao J, Lepist EI, Babusis D, Ray AS. Implications of efficient hepatic delivery by tenofovir alafenamide (GS-7340) for hepatitis B virus therapy. *Antimicrob Agents Chemother* 2015; **59**: 3563-3569 [PMID: 25870059 DOI: 10.1128/AAC.00128-15]
9 **Chinese Society of Hepatology**; Chinese Medical Association. [Expert opinion on expanding anti-HBV treatment for chronic hepatitis B]. *Zhonghua Gan Zang Bing Za Zhi* 2022; **30**: 131-136 [PMID: 35359064 DOI: 10.3760/cma.j.cn501113-20220209-00060]
10 **Mehellou Y**, Rattan HS, Balzarini J. The ProTide Prodrug Technology: From the Concept to the Clinic. *J Med Chem* 2018; **61**: 2211-2226 [PMID: 28792763 DOI: 10.1021/acs.jmedchem.7b00734]
11 **Hong X**, Cai Z, Zhou F, Jin X, Wang G, Ouyang B, Zhang J. Improved pharmacokinetics of tenofovir ester prodrugs strengthened the inhibition of HBV replication and the rebalance of hepatocellular metabolism in preclinical models. *Front Pharmacol* 2022; **13**: 932934 [PMID: 36105197 DOI: 10.3389/fphar.2022.932934]
12 **Liu Z**, Jin Q, Zhang Y, Gong G, Wu G, Yao L, Wen X, Gao Z, Huang Y, Yang D, Chen E, Mao Q, Lin S, Shang J, Gong H, Zhong L, Yin H, Wang F, Hu P, Xiao L, Li C, Wu Q, Sun C, Niu J, Hou J; TMF Study Group. Randomised clinical trial: 48 weeks of treatment with tenofovir amibufenamide versus tenofovir disoproxil fumarate for patients with chronic hepatitis B. *Aliment Pharmacol Ther* 2021; **54**: 1134-1149 [PMID: 34587302 DOI: 10.1111/apt.16611]
13 **Liu Z**, Jin Q, Zhang Y, Gong G, Wu G, Yao L, Wen X, Gao Z, Huang Y, Yang D, Chen E, Mao Q, Lin S, Shang J, Gong H, Zhong L, Yin H, Wang F, Hu P, Wu Q, Pan C, Jia W, Li C, Sun C, Niu J, Hou J; TMF Study Group. 96-Week Treatment of Tenofovir Amibufenamide and Tenofovir Disoproxil Fumarate in Chronic Hepatitis B Patients. *J Clin Transl Hepatol* 2023; **11**: 649-660 [PMID: 36969889 DOI: 10.14218/JCTH.2022.00058]
14 **Sterling RK**, Lissen E, Clumeck N, Sola R, Correa MC, Montaner J, S Sulkowski M, Torriani FJ, Dieterich DT, Thomas DL, Messinger D, Nelson M; APRICOT Clinical Investigators. Development of a simple noninvasive index to predict significant fibrosis in patients with HIV/HCV coinfection. *Hepatology* 2006; **43**: 1317-1325 [PMID: 16729309 DOI: 10.1002/hep.21178]
15 **Beadle JR**, Aldern KA, Zhang XQ, Valiaeva N, Hostetler KY, Schooley RT. Octadecyloxyethyl benzyl tenofovir: A novel tenofovir diester provides sustained intracellular levels of tenofovir diphosphate. *Antiviral Res* 2019; **171**: 104614 [PMID: 31550449 DOI: 10.1016/j.antiviral.2019.104614]
16 **Wang A**, Wu S, Tao Z, Li X, Lv K, Ma C, Li Y, Li L, Liu M. Design, Synthesis, and Anti-HBV Activity of New Bis(l-amino acid) Ester Tenofovir Prodrugs. *ACS Med Chem Lett* 2019; **10**: 991-995 [PMID: 31223460 DOI: 10.1021/acsmedchemlett.9b00184]
17 **Zhang H**, Hu Y, Wu M, Liu J, Zhu X, Li X, Chen H, Li C, Liu C, Niu J, Ding Y. Randomised clinical trial: safety, efficacy and pharmacokinetics of HS-10234 versus tenofovir for the treatment of chronic hepatitis B infection. *Aliment Pharmacol Ther* 2021; **53**: 243-252 [PMID: 33249630 DOI: 10.1111/apt.16196]
18 **Agarwal K**, Brunetto M, Seto WK, Lim YS, Fung S, Marcellin P, Ahn SH, Izumi N, Chuang WL, Bae H, Sharma M, Janssen HLA, Pan CQ,

Çelen MK, Furusyo N, Shalimar D, Yoon KT, Trinh H, Flaherty JF, Gaggar A, Lau AH, Cathcart AL, Lin L, Bhardwaj N, Suri V, Mani Subramanian G, Gane EJ, Buti M, Chan HLY; GS-US-320-0110; GS-US-320-0108 Investigators. 96 weeks treatment of tenofovir alafenamide vs. tenofovir disoproxil fumarate for hepatitis B virus infection. *J Hepatol* 2018; **68**: 672-681 [PMID: 29756595 DOI: 10.1016/j.jhep.2017.11.039]

19 **Wong GL**, Chan HL, Tse YK, Yip TC, Lam KL, Lui GC, Wong VW. Normal on-treatment ALT during antiviral treatment is associated with a lower risk of hepatic events in patients with chronic hepatitis B. *J Hepatol* 2018; **69**: 793-802 [PMID: 29758335 DOI: 10.1016/j.jhep.2018.05.009]

20 **Wong GL**, Seto WK, Wong VW, Yuen MF, Chan HL. Review article: long-term safety of oral anti-viral treatment for chronic hepatitis B. *Aliment Pharmacol Ther* 2018; **47**: 730-737 [PMID: 29359487 DOI: 10.1111/apt.14497]

21 **Samuels R**, Bayerri CR, Sayer JA, Price DA, Payne BAI. Tenofovir disoproxil fumarate-associated renal tubular dysfunction: noninvasive assessment of mitochondrial injury. *AIDS* 2017; **31**: 1297-1301 [PMID: 28323756 DOI: 10.1097/QAD.0000000000001466]

22 **Gilead Sciences**. Prescribing information for VEMLIDY (tenofovir alafenamide). Available from: https://www.gilead.com/-/media/files/pdfs/medicines/liver-disease/vemlidy/vemlidy_pi.pdf

23 **Lo AO**, Wong GL. Current developments in nucleoside/nucleotide analogues for hepatitis B. *Expert Rev Gastroenterol Hepatol* 2014; **8**: 607-622 [PMID: 24787673 DOI: 10.1586/17474124.2014.909724]

24 **Buti M**, Gane E, Seto WK, Chan HL, Chuang WL, Stepanova T, Hui AJ, Lim YS, Mehta R, Janssen HL, Acharya SK, Flaherty JF, Massetto B, Cathcart AL, Kim K, Gaggar A, Subramanian GM, McHutchison JG, Pan CQ, Brunetto M, Izumi N, Marcellin P; GS-US-320-0108 Investigators. Tenofovir alafenamide versus tenofovir disoproxil fumarate for the treatment of patients with HBeAg-negative chronic hepatitis B virus infection: a randomised, double-blind, phase 3, non-inferiority trial. *Lancet Gastroenterol Hepatol* 2016; **1**: 196-206 [PMID: 28404092 DOI: 10.1016/S2468-1253(16)30107-8]

25 **Kauppinen KJ**, Kivelä P, Sutinen J. Switching from Tenofovir Disoproxil Fumarate to Tenofovir Alafenamide Significantly Worsens the Lipid Profile in a Real-World Setting. *AIDS Patient Care STDS* 2019; **33**: 500-506 [PMID: 31742421 DOI: 10.1089/apc.2019.0236]

26 **Hagins D**, Orkin C, Daar ES, Mills A, Brinson C, DeJesus E, Post FA, Morales-Ramirez J, Thompson M, Osiyemi O, Rashbaum B, Stellbrink HJ, Martorell C, Liu H, Liu YP, Porter D, Collins SE, SenGupta D, Das M. Switching to coformulated rilpivirine (RPV), emtricitabine (FTC) and tenofovir alafenamide from either RPV, FTC and tenofovir disoproxil fumarate (TDF) or efavirenz, FTC and TDF: 96-week results from two randomized clinical trials. *HIV Med* 2018; **19**: 724-733 [PMID: 30101539 DOI: 10.1111/hiv.12664]

27 **Li L**, Zhou J, Li Y, Wang F, Zhang D, Wang M, Tao Y, Chen E. Effectiveness and safety of tenofovir amibufenamide and its comparison with tenofovir alafenamide in patients with chronic hepatitis B: results from a retrospective real-world study. *Front Pharmacol* 2023; **14**: 1165990 [PMID: 37324480 DOI: 10.3389/fphar.2023.1165990]

28 **Mokdad AA**, Lopez AD, Shahraz S, Lozano R, Mokdad AH, Stanaway J, Murray CJ, Naghavi M. Liver cirrhosis mortality in 187 countries between 1980 and 2010: a systematic analysis. *BMC Med* 2014; **12**: 145 [PMID: 25242656 DOI: 10.1186/s12916-014-0145-y]

World Journal of Gastroenterology

Submit a Manuscript: https://www.f6publishing.com

World J Gastroenterol 2023 November 28; 29(44): 5919-5934

DOI: 10.3748/wjg.v29.i44.5919

ISSN 1007-9327 (print) ISSN 2219-2840 (online)

ORIGINAL ARTICLE

Basic Study

Tousled-like kinase 1 promotes gastric cancer progression by regulating the tumor growth factor-beta signaling pathway

Ruo-Chuan Sun, Jing Li, Ya-Xian Li, Hui-Zhen Wang, Emre Dal, Ming-Liang Wang, Yong-Xiang Li

Specialty type: Gastroenterology and hepatology

Provenance and peer review: Unsolicited article; Externally peer reviewed.

Peer-review model: Single blind

Peer-review report's scientific quality classification

Grade A (Excellent): 0
Grade B (Very good): B, B
Grade C (Good): C
Grade D (Fair): 0
Grade E (Poor): 0

P-Reviewer: Buechler C, Germany; Cucu D, Romania; Ocker M, Germany

Received: July 20, 2023
Peer-review started: July 20, 2023
First decision: October 9, 2023
Revised: October 23, 2023
Accepted: November 14, 2023
Article in press: November 14, 2023
Published online: November 28, 2023

Ruo-Chuan Sun, Jing Li, Ya-Xian Li, Hui-Zhen Wang, Ming-Liang Wang, Yong-Xiang Li, Department of General Surgery, The First Affiliated Hospital of Anhui Medical University, Hefei 230022, Anhui Province, China

Emre Dal, Department of Oncological Sciences, University of Utah, Salt Lake City, UT 84112, United States

Corresponding author: Yong-Xiang Li, Doctor, Department of General Surgery, The First Affiliated Hospital of Anhui Medical University, No. 218 Jixi Road, Shushan District, Hefei 230022, Anhui Province, China. liyongxiang@ahmu.edu.cn

Abstract

BACKGROUND

The role of Tousled-like kinase 1 (TLK1) in in gastric cancer (GC) remains unclear.

AIM

To investigate the expression, biological function, and underlying mechanisms of TLK1 in GC.

METHODS

We measured TLK1 protein expression levels and localized TLK1 in GC cells and tissues by western blot and immunofluorescence, respectively. We transfected various GC cells with lentiviruses to create TLK1 overexpression and knockdown lines and established the functional roles of TLK1 through *in vitro* colony formation, 5-ethynyl-2`-deoxyuridine, and Transwell assays as well as flow cytometry. We applied bioinformatics to elucidate the signaling pathways associated with TLK1. We performed *in vivo* validation of TLK1 functions by inducing subcutaneous xenograft tumors in nude mice.

RESULTS

TLK1 was significantly upregulated in GC cells and tissues compared to their normal counterparts and was localized mainly to the nucleus. TLK1 knockdown significantly decreased colony formation, proliferation, invasion, and migration but increased apoptosis in GC cells. TLK1 overexpression had the opposite effects. Bioinformatics revealed, and subsequent experiments verified, that the tumor growth factor-beta signaling pathway was implicated in TLK1-mediated GC progression. The *in vivo* assays confirmed that TLK1 promotes tumorigenesis in GC.

CONCLUSION
The findings of the present study indicated that TLK1 plays a crucial role in GC progression and is, therefore, promising as a therapeutic target against this disease.

Key Words: Gastric cancer; Tousled-like kinase 1; Tumor growth factor-beta; Tumour progression; Targeted therapy

Core Tip: We demonstrated that Tousled-like kinase 1 (TLK1) is highly expressed in gastric cancer (GC), localized mainly to the nucleus, significantly promotes GC cell proliferation, invasion, and migration, and inhibits apoptosis. TLK1 may facilitate GC progression by modulating tumor growth factor-beta expression. We believe that TLK1 could be a crucial therapeutic target for GC, and propose that future investigations evaluate the feasibility and practicality of targeting TLK1 in GC treatment.

Citation: Sun RC, Li J, Li YX, Wang HZ, Dal E, Wang ML, Li YX. Tousled-like kinase 1 promotes gastric cancer progression by regulating the tumor growth factor-beta signaling pathway. *World J Gastroenterol* 2023; 29(44): 5919-5934
URL: https://www.wjgnet.com/1007-9327/full/v29/i44/5919.htm
DOI: https://dx.doi.org/10.3748/wjg.v29.i44.5919

INTRODUCTION

Gastric cancer (GC) is the fifth most prevalent cancer and the third leading cause of cancer-related mortality worldwide [1]. Endoscopy is the mainstay of early-stage GC treatment whereas advanced GC must be managed through surgery and other interventions including chemotherapy and targeted therapy[2]. Despite significant progress in GC control, however, its overall survival remains unsatisfactory. Hence, potential therapeutic targets against this disease are urgently required.

Tousled kinase and Tousled-like kinase (TLK) are serine-threonine enzymes implicated in DNA replication[3], transcription[4,5], and chromatin assembly[6]. TLK promotes glioma progression[7] and modulates latent viral activation [8]. Thus, it plays a critical role in various cellular processes. The two known TLK genes are TLK1 and TLK2. However, the former has received more research attention than the latter, and prior investigations focused primarily on the mechanisms by which TLK1 regulates DNA replication and repair. It interacts with Aurora kinase and chromatin assembly factors, and together they precisely control spindle assembly and S-phase progression[9]. The ataxia-telangiectasia-mutated-checkpoint kinase (Chk1)-TLK pathway uses TLK1 as a target to direct chromatin assembly[10, 11]. TLK1 collaborates with Chk1 to regulate RAD9 checkpoint clamp component A (Rad9A) phosphorylation and, by extension, modulate the DNA damage response[12,13]. It also confers resistance to ultraviolet irradiation and, therefore, helps maintain cellular integrity and survival[14-17].

Recent research efforts have aimed to clarify the roles of TLK1 in cancers. TLK1 mediates prostate cancer progression *via* the TLK1-MAPK-activated protein kinase 5 and TLK1-NIMA-related kinase 1 axes[18-21]. The phenothiazine analog J54 is a potent TLK1 inhibitor and a possible therapeutic agent against prostate cancer[22]. TLK1 may promote the progression of glioma[23-25] and oral cancer[26]. However, the expression patterns and functional relevance of TLK1 in GC remain to be determined. Hence, the present study aimed to elucidate the functional significance of TLK1 in GC cells and potentially identify a novel therapeutic target against this disease.

MATERIALS AND METHODS

Bioinformatics analysis

The RNA-sequencing data obtained from The Cancer Genome Atlas (TCGA) website (https://portal.gdc.cancer.gov/) was subjected to a transcriptome analysis in R v. 4.1.2 (R Core Team, Vienna, Austria) to determine the functional relevance of TLK1 to GC. Differential gene expression between the high- and low-TLK1 expression groups was evaluated. The differentially expressed genes were then subjected to a Kyoto Encyclopedia of Genes and Genomes analysis (http://www.kegg.jp/) to identify and characterize the enrichment pathways with which they were associated. A gene set enrichment analysis was then used to analyze specific pathways and identify the interactions between them and TLK1 in GC. This multifaceted approach established novel molecular mechanisms and regulatory pathways underlying TLK1-mediated GC progression and elucidated GC biology.

Cell culture

The normal gastric epithelial cell line GES-1 as well as the AGS, SGC7901, MGC803, BGC823, and HGC27 GC cell lines were sourced from GeneChem (Shanghai, China) in December 2021. Short tandem repeat analyses verified the authenticity of each cell line and the final test was conducted on March 30, 2022. The cells were cultured in PMIS-1640 medium (Corning Inc., Corning, NY, United States) supplemented with 10% fetal bovine serum (FBS; Clark Bioscience, Richmond,

VA, United States), 1% penicillin, and 1% streptomycin (HyClone Laboratories, Logan, UT, United States) and incubated in a Thermo Fisher incubator (Thermo Fisher Scientific, Waltham, MA, United States) under a 5% CO_2 atmosphere at 37°C. They were then subcultured after they reached 80% confluence and maintained in the log phase. Strict quality control measures including regular mycoplasma testing were implemented to mitigate the risk of contamination.

Western blotting

Total protein was extracted with M-PER Mammalian Protein Extraction Reagent (Thermo Fisher Scientific) supplemented with phosphatase and protease inhibitors (BBI Life Sciences Corporation, Shanghai, China). Denatured sodium dodecyl sulfate-polyacrylamide gel electrophoresis was used to separate the proteins and they were then blotted onto polyvinylidene fluoride (PVDF) membranes. The latter were blocked with 5% skim milk for 1 h and incubated at 4°C overnight with primary antibodies including anti-GAPDH (1:2,500; No. 7074T; Cell Signaling Technology, Danvers, MA, United States), anti-TLK1 (1:1,000; No. 13564-1-AP; Proteintech Group, Rosemont, IL, United States), and anti-tumor growth factor-beta (TGF-β) (1:1,000; No. 346599; ZenBio, Chengdu, China) to detect the protein expression levels. The PVDF membranes were then washed with Tris-buffered saline with Tween-20 (TBST), incubated with secondary antibody at room temperature for 1 h, rinsed again with TBST, and visualized by enhanced chemiluminescence (ECL; Bridgen, Beijing, China). The ECL signals were captured on a Tanon-5200 multi-platform (Tanon Science & Technology Co. Ltd., Shanghai, China). The protein band gray values were then quantified with ImageJ software (National Institutes of Health (NIH), Bethesda, MD, United States).

Immunofluorescence staining

Sterile slides were placed in a 24-well plate, drops of cell suspension were dispensed onto them, and they were incubated overnight. The following day, the cells were fixed with 4% formaldehyde, blocked with 5% bovine serum albumin (BSA) for 1 h, and incubated at 4°C overnight with anti-TLK1 antibody (1:1,000; No. 13564-1-AP; Proteintech Group). The next day, the slides were subjected to fluorescent secondary antibody (1:250; No. A11012; Thermo Fisher Scientific) at room temperature for 1 h. Then 4`,6-diamidino-2-phenylindole (DAPI; 1:100; No. D9542; Sigma-Aldrich Corp., Roedermark, Germany) nuclear stain was applied to them for 15 min and they were observed and photographed under a confocal laser scanning microscope (CLSM; No. LSM800; Carl Zeiss AG, Jena, Germany).

Lentivirus infection

Three distinct small hairpin RNAs (shRNAs) targeting human TLK1 and a lentiviral TLK1 overexpression construct were procured from GeneChem (Shanghai, China). Cells were seeded in 12-well plates and the lentiviral particles were added to them at a multiplicity of infection = 10 in the presence of a transfection aid per the manufacturer's instructions. The medium was replaced and the cells were passaged after 24 h and 48 h, respectively. Successful lentiviral infection was confirmed by screening the cells with a medium containing puromycin. Transfection efficiency was assessed *via* protein extraction. The shRNA sequences used in the experiment were as follows: sh1: 5`-GAUACAGAUACGUUUUGUACA-dTdT-3`; sh2: 5`-CUCGUAGGGUAGAAACCAAUAdTdT-3`; and sh3: 5`-GCAGGCACUUACUGGUAUUUAdTdT-3`.

Colony formation assay

Cells were seeded in six-well plates at a density of 800/well and incubated with gentle agitation under optimal conditions. The culture medium was renewed every 3 d and the experiment was terminated when cell colonies emerged. The cells were then fixed with 4% formaldehyde for 20 min, washed thrice with phosphate-buffered saline (PBS), stained with 0.1% crystal violet for 15 min, air-dried, and imaged.

5-ethynyl-2`-deoxyuridine assay

An 5-ethynyl-2`-deoxyuridine (EdU) Kit (No. C0078S; Beyotime Biotechnology, Shanghai, China) was utilized for this assay. Sterile slides were aseptically placed in 12-well plates. Cells were seeded onto them and incubated overnight until the optimal cell density was attained. The next day, a 2 EdU solution was prepared according to the manufacturer's instructions and mixed in equal proportions with the culture medium. The mixture was then added to the 12-well plates and incubated at 37°C for 2 h. The culture medium was removed and the cells were fixed with 4% paraformaldehyde for 15 min and washed with PBS containing 3% BSA (Beyotime Biotechnology). Then 0.3% Triton X-100 was added and the cells were incubated at room temperature for 15 min. The cells were rinsed and a pre-configured Click reaction solution was added to the 12-well plates. The cells were incubated for 30 min and their nuclei were stained with Hoechst33342 for 10 min. An anti-quenching agent was added and the cells were viewed under a microscope (Leica Microsystems GmbH, Wetzlar, Germany).

Transwell assays

Cells in the log phase were seeded at optimal density and subjected to serum deprivation for 24 h. Matrigel Basement Membrane Matrix (BD Biosciences, Shanghai, China) was diluted to a working concentration and uniformly spread onto the upper layer of a Transwell chamber (Corning Inc.). The latter was incubated at 37°C for 5 h. The cell concentration was adjusted and maintained at 8 10^5/mL. One hundred microliters cell suspension was added to the upper chamber, 650 μL high-serum medium was added to the lower chamber, and the Transwell was incubated in a suitable environment. After a predetermined incubation period, the Transwell chambers were extracted. Their contents were then fixed with 4% paraformaldehyde, stained with 0.1% crystal violet, and observed and photographed under a microscope (Leica Microsystems GmbH).

Flow cytometry

An Annexin V-fluorescein isothiocyanate (FITC)/propidium iodide (PI) Apoptosis Kit (Yeasen Biotechnology, Shanghai, China) was used for this assay. Cell supernatant and digested cells were collected in a centrifuge tube, washed with PBS, and resuspended in 100 μL of 1 × binding buffer. Then 5 μL Annexin V-FITC and 10 μL PI staining solution were added and the suspension was incubated in the dark at room temperature for 15 min. Then a CytoFLEX Flow Cytometry Platform (Beckman Coulter, Brea, CA, United States) was used to detect apoptosis.

Xenograft mouse model

Four-Week-old male BALB/C nude mice were obtained from GemPharmatech, Jiangsu, China, and maintained under specific pathogen-free conditions. The control and experimental groups each included six mice. SGC7901 cells were digested and resuspended in PBS and 5 x 10^6 were subcutaneously injected into the left underarm of each mouse. During the experiment, the mice were provided with sufficient food and water, and their body weight was periodically measured. The volumes of any subcutaneous tumors that had formed were determined every 4 d. Humane euthanasia was performed when the body weight decreased by ≥ 20% and/or the tumor diameter was > 1.5 cm.

Immunohistochemical staining

Immunohistochemical (IHC) staining was conducted per established methods[27]. Protein expression levels were independently evaluated by two pathologists blinded to the clinical information of the patients. The IHC score was calculated based on the staining intensity and area to assess the protein expression levels.

Statistical analysis

All data were analyzed with SPSS v. 22.0 (SPSS Inc., Chicago, IL, United States), GraphPad Prism v. 7.0 (GraphPad Software, La Jolla, CA, United States), and R v. 4.1.2 (R Core Team, Vienna, Austria). Student's *t*-test or one-way ANOVA was used to detect significant differences between treatments. $P < 0.05$ was considered statistically significant ($^aP < 0.05$).

Ethics statement

Studies involving human participants were reviewed and approved (No. 20180323) by the Ethics Committee of Anhui Medical University, Anhui, China. All patients and participants provided written informed consent. All animal experiments were approved (No. 20180345) by the Institutional Animal Care and Use Committee of Anhui Medical University.

RESULTS

TLK1 was significantly upregulated in GC cells and tissues and localized mainly to the nucleus

We performed a bioinformatics analysis using TCGA to determine TLK1 expression and localization in GC. We found that TLK1 was upregulated in GC and other tumors of the digestive tract (Figure 1A). We then conducted a western blot analysis to determine the TLK1 expression levels in the GC cells and tissues. We measured TLK1 protein expression in normal gastric epithelial cells (GES-1) and the GC cells AGS, SGC7901, MGC803, BGC823, and HGC27 to clarify the association between the expression and localization of TLK1 in GC. TLK1 expression was significantly higher in GC than in GES-1 cells (Figure 1B and C). We then measured TLK1 expression in GC and their adjacent normal tissues and found that it was significantly higher in the former than in the latter (Figure 1D and E). We then subjected HGC27 and MGC803 GC cells to immunofluorescence staining and observed that TLK1 was localized mainly to their nuclei (Figure 1F). The foregoing findings suggest that TLK1 is upregulated in GC cells and tissues and is localized to the nucleus.

TLK1 significantly enhanced GC cell clonogenesis, proliferation, invasion, and migration in vitro

We increased TLK1 expression in SGC7901 cells *via* lentiviral transfection and verified its upregulation *via* western blot to elucidate its role in GC cells (Figure 2A). We then used a colony formation assay to assess the impact of TLK1 overexpression on GC cell proliferation. TLK overexpression substantially increased the number of SGC7901 cell colonies compared to the control (Figure 2B and C). The EdU assay demonstrated a dramatic increase in the proportion of proliferative SGC7901 cells in response to TLK1 overexpression (Figure 2D and E). The preceding experiments showed that TLK1 overexpression augments SGC7901 cell proliferation.

A Transwell assay showed that TLK1 overexpression significantly increased SGC7901 GC cell migration and invasion relative to the control (Figure 2F and G). Overall, TLK1 overexpression promoted clonal expansion, proliferation, invasion, and migration in SGC7901 GC cells.

TLK1 knockdown inhibited GC cell clonal formation, invasion, and migration

We transfected AGS and HGC27 cells with three lentiviral sequences designed to knock down/silence TLK1 and used western blot analysis to assess transfection efficiency. We selected sh2 and sh3 for the subsequent experiments as they exhibited superior knockdown efficacy (Figure 3A). A colony formation assay demonstrated that TLK1 knockdown markedly reduced the number of AGS and HGC27 cell colonies compared with the control (Figure 3B and C).

A Transwell assay revealed that TLK1 knockdown significantly diminished AGS GC cell invasion and migration relative to the control (Figure 3D and E). Similar results were obtained for HGC27 cells subjected to TLK1 knockdown (Figure 3F and G). The foregoing findings suggest that TLK1 knockdown effectively suppresses clonal formation,

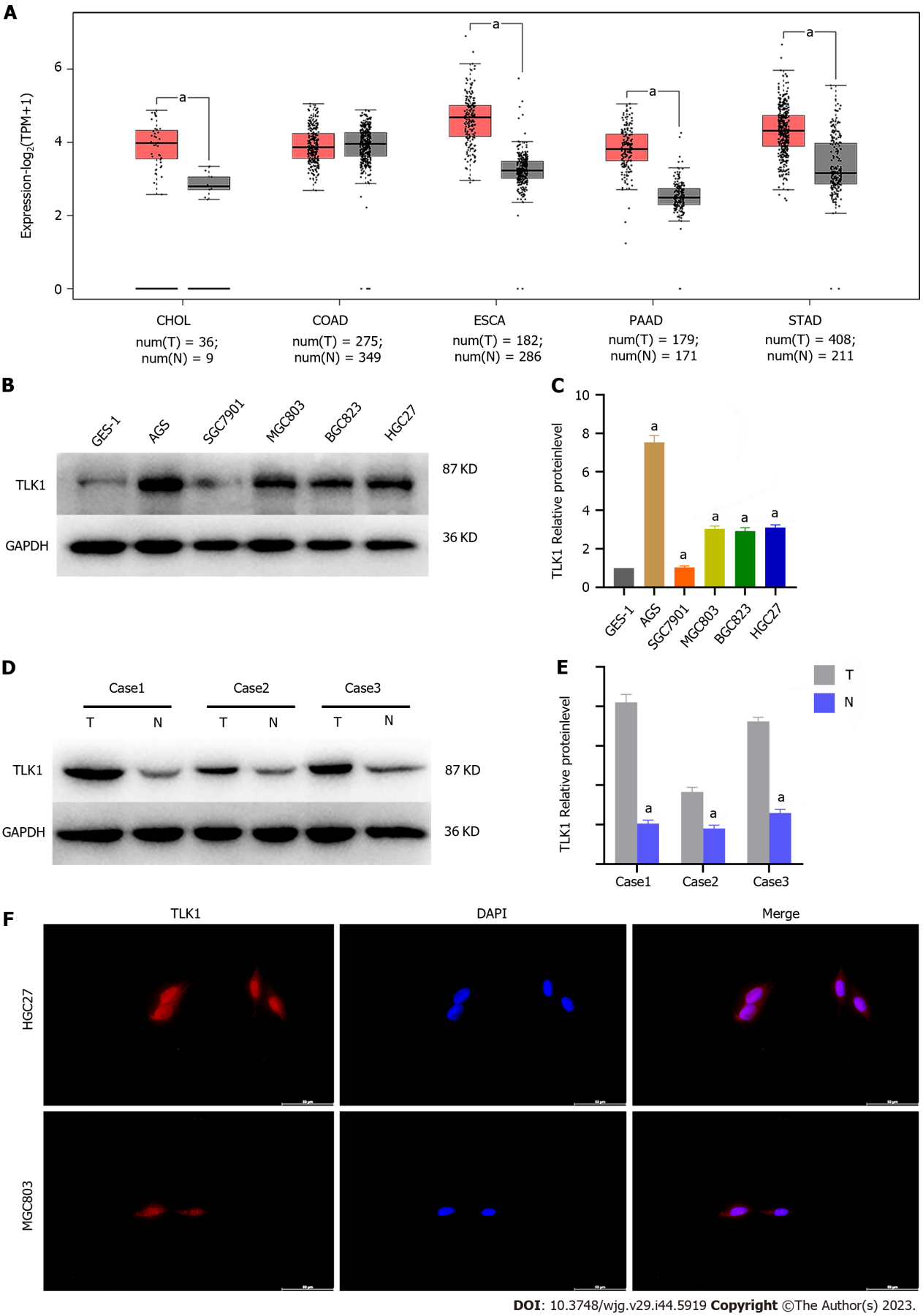

DOI: 10.3748/wjg.v29.i44.5919 **Copyright** ©The Author(s) 2023.

Figure 1 Tousled-like kinase 1 was upregulated and localized mainly to the nucleus in gastric cancers. A: Tousled-like kinase 1 (TLK1) expression in various tumors was explored using The Cancer Genome Atlas database; B and C: Western blot measuring TLK1 expression in normal gastric epithelial

cells GES-1 and in gastric cancer (GC) cell lines; D and E: Western blot detecting differential TLK1 expression between GC and adjacent non-neoplastic tissues; F: Immunofluorescence detecting subcellular TLK1 compartmentalization in HGC27 and MGC803 cell lines. [a]*P* < 0.05. TLK1: Tousled-like kinase 1; CHOL: Cholangiocarcinoma; COAD: Colon adenocarcinoma; ESCA: Esophageal carcinoma; PAAD: Pancreatic adenocarcinoma; STAD: Stomach adenocarcinoma.

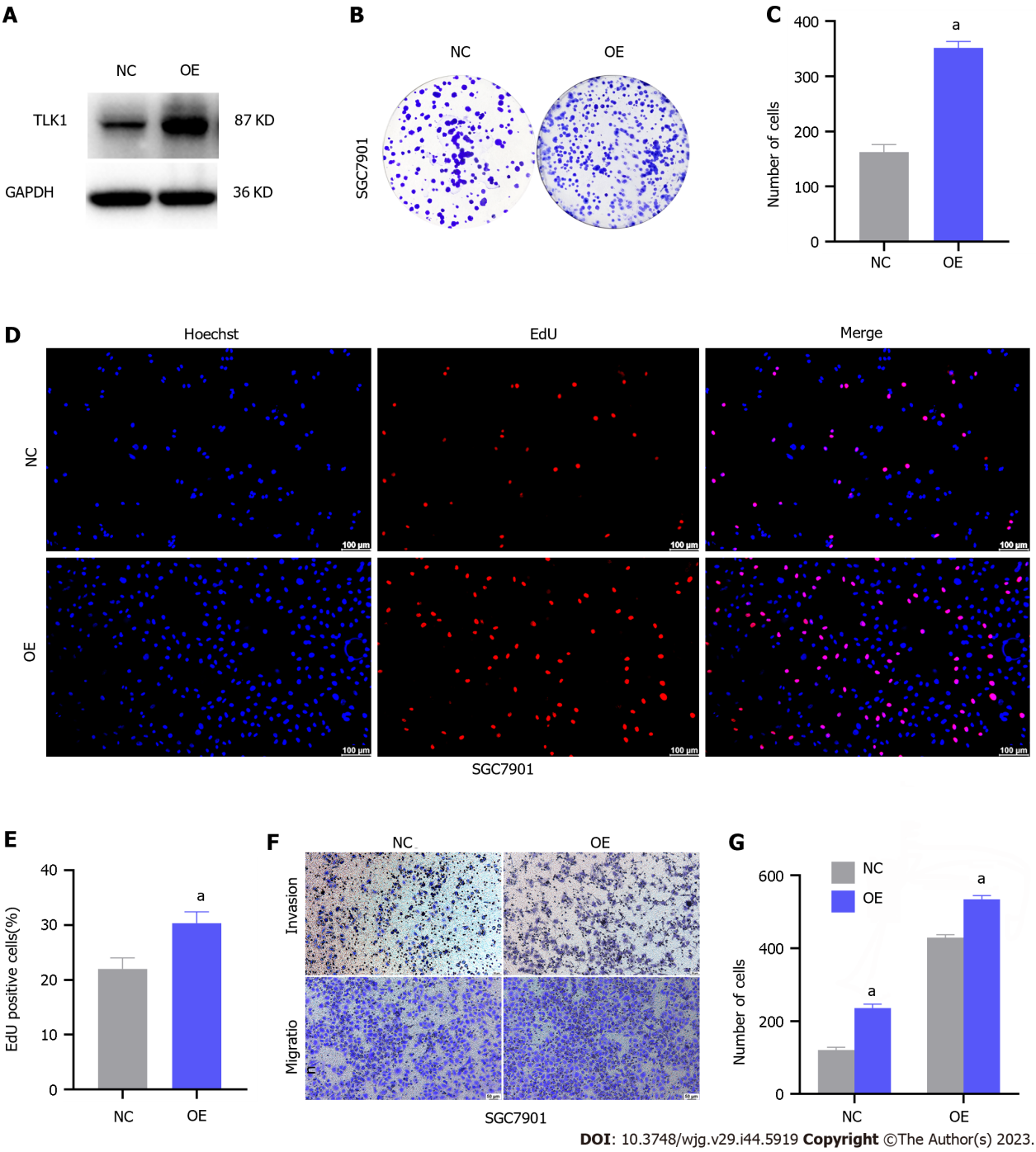

DOI: 10.3748/wjg.v29.i44.5919 **Copyright** ©The Author(s) 2023.

Figure 2 Tousled-like kinase 1 upregulation potentiated tumorigenesis in gastric cancer cell lines. A: Western blot demonstrated the effects of Tousled-like kinase 1 (TLK1) overexpression in SGC7901 cells; B and C: Impact of TLK1 overexpression on clonogenesis in SGC7901 cells; D and E: 5-ethynyl-2`-deoxyuridine assay evaluating the influence of TLK1 overexpression on SGC7901 cell proliferation; F and G: Transwell assay showing the effects of TLK1 overexpression on SGC7901 cell invasion and migration. [a]*P* < 0.05. TLK1: Tousled-like kinase 1; NC: Negative control; OE: Overexpression; EdU: 5-ethynyl-2`-deoxyuridine.

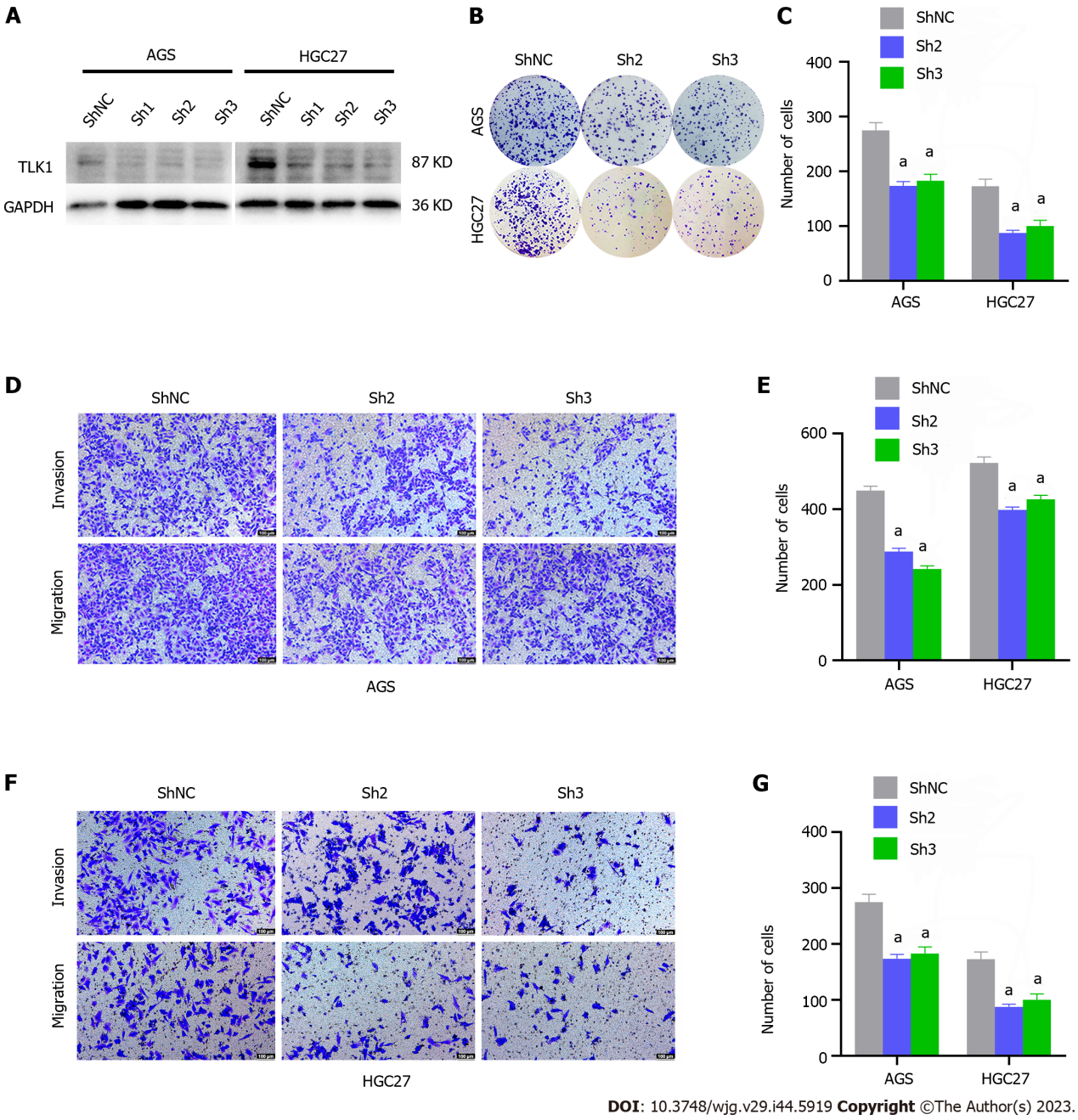

DOI: 10.3748/wjg.v29.i44.5919

Figure 3 Tousled-like kinase 1 knockdown attenuated clonal formation, invasion, and migration in gastric cancer cell lines. A: Western blot revealing the impact of Tousled-like kinase 1 (TLK1) knockdown on AGS and HGC27 cell lines; B and C: Effects of TLK1 suppression on clonogenesis in AGS and HGC27 cell lines; D and E: Transwell assay disclosing the effects of TLK1 knockdown on AGS cell invasion and migration; F and G: Transwell assay demonstrating the influences of TLK1 suppression on HGC27 cell invasion and migration. [a]$P < 0.05$. TLK1: Tousled-like kinase 1; shNC: Short hairpin RNA of negative control.

invasion, and migration in GC cells.

TLK1 knockdown diminished proliferation and augmented apoptosis in GC cells

An EdU assay disclosed that TLK1 knockdown substantially inhibited AGS cell proliferation compared to the control (Figure 4A and B). Similar results were obtained for HGC27 cells (Figure 4C and D). Flow cytometry also showed that TLK1 knockdown considerably increased the apoptosis ratios in AGS and HGC27 relative to the control (Figure 4E and F).

TLK1 promotes GC progression by regulating the TGF-β signaling pathway

We applied bioinformatics to identify the genes associated with TLK1 and elucidate the mechanisms by which TLK1 affects GC cell clonal formation, proliferation, invasion, and migration. The expression levels of DDB1- and CUL4-associated factor 17 (DCAF17), enhancer of polycomb homolog 2 (EPC2), and membrane-associated ring-CH-type finger 7 (MARCH7) were positively correlated with that of TLK1 (Figure 5A) whereas those of COPI coat complex subunit epsilon (COPE), RNA pseudouridine synthase domain containing 1 (RPUSD1), and protein phosphatase 4, catalytic subunit

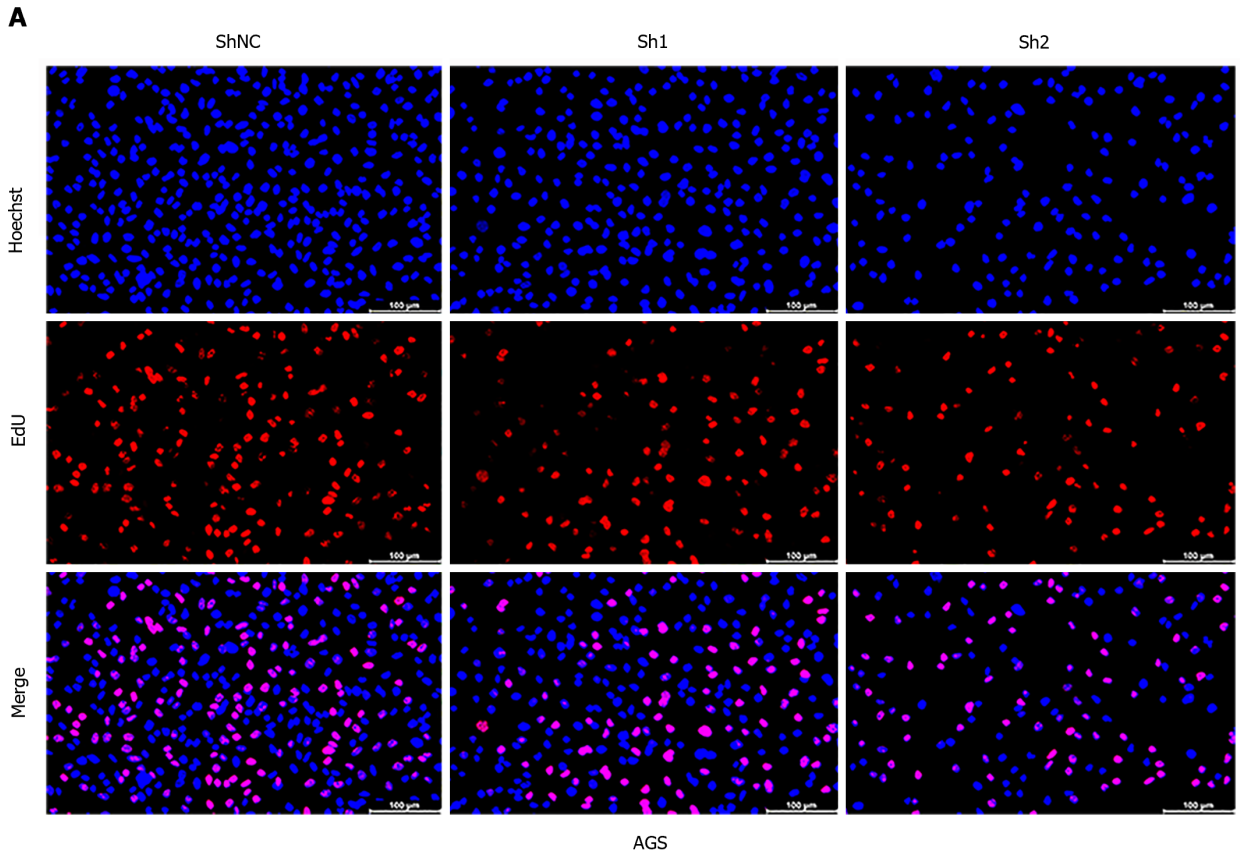
A
ShNC
Sh1
Sh2
Hoechst
EdU
Merge
AGS

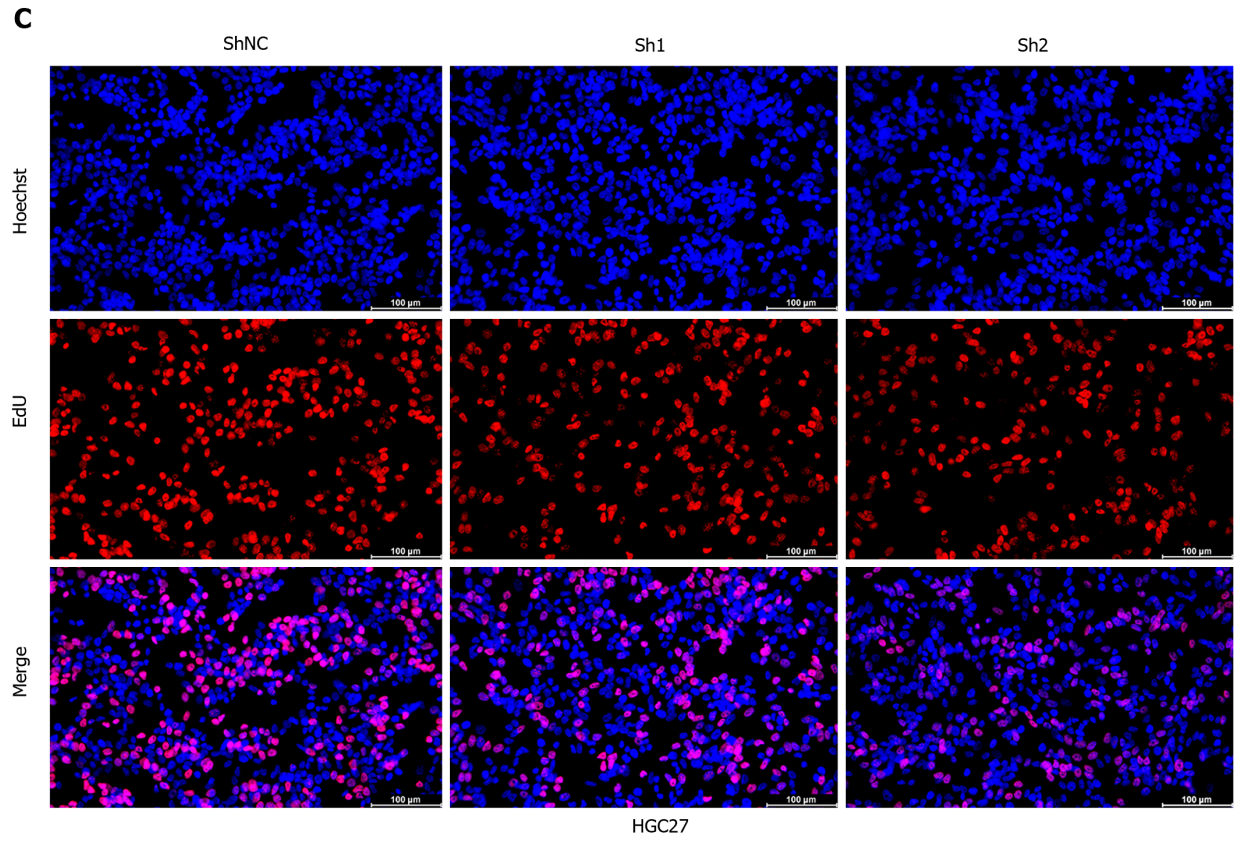
C
ShNC
Sh1
Sh2
Hoechst
EdU
Merge
HGC27

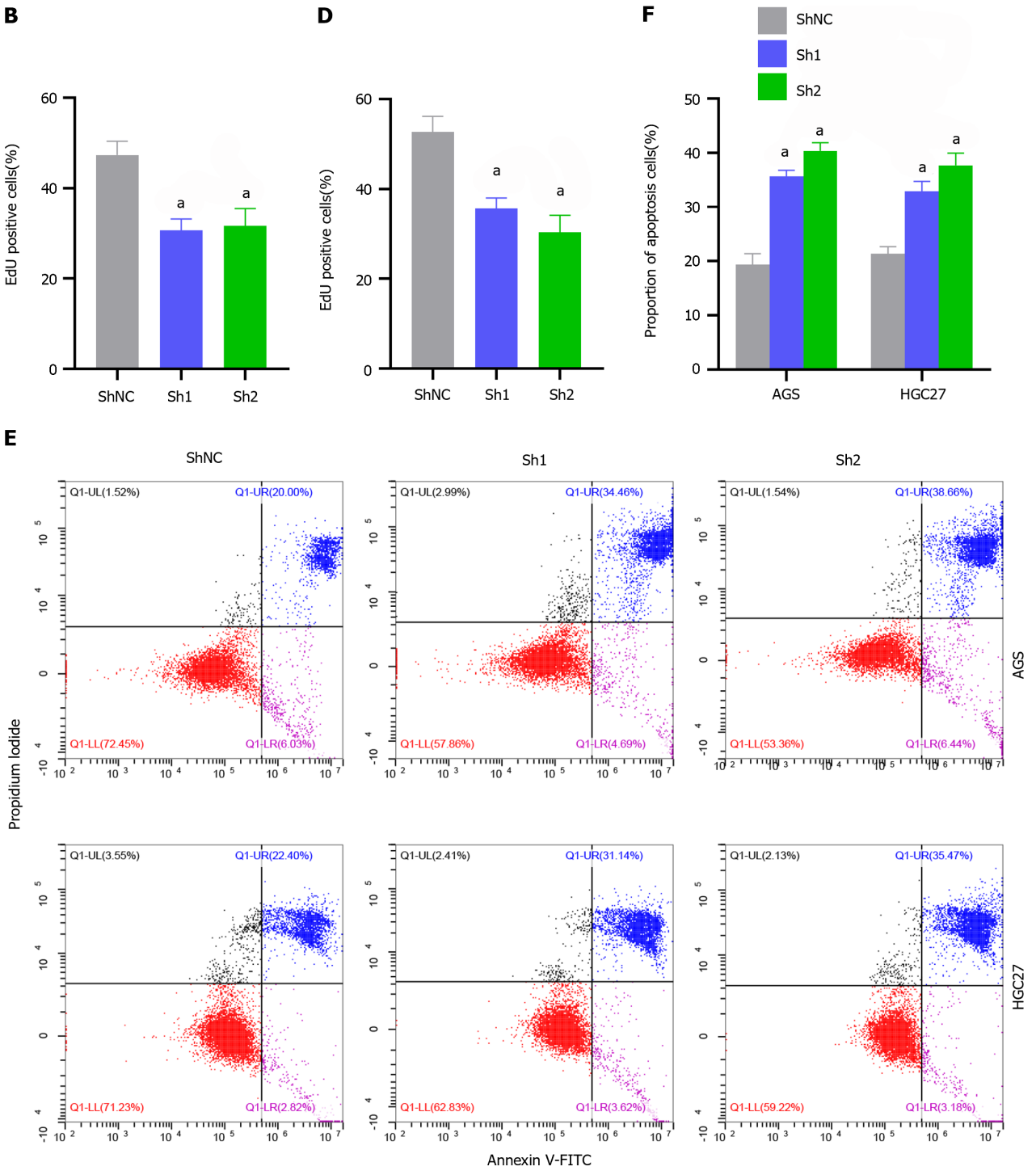

DOI: 10.3748/wjg.v29.i44.5919

Figure 4 Tousled-like kinase 1 inhibition diminished proliferation and augmented apoptosis in gastric cancer cell lines. A and B: 5-ethynyl-2`-deoxyuridine (EdU) assay showing the effects of Tousled-like kinase 1 (TLK1) suppression on AGS cell proliferation; C and D: EdU assay revealing the impact of TLK1 knockdown on HGC27 cell proliferation; E and F: Flow cytometry evaluating the effects of TLK1 inhibition on apoptosis in AGS and HGC27 cell lines. $^{a}P < 0.05$. EdU: 5-ethynyl-2`-deoxyuridine; shNC: Short hairpin RNA of negative control.

(PPP4C) were negatively correlated with it (Figure 5B).

We then discovered that the TGF-β signaling pathway might mediate the impact of TLK1 on the clonal formation, proliferation, invasion, and migration of GC cells (Figure 5C and D). We then used western blot to measure TGF-β protein expression in GC cells subjected to TLK1 knockdown and overexpression. We observed that the former downregulated TGF-β in AGS and HGC27 cells whereas the latter upregulated TGF-β in SGC7901 cells. Hence, TGF-β signaling determines the influence of TLK1 on GC progression (Figure 5E-G).

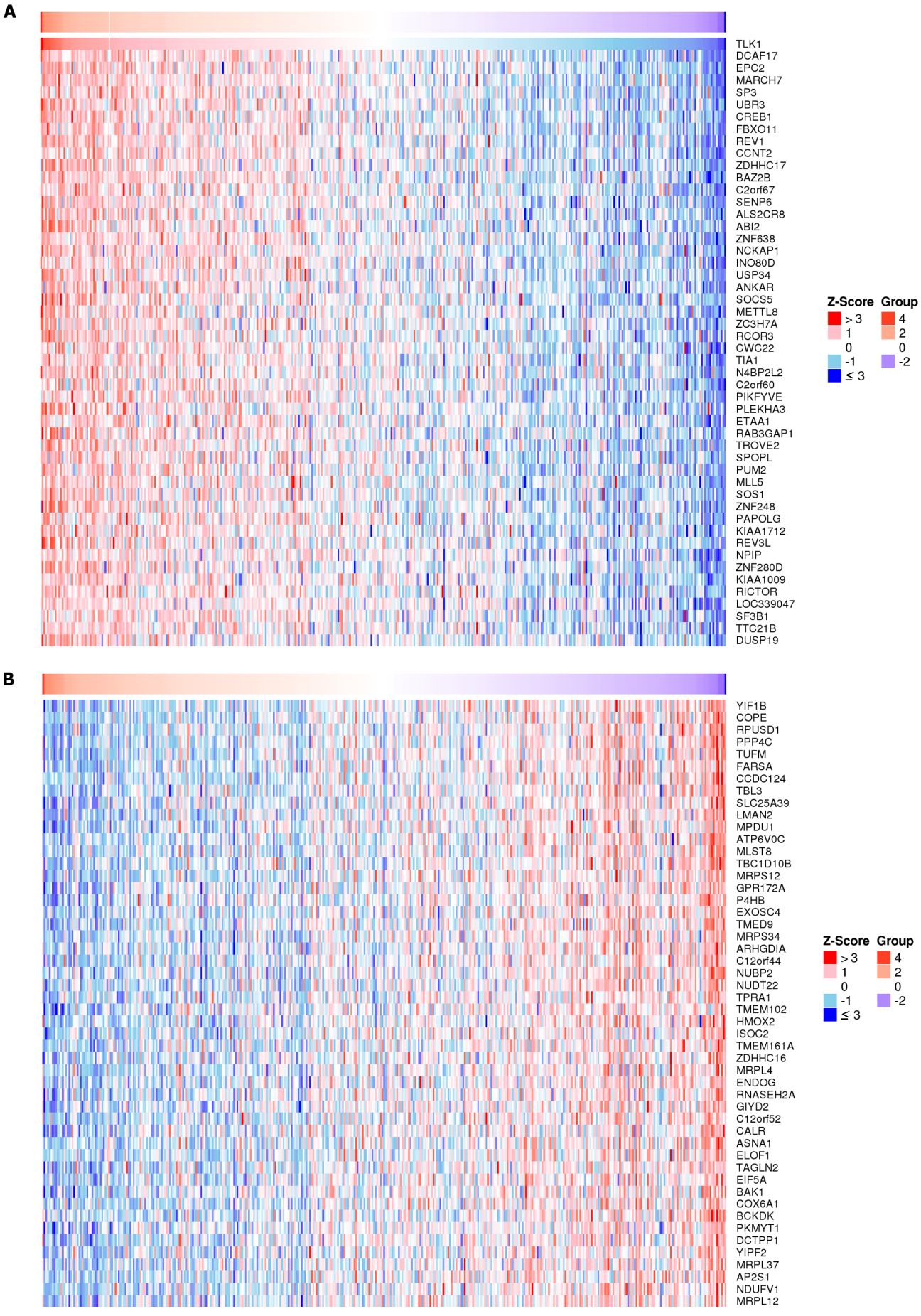
A
TLK1
DCAF17
EPC2
MARCH7
SP3
UBR3
CREB1
FBXO11
REV1
CCNT2
ZDHHC17
BAZ2B
C2orf67
SENP6
ALS2CR8
ABI2
ZNF638
NCKAP1
INO80D
USP34
ANKAR
SOCS5
METTL8
ZC3H7A
RCOR3
CWC22
TIA1
N4BP2L2
C2orf60
PIKFYVE
PLEKHA3
ETAA1
RAB3GAP1
TROVE2
SPOPL
PUM2
MLL5
SOS1
ZNF248
PAPOLG
KIAA1712
REV3L
NPIP
ZNF280D
KIAA1009
RICTOR
LOC339047
SF3B1
TTC21B
DUSP19
Z-Score
> 3
1
0
-1
≤ 3
Group
4
2
0
-2
B
YIF1B
COPE
RPUSD1
PPP4C
TUFM
FARSA
CCDC124
TBL3
SLC25A39
LMAN2
MPDU1
ATP6V0C
MLST8
TBC1D10B
MRPS12
GPR172A
P4HB
EXOSC4
TMED9
MRPS34
ARHGDIA
C12orf44
NUBP2
NUDT22
TPRA1
TMEM102
HMOX2
ISOC2
TMEM161A
ZDHHC16
MRPL4
ENDOG
RNASEH2A
GIYD2
C12orf52
CALR
ASNA1
ELOF1
TAGLN2
EIF5A
BAK1
COX6A1
BCKDK
PKMYT1
DCTPP1
YIPF2
MRPL37
AP2S1
NDUFV1
MRPL12
Z-Score
> 3
1
0
-1
≤ 3
Group
4
2
0
-2

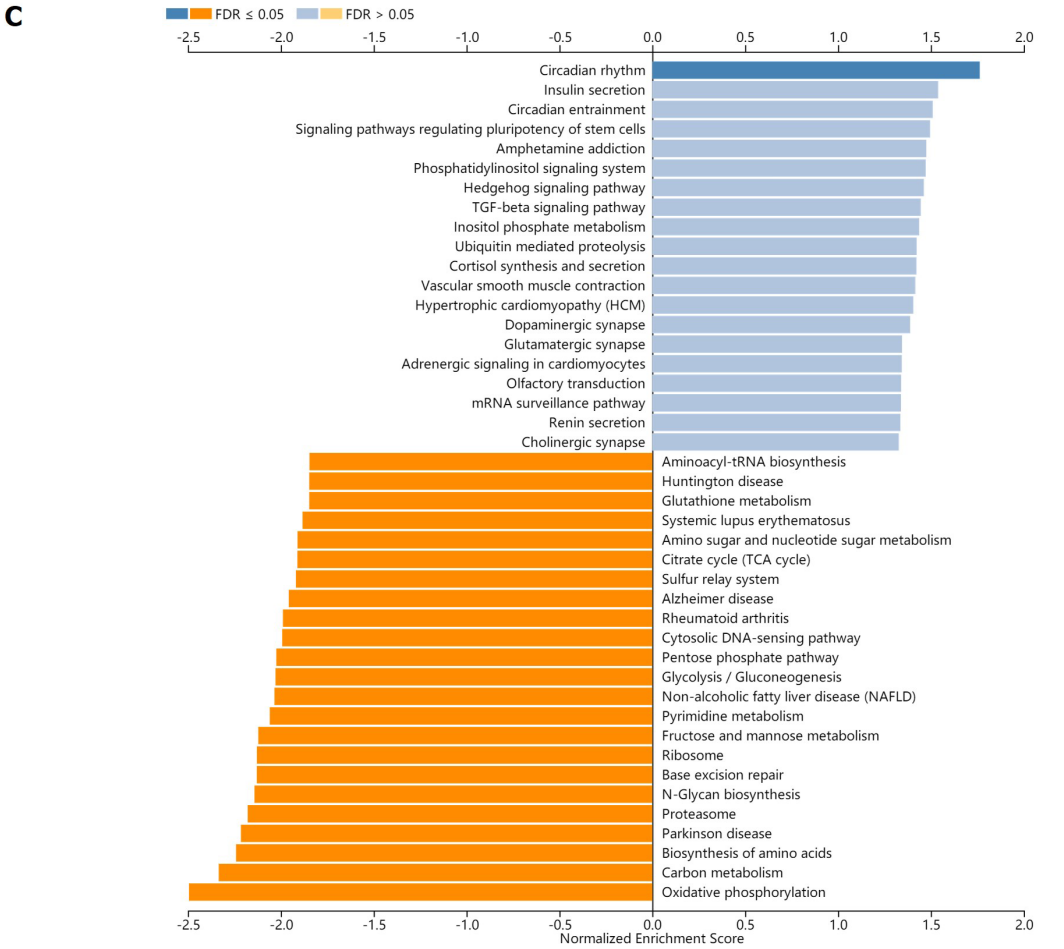
C
FDR ≤ 0.05
FDR > 0.05
-2.5 -2.0 -1.5 -1.0 -0.5 0.0 0.5 1.0 1.5 2.0
Circadian rhythm
Insulin secretion
Circadian entrainment
Signaling pathways regulating pluripotency of stem cells
Amphetamine addiction
Phosphatidylinositol signaling system
Hedgehog signaling pathway
TGF-beta signaling pathway
Inositol phosphate metabolism
Ubiquitin mediated proteolysis
Cortisol synthesis and secretion
Vascular smooth muscle contraction
Hypertrophic cardiomyopathy (HCM)
Dopaminergic synapse
Glutamatergic synapse
Adrenergic signaling in cardiomyocytes
Olfactory transduction
mRNA surveillance pathway
Renin secretion
Cholinergic synapse
Aminoacyl-tRNA biosynthesis
Huntington disease
Glutathione metabolism
Systemic lupus erythematosus
Amino sugar and nucleotide sugar metabolism
Citrate cycle (TCA cycle)
Sulfur relay system
Alzheimer disease
Rheumatoid arthritis
Cytosolic DNA-sensing pathway
Pentose phosphate pathway
Glycolysis / Gluconeogenesis
Non-alcoholic fatty liver disease (NAFLD)
Pyrimidine metabolism
Fructose and mannose metabolism
Ribosome
Base excision repair
N-Glycan biosynthesis
Proteasome
Parkinson disease
Biosynthesis of amino acids
Carbon metabolism
Oxidative phosphorylation
Normalized Enrichment Score

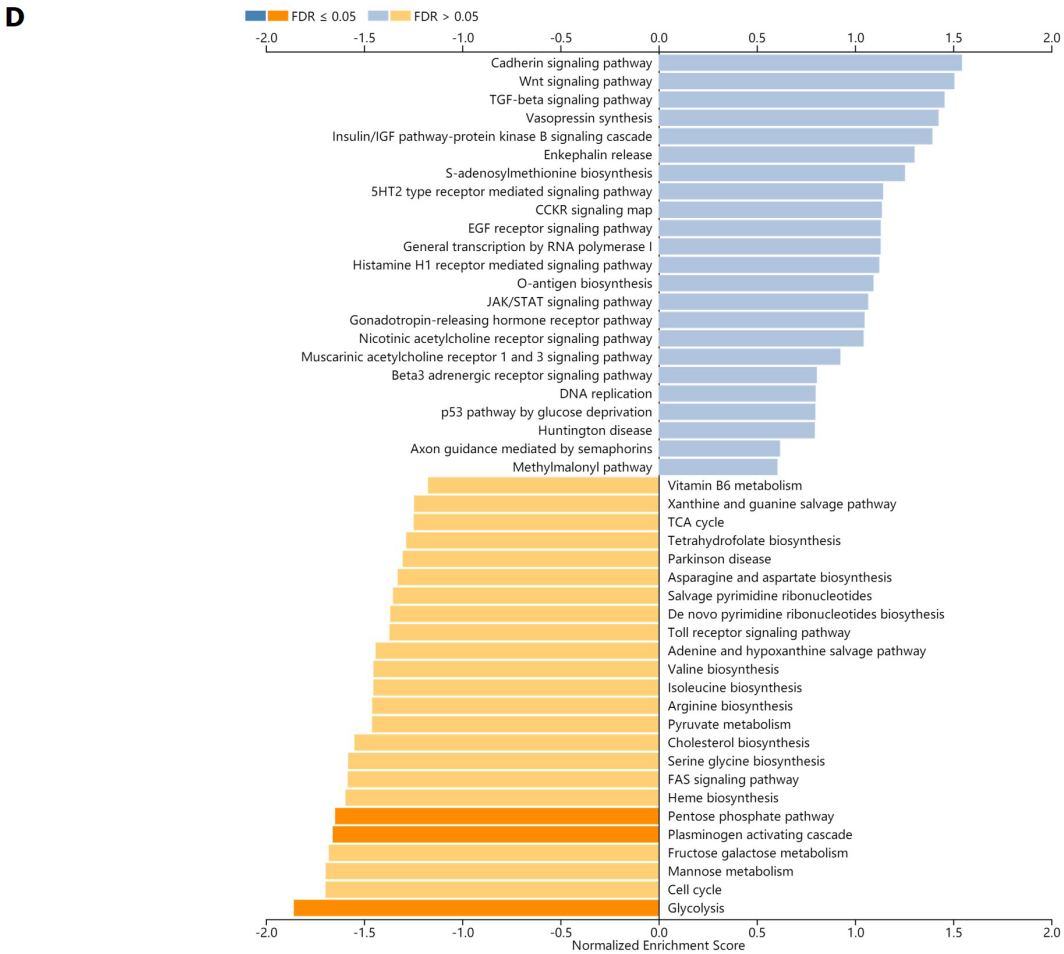
D
FDR ≤ 0.05
FDR > 0.05
-2.0 -1.5 -1.0 -0.5 0.0 0.5 1.0 1.5 2.0
Cadherin signaling pathway
Wnt signaling pathway
TGF-beta signaling pathway
Vasopressin synthesis
Insulin/IGF pathway-protein kinase B signaling cascade
Enkephalin release
S-adenosylmethionine biosynthesis
5HT2 type receptor mediated signaling pathway
CCKR signaling map
EGF receptor signaling pathway
General transcription by RNA polymerase I
Histamine H1 receptor mediated signaling pathway
O-antigen biosynthesis
JAK/STAT signaling pathway
Gonadotropin-releasing hormone receptor pathway
Nicotinic acetylcholine receptor signaling pathway
Muscarinic acetylcholine receptor 1 and 3 signaling pathway
Beta3 adrenergic receptor signaling pathway
DNA replication
p53 pathway by glucose deprivation
Huntington disease
Axon guidance mediated by semaphorins
Methylmalonyl pathway
Vitamin B6 metabolism
Xanthine and guanine salvage pathway
TCA cycle
Tetrahydrofolate biosynthesis
Parkinson disease
Asparagine and aspartate biosynthesis
Salvage pyrimidine ribonucleotides
De novo pyrimidine ribonucleotides biosythesis
Toll receptor signaling pathway
Adenine and hypoxanthine salvage pathway
Valine biosynthesis
Isoleucine biosynthesis
Arginine biosynthesis
Pyruvate metabolism
Cholesterol biosynthesis
Serine glycine biosynthesis
FAS signaling pathway
Heme biosynthesis
Pentose phosphate pathway
Plasminogen activating cascade
Fructose galactose metabolism
Mannose metabolism
Cell cycle
Glycolysis
Normalized Enrichment Score

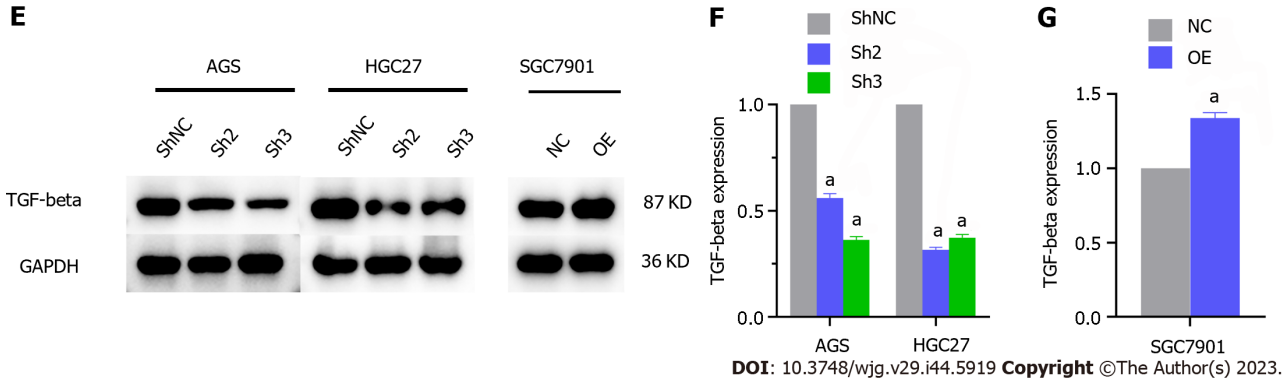

DOI: 10.3748/wjg.v29.i44.5919

Figure 5 Tousled-like kinase 1 drives gastric cancer progression by modulating the tumor growth factor-beta signaling pathway. A and B: Genes positively and negatively correlated with Tousled-like kinase 1 (TLK1) were identified from The Cancer Genome Atlas database; C: Kyoto Encyclopedia of Genes and Genomes analysis identifying the differentially expressed genes and their associated enriched pathways; D: Gene set enrichment analysis of pathway enrichment; E–G: Western blot evaluating tumor growth factor-beta expression in gastric cancer cell lines in response to TLK1 knockdown or overexpression. $^{a}P < 0.05$. TGF-beta: Tumor growth factor-beta; shNC: Short hairpin RNA of negative control; NC: Negative control; OE: Overexpression.

In vivo assays confirmed that TLK1 drives GC progression

We then validated the impact of TLK1 on GC progression through subcutaneous xenograft tumor induction in nude mice. The study included control and TLK1 overexpression groups (Figure 6A). Compared to the former, the latter presented significantly larger tumor size, volume, and mass (Figure 6B–D). Western blot and IHC verified that the TLK1 and TGF-β expression levels were considerably higher in the treatment group presenting large tumors than in the control group exhibiting small tumors (Figure 6E-G).

Antigen Kiel 67 staining of the tumors revealed that cancer proliferation was markedly higher in the TLK1 overexpression group than in the control group (Figure 6H and I). Hematoxylin and eosin and terminal deoxynucleotidyl transferase dUTP nick end labeling staining exposed substantially greater apoptotic necrosis in the control group than in the TLK1 overexpression group (Figure 6J and K).

DISCUSSION

The mortality rate of advanced GC remains high despite the progress that has been made in the therapeutic approaches used against it[28]. Hence, novel treatments for GC are urgently needed. TLK promotes the progression of various malignancies. Therefore, research on TLK in the context of cancer therapy should be prioritized[18-21,23-26]. Here, we examined TLK1 expression in GC cells, investigated its effects on their functions, and used *in vivo* experiments to clarify how it modulates GC progression.

Previous studies reported that TLK1 was upregulated in gliomas[23,25]. In the present work, we discovered that TLK1 was significantly overexpressed in GC cells and tissues (Figure 1B–E). Immunofluorescence staining also revealed that TLK1 was localized mainly to GC cell nuclei (Figure 1F).

We then assessed the impact of TLK1 on GC cell function. TLK1 was overexpressed in the SGC7901 cell line (Figure 2A). Colony formation, EdU, and Transwell assays disclosed that TLK1 overexpression promoted SGC7901 cell proliferation, invasion, and migration (Figure 2B–G). TLK1 knockdown had the opposite effects on AGS and HGC27 cell lines (Figures 3 and 4). An earlier study reported similar findings for the roles of TLK1 in other cancer types[25]. Taken together, these results suggest that TLK1 contributes to GC progression. Our bioinformatics analysis revealed that the mechanism of TLK1 was associated with the TGF-β signaling pathway in GC (Figure 5C and D). The TGF-β signaling pathway comprises TGF-β itself, activins, nodal, bone morphogenetic proteins, growth and differentiation factors, and other factors[29,30] and plays vital roles in human embryonic development and homeostasis[31]. A recent study showed that alterations in TGF-β signaling may result in immunocompromise, fibrosis, and carcinogenesis[32]. The TGF-β signaling pathway may either inhibit or promote tumorigenesis depending upon the tumor microenvironment or cancer stage[29,33,34]. We used western blot to measure TGF-β expression in response to TLK1 overexpression or knockdown and found a positive correlation between TLK1 and TGF-β (Figure 5E and F). Thus, TLK1 may promote GC progression by upregulating TGF-β. We validated this mechanism *in vivo* by inducing subcutaneous xenograft tumor formation in nude mice (Figure 6) and substantiated the critical role of TLK1 in GC progression. To the best of our knowledge, the present work is one of the first to delineate the expression, localization, and functional impact of TLK1 in GC.

CONCLUSION

We demonstrated that TLK1 is highly expressed in GC, localized mainly to the nucleus, significantly promotes GC cell proliferation, invasion, and migration, and inhibits apoptosis. TLK1 may facilitate GC progression by modulating TGF-β

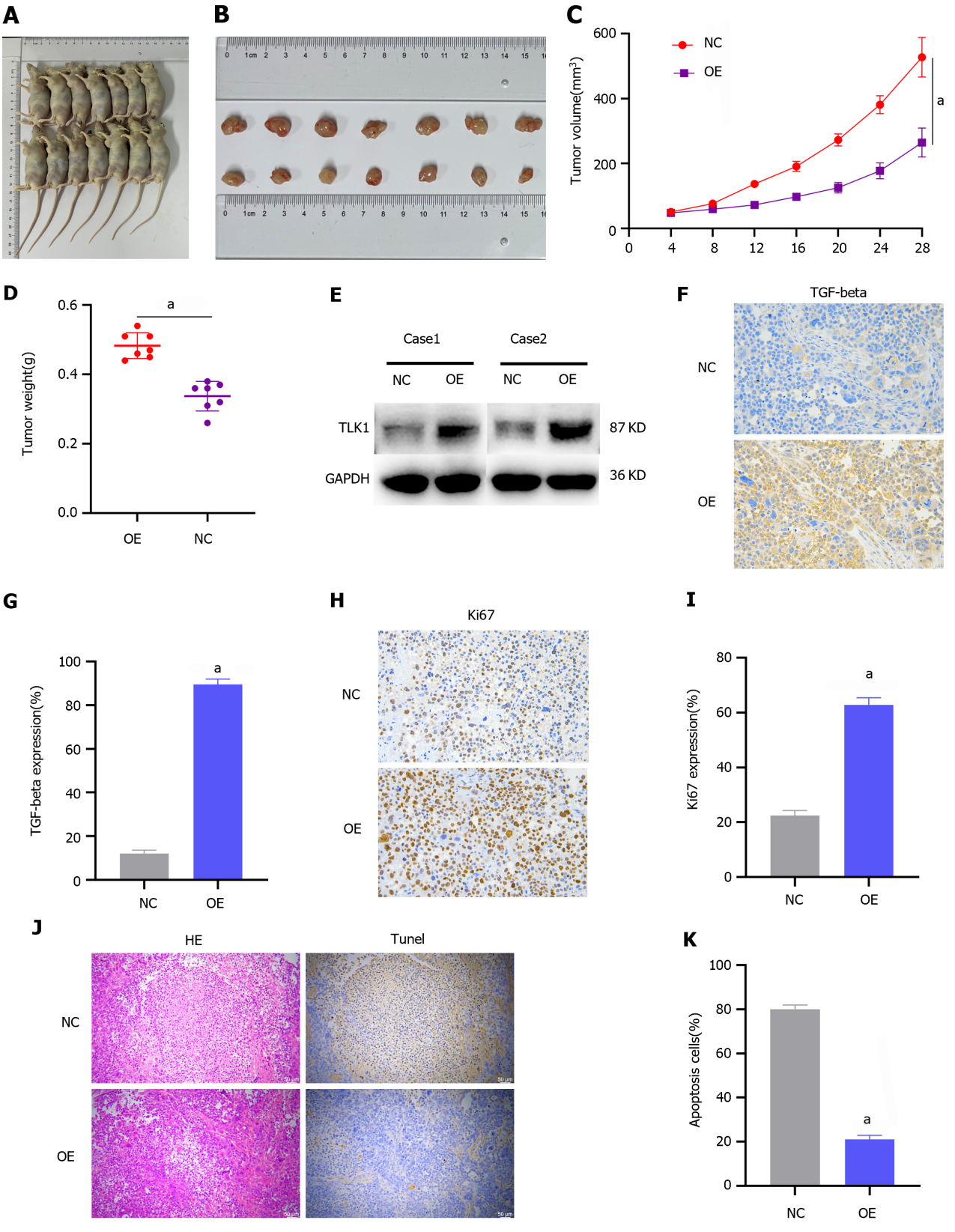

DOI: 10.3748/wjg.v29.i44.5919

Figure 6 *In vivo* confirmation of the role of Tousled-like kinase 1 in gastric cancer progression. A and B: Relative tumorigenesis between the control and Tousled-like kinase 1 (TLK1) overexpression groups; C and D: Differences in tumor volume and mass between the control and TLK1 overexpression groups; E: Western blot verifying differential TLK1 expression in tumor tissues; F and G: Immunohistochemical (IHC) staining detecting the differences in tumor growth factor-beta expression between the control and TLK1 overexpression groups; H and I: IHC staining showing the differences in Ki-67 expression between the control and TLK1 overexpression groups; J and K: IHC and HE staining disclosing the differences in apoptosis between the control and TLK1 overexpression groups. $^{a}P < 0.05$. TGF-beta: Tumor growth factor-beta; NC: Negative control; OE: Overexpression.

expression. We believe that TLK1 could be a crucial therapeutic target for GC, and propose that future investigations evaluate the feasibility and practicality of targeting TLK1 in GC treatment.

ARTICLE HIGHLIGHTS

Research background

Gastric cancer (GC) is the fifth most prevalent cancer and the third leading cause of cancer-related mortality worldwide. Endoscopy is the mainstay of early-stage GC treatment whereas advanced GC must be managed through surgery and other interventions including chemotherapy and targeted therapy. Despite significant progress in GC control, however, its overall survival remains unsatisfactory.

Research motivation

Potential therapeutic targets against GC are urgently required.

Research objectives

The present study aimed to elucidate the functional significance of Tousled-like kinase 1 (TLK1) in GC cells and potentially identify a novel therapeutic target against this disease.

Research methods

We measured TLK1 protein expression levels and localized TLK1 in GC cells and tissues by western blot and immunofluorescence, respectively. We transfected various GC cells with lentiviruses to create TLK1 overexpression and knockdown lines and established the functional roles of TLK1 through *in vitro* colony formation, 5-ethynyl-2`-deoxyuridine, and Transwell assays as well as flow cytometry. We applied bioinformatics to elucidate the signaling pathways associated with TLK1. We performed *in vivo* validation of TLK1 functions by inducing subcutaneous xenograft tumors in nude mice.

Research results

TLK1 was significantly upregulated in GC cells and tissues compared to their normal counterparts and was localized mainly to the nucleus. TLK1 knockdown significantly decreased colony formation, proliferation, invasion, and migration but increased apoptosis in GC cells. TLK1 overexpression had the opposite effects. Bioinformatics revealed, and subsequent experiments verified, that the tumor growth factor-beta (TGF-β) signaling pathway was implicated in TLK1-mediated GC progression. The *in vivo* assays confirmed that TLK1 promotes tumorigenesis in GC.

Research conclusions

We demonstrated that TLK1 is highly expressed in GC, localized mainly to the nucleus, significantly promotes GC cell proliferation, invasion, and migration, and inhibits apoptosis. TLK1 may facilitate GC progression by modulating TGF-β expression. We believe that TLK1 could be a crucial therapeutic target for GC.

Research perspectives

Future investigations evaluate the feasibility and practicality of targeting TLK1 in GC treatment.

ACKNOWLEDGEMENTS

The authors thank the personnel at the Center for Scientific Research of the First Affiliated Hospital of Anhui Medical University for their valuable assistance with our experiments.

FOOTNOTES

Co-first authors: Ruo-Chuan Sun and Jing Li.

Co-corresponding authors: Ming-Liang Wang and Yong-Xiang Li.

Author contributions: Li YX and Wang ML conceived the study design; Wang HZ and Dal E wrote the manuscript. Sun RC and Li J performed the experiments; Li YX participated in the cell culture and *in vitro* experiments; All authors contributed to the article and approved the final submitted version. Li YX and Wang ML contributed equally to this work as co-corresponding authors. The reasons for designating Li YX and Wang ML as co-corresponding authors are twofold. First, the main design of this project is completed by Li YX and Wang ML, which makes our project more rigorous. Second, the choice of these researchers as co-corresponding authors acknowledges and respects this equal contribution, while recognizing the spirit of teamwork and collaboration of this study. Sun RC and Li J contributed equally to this work as co-first authors. The reasons for designating Sun RC and Li J as co-first authors are also twofold. Sun RC and Li J completed all *in vitro* and *in vivo* experiments of this study, and made great contributions to this study. They contributed efforts of equal substance throughout the research process. Second, the research was performed as a collaborative effort, and

the designation of co-first authorship accurately reflects the distribution of responsibilities and burdens associated with the time and effort required to complete the study and the resultant paper. This also ensures effective communication and management of post-submission matters, ultimately enhancing the paper's quality and reliability. summary, we believe that designating Li YX and Wang ML as co-corresponding authors and Sun RC and Li J as co-first authors of is fitting for our manuscript as it accurately reflects our team's collaborative spirit, equal contributions, and diversity.

Supported by the Key Programs of the Educational Commission of Anhui Province, No. 2023AH053313; and the Research Project of Higher Education in Anhui Province in 2022, No. 2022AH051192.

Institutional review board statement: Institutional review board statement: The study was reviewed and approved by the the Ethics Committee of Anhui Medical University (Approval No. 20180323).

Institutional animal care and use committee statement: All procedures involving animals were reviewed and approved by the Institutional Animal Care and Use Committee of Anhui Medical University (No. 20180345).

Conflict-of-interest statement: The authors have no conflict of interest to declare.

Data sharing statement: Technical appendix, statistical code, and dataset available from the corresponding author at liyongxiang@ahmu.edu.cn.

ARRIVE guidelines statement: The authors have read the ARRIVE Guidelines, and the manuscript was prepared and revised according to the ARRIVE Guidelines.

Country/Territory of origin: China

ORCID number: Jing Li 0009-0006-4499-5427; Hui-Zhen Wang 0000-0002-3377-7284; Ming-Liang Wang 0000-0002-4830-9467; Yong-Xiang Li 0000-0001-7183-9485.

S-Editor: Lin C
L-Editor: A
P-Editor: Chen YX

REFERENCES

1 **Bray F**, Ferlay J, Soerjomataram I, Siegel RL, Torre LA, Jemal A. Global cancer statistics 2018: GLOBOCAN estimates of incidence and mortality worldwide for 36 cancers in 185 countries. *CA Cancer J Clin* 2018; **68**: 394-424 [PMID: 30207593 DOI: 10.3322/caac.21492]
2 **Smyth EC**, Nilsson M, Grabsch HI, van Grieken NC, Lordick F. Gastric cancer. *Lancet* 2020; **396**: 635-648 [PMID: 32861308 DOI: 10.1016/S0140-6736(20)31288-5]
3 **Silljé HH**, Takahashi K, Tanaka K, Van Houwe G, Nigg EA. Mammalian homologues of the plant Tousled gene code for cell-cycle-regulated kinases with maximal activities linked to ongoing DNA replication. *EMBO J* 1999; **18**: 5691-5702 [PMID: 10523312 DOI: 10.1093/emboj/18.20.5691]
4 **Han Z**, Saam JR, Adams HP, Mango SE, Schumacher JM. The C. elegans Tousled-like kinase (TLK-1) has an essential role in transcription. *Curr Biol* 2003; **13**: 1921-1929 [PMID: 14614817 DOI: 10.1016/j.cub.2003.10.035]
5 **Giménez AC**, Tamajón LG. Analysis of the third-order structuring of Shalom Schwartz's theory of basic human values. *Heliyon* 2019; **5**: e01797 [PMID: 31198868 DOI: 10.1016/j.heliyon.2019.e01797]
6 **Silljé HH**, Nigg EA. Identification of human Asf1 chromatin assembly factors as substrates of Tousled-like kinases. *Curr Biol* 2001; **11**: 1068-1073 [PMID: 11470414 DOI: 10.1016/s0960-9822(01)00298-6]
7 **Han Z**, Riefler GM, Saam JR, Mango SE, Schumacher JM. The C. elegans Tousled-like kinase contributes to chromosome segregation as a substrate and regulator of the Aurora B kinase. *Curr Biol* 2005; **15**: 894-904 [PMID: 15916946 DOI: 10.1016/j.cub.2005.04.019]
8 **Dillon PJ**, Gregory SM, Tamburro K, Sanders MK, Johnson GL, Raab-Traub N, Dittmer DP, Damania B. Tousled-like kinases modulate reactivation of gammaherpesviruses from latency. *Cell Host Microbe* 2013; **13**: 204-214 [PMID: 23414760 DOI: 10.1016/j.chom.2012.12.005]
9 **Li Z**, Gourguechon S, Wang CC. Tousled-like kinase in a microbial eukaryote regulates spindle assembly and S-phase progression by interacting with Aurora kinase and chromatin assembly factors. *J Cell Sci* 2007; **120**: 3883-3894 [PMID: 17940067 DOI: 10.1242/jcs.007955]
10 **Krause DR**, Jonnalagadda JC, Gatei MH, Sillje HH, Zhou BB, Nigg EA, Khanna K. Suppression of Tousled-like kinase activity after DNA damage or replication block requires ATM, NBS1 and Chk1. *Oncogene* 2003; **22**: 5927-5937 [PMID: 12955071 DOI: 10.1038/sj.onc.1206691]
11 **Groth A**, Lukas J, Nigg EA, Silljé HH, Wernstedt C, Bartek J, Hansen K. Human Tousled like kinases are targeted by an ATM- and Chk1-dependent DNA damage checkpoint. *EMBO J* 2003; **22**: 1676-1687 [PMID: 12660173 DOI: 10.1093/emboj/cdg151]
12 **Sunavala-Dossabhoy G**, De Benedetti A. Tousled homolog, TLK1, binds and phosphorylates Rad9; TLK1 acts as a molecular chaperone in DNA repair. *DNA Repair (Amst)* 2009; **8**: 87-102 [PMID: 18940270 DOI: 10.1016/j.dnarep.2008.09.005]
13 **Kelly R**, Davey SK. Tousled-like kinase-dependent phosphorylation of Rad9 plays a role in cell cycle progression and G2/M checkpoint exit. *PLoS One* 2013; **8**: e85859 [PMID: 24376897 DOI: 10.1371/journal.pone.0085859]
14 **Sen SP**, De Benedetti A. TLK1B promotes repair of UV-damaged DNA through chromatin remodeling by Asf1. *BMC Mol Biol* 2006; **7**: 37

[PMID: 17054786 DOI: 10.1186/1471-2199-7-37]

15 **Sunavala-Dossabhoy G**, Balakrishnan SK, Sen S, Nuthalapaty S, De Benedetti A. The radioresistance kinase TLK1B protects the cells by promoting repair of double strand breaks. *BMC Mol Biol* 2005; **6**: 19 [PMID: 16156902 DOI: 10.1186/1471-2199-6-19]

16 **Canfield C**, Rains J, De Benedetti A. TLK1B promotes repair of DSBs *via* its interaction with Rad9 and Asf1. *BMC Mol Biol* 2009; **10**: 110 [PMID: 20021694 DOI: 10.1186/1471-2199-10-110]

17 **Sunavala-Dossabhoy G**, Fowler M, De Benedetti A. Translation of the radioresistance kinase TLK1B is induced by gamma-irradiation through activation of mTOR and phosphorylation of 4E-BP1. *BMC Mol Biol* 2004; **5**: 1 [PMID: 15070431 DOI: 10.1186/1471-2199-5-1]

18 **Khalil MI**, De Benedetti A. The TLK1-MK5 Axis Regulates Motility, Invasion, and Metastasis of Prostate Cancer Cells. *Cancers (Basel)* 2022; **14** [PMID: 36497211 DOI: 10.3390/cancers14235728]

19 **Khalil MI**, Singh V, King J, De Benedetti A. TLK1-mediated MK5-S354 phosphorylation drives prostate cancer cell motility and may signify distinct pathologies. *Mol Oncol* 2022; **16**: 2537-2557 [PMID: 35064619 DOI: 10.1002/1878-0261.13183]

20 **Singh V**, Khalil MI, De Benedetti A. The TLK1/Nek1 axis contributes to mitochondrial integrity and apoptosis prevention *via* phosphorylation of VDAC1. *Cell Cycle* 2020; **19**: 363-375 [PMID: 31914854 DOI: 10.1080/15384101.2019.1711317]

21 **Singh V**, Jaiswal PK, Ghosh I, Koul HK, Yu X, De Benedetti A. The TLK1-Nek1 axis promotes prostate cancer progression. *Cancer Lett* 2019; **453**: 131-141 [PMID: 30928383 DOI: 10.1016/j.canlet.2019.03.041]

22 **Singh V**, Bhoir S, Chikhale RV, Hussain J, Dwyer D, Bryce RA, Kirubakaran S, De Benedetti A. Generation of Phenothiazine with Potent Anti-TLK1 Activity for Prostate Cancer Therapy. *iScience* 2020; **23**: 101474 [PMID: 32905878 DOI: 10.1016/j.isci.2020.101474]

23 **Wang Z**, Chen X, Liang Q, An Y, Wei M, Shi W. Inhibiting of circ-TLK1 inhibits the progression of glioma through down-regulating PANX1 *via* targeting miR-17-5p. *J Mol Histol* 2021; **52**: 1007-1020 [PMID: 34181173 DOI: 10.1007/s10735-021-09993-x]

24 **Zhang Z**, Liu S. The interaction between ASF1B and TLK1 promotes the malignant progression of low-grade glioma. *Ann Med* 2023; **55**: 1111-1122 [PMID: 36947060 DOI: 10.1080/07853890.2023.2169751]

25 **Ibrahim K**, Abdul Murad NA, Harun R, Jamal R. Knockdown of Tousledlike kinase 1 inhibits survival of glioblastoma multiforme cells. *Int J Mol Med* 2020; **46**: 685-699 [PMID: 32468002 DOI: 10.3892/ijmm.2020.4619]

26 **Hu S**, Wang H, Yan D, Lu W, Gao P, Lou W, Kong X. Loss of miR-16 contributes to tumor progression by activation of tousled-like kinase 1 in oral squamous cell carcinoma. *Cell Cycle* 2018; **17**: 2284-2295 [PMID: 30252587 DOI: 10.1080/15384101.2018.1526601]

27 **Sun R**, Wu J, Chen Y, Lu M, Zhang S, Lu D, Li Y. Down regulation of Thrombospondin2 predicts poor prognosis in patients with gastric cancer. *Mol Cancer* 2014; **13**: 225 [PMID: 25262009 DOI: 10.1186/1476-4598-13-225]

28 **Joshi SS**, Badgwell BD. Current treatment and recent progress in gastric cancer. *CA Cancer J Clin* 2021; **71**: 264-279 [PMID: 33592120 DOI: 10.3322/caac.21657]

29 **David CJ**, Massagué J. Contextual determinants of TGFβ action in development, immunity and cancer. *Nat Rev Mol Cell Biol* 2018; **19**: 419-435 [PMID: 29643418 DOI: 10.1038/s41580-018-0007-0]

30 **Saito A**, Horie M, Nagase T. TGF-β Signaling in Lung Health and Disease. *Int J Mol Sci* 2018; **19** [PMID: 30127261 DOI: 10.3390/ijms19082460]

31 **Xu X**, Zheng L, Yuan Q, Zhen G, Crane JL, Zhou X, Cao X. Transforming growth factor-β in stem cells and tissue homeostasis. *Bone Res* 2018; **6**: 2 [PMID: 29423331 DOI: 10.1038/s41413-017-0005-4]

32 **Liu S**, Ren J, Ten Dijke P. Targeting TGFβ signal transduction for cancer therapy. *Signal Transduct Target Ther* 2021; **6**: 8 [PMID: 33414388 DOI: 10.1038/s41392-020-00436-9]

33 **Neuzillet C**, Tijeras-Raballand A, Cohen R, Cros J, Faivre S, Raymond E, de Gramont A. Targeting the TGFβ pathway for cancer therapy. *Pharmacol Ther* 2015; **147**: 22-31 [PMID: 25444759 DOI: 10.1016/j.pharmthera.2014.11.001]

34 **Colak S**, Ten Dijke P. Targeting TGF-β Signaling in Cancer. *Trends Cancer* 2017; **3**: 56-71 [PMID: 28718426 DOI: 10.1016/j.trecan.2016.11.008]

World Journal of Gastroenterology

Submit a Manuscript: https://www.f6publishing.com

World J Gastroenterol 2023 November 28; 29(44): 5935-5944

DOI: 10.3748/wjg.v29.i44.5935

ISSN 1007-9327 (print) ISSN 2219-2840 (online)

CASE REPORT

Mucosal esophageal carcinoma following endoscopic submucosal dissection with giant gastric metastasis: A case report and review of literature

Mei-Qi Yang, Ming-Jun Sun, Hui-Jing Zhang

Specialty type: Gastroenterology and hepatology

Provenance and peer review: Unsolicited article; Externally peer reviewed.

Peer-review model: Single blind

Peer-review report's scientific quality classification

Grade A (Excellent): A
Grade B (Very good): B
Grade C (Good): 0
Grade D (Fair): 0
Grade E (Poor): 0

P-Reviewer: Lu P, United States; Mori F, Italy

Received: September 19, 2023
Peer-review started: September 19, 2023
First decision: October 8, 2023
Revised: October 15, 2023
Accepted: November 14, 2023
Article in press: November 14, 2023
Published online: November 28, 2023

Mei-Qi Yang, Hui-Jing Zhang, Department of Gastroenterology, The First Hospital of China Medical University, Shenyang 110000, Liaoning Province, China

Ming-Jun Sun, Department of Endoscopy, The First Affiliated Hospital of China Medical University, Shenyang 110000, Liaoning Province, China

Corresponding author: Hui-Jing Zhang, PhD, Professor, Department of Gastroenterology, The First Hospital of China Medical University, No. 155 Beier Road, Nanjing Street, Shenyang 110000, Liaoning Province, China. hjzhang@cmu.edu.cn

Abstract

BACKGROUND

Esophageal carcinoma is a highly aggressive digestive cancer responsible for a notable proportion of cancer-related deaths worldwide. Its elevated metastatic rate contributes to a poor prognosis in affected patients. In this case review, we aim to summarize the metastatic characteristics of intramural gastric metastasis (IGM) in mucosal esophageal squamous carcinoma.

CASE SUMMARY

A 56-year-old man was admitted to our hospital because of a dry cough with an esophageal sensation for one year. Endoscopic examination revealed a 2.0 cm 1.0 cm, superficial esophageal squamous cell carcinoma, and the patient underwent endoscopic submucosal dissection (ESD). Fifteen months after ESD, positron emission tomography/computed tomography revealed that the metabolism of the stomach cardia wall had increased slightly. However, the mucosa of the gastric cardia was smooth under gastroendoscopy. Two years after ESD, endoscopic examination revealed a giant gastric cardia carcinoma, while the esophageal mucosa was smooth, and no advanced cancer was found. A biopsy of the gastric cardia indicated squamous-cell carcinoma. The patient received immunochemotherapy and radiotherapy for esophageal cancer for 8 mo and is currently under follow-up.

CONCLUSION

Early-stage esophageal carcinoma with IGM is rare. Despite the ESD of the primary lesion, IGM may still occur and should be closely monitored after ESD.

Key Words: Esophageal squamous cell carcinoma; Intramural metastasis; Endoscopic submucosal dissection; Case report

Core Tip: This study presents a rare case of mucosal esophageal squamous cell carcinoma (ESCC) post endoscopic submucosal dissection with giant gastric cardia metastasis. intramural gastric metastasis has also been reported to plays a role in distant metastasis, particularly in the liver. Preoperative and postoperative endoscopic follow-up of patients with ESCC of any stage, although the depth of an esophageal cancer may be T1.

Citation: Yang MQ, Sun MJ, Zhang HJ. Mucosal esophageal carcinoma following endoscopic submucosal dissection with giant gastric metastasis: A case report and review of literature. *World J Gastroenterol* 2023; 29(44): 5935-5944
URL: https://www.wjgnet.com/1007-9327/full/v29/i44/5935.htm
DOI: https://dx.doi.org/10.3748/wjg.v29.i44.5935

INTRODUCTION

Globally, esophageal squamous cell carcinoma (SCC) (ESCC) is the sixth leading cause of cancer-related deaths. In Asian countries, SCC is the most common pathological type of esophageal cancer. The prognosis of ESCC is poor owing to its increased tendencyfor direct spread and metastasis. The 5-year survival rate of ESCC patients with metastatic disease is less than 5%[1]. ESCC often metastasizes to the lymph nodes and distant organs, and intramural metastasis (IM) occasionally occurs, which is seen in approximately 10% of esophageal carcinomas[2,3]. IM is a form that tumor can occur as a skip lesion in the other parts of esophagus or to the stomach. IM incidence in ESCC in the head and neck is 25%, compared with 11% in stage I ESCC[4]. However, the reported intramural gastric metastasis (IGM) is seldom, accounting for only 1%–4.58% of ESCC through surgical treatment[5-9]. A higher incidence of IGM has been reported in the advanced ESCC, whereas only a few cases of IGM have been reported in the early-stage ESCC[10-13]. Herein, we report a case of mucosal esophageal carcinoma with multi-pathway and multi-organ metastases (including IGM, lymphatic metastasis of celiac lymph nodes, and hematogenous metastasis of the liver and right adrenal gland) that occurred in a metachronous manner, while the IGM progressed rapidly over 1 year. We hope that this case will guideclinicians in identifying unique metastasis of ESCC in some cases when making a treatment plan.

CASE PRESENTATION

Chief complaints

In August 2020, a 56-year-old man was admitted to our hospital for a dry cough with an esophageal sensation.

History of present illness

The symptoms started 1 year before presentation.

History of past illness

The patient had no relevant past illness.

Personal and family history

The patient had a smoking history for 20 years, with 20 cigarettes daily and drinking approximately 4000 mL of beer 3–4 times a week for 20 years.

Physical examination

There was no abnormal in physical examination.

Laboratory examinations

All blood test results, including tumor markers, were within normal limits.

Imaging examinations

Gastroendoscopy showed a 2.0 cm × 1.0 cm, superficial, flat, slightly rough, and red esophageal lesion 30 cm from the incisor teeth. Magnifying endoscopy with narrow-band imaging observations showed that the background mucus was brown, and the intrapapillary capillary loop was Type B1 (JES). Iodine staining showed no stain but showed its apparent margins more, and the pink sign was positive in the central part. The remaining esophageal mucosa was scattered in patchy light-stained areas, ranging from 0.2–0.4 cm (Figure 1A). Computed tomography (CT) revealed a small cyst in the

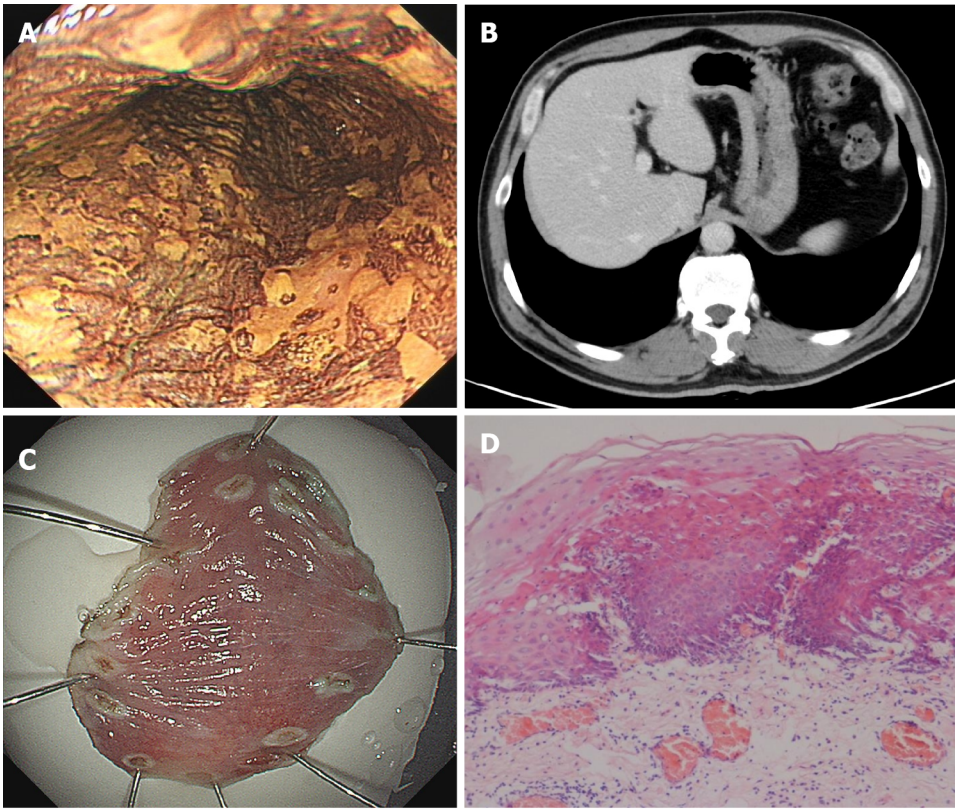

DOI: 10.3748/wjg.v29.i44.5935 **Copyright** ©The Author(s) 2023.

Figure 1 The first gastroendoscopy examination in August 2020. A: After iodine staining, the esophageal mucosa was scattered in patchy light-stained areas, ranging from 0.2 cm to 0.4 cm, and a 2.0 cm × 1.0 cm, superficial, flat lesion (30 cm from the incisor teeth) did not stain, whereas the pink areas were positive; B: Computed tomography showed no abnormal thickening in the gastrointestinal wall; C: Endoscopic submucosal dissection was performed 1 wk after gastroendoscopy; D: Postoperative pathology revealed moderate to severe dysplasia of squamous epithelium.

liver; however, no abnormal thickening of the gastrointestinal wall was observed (Figure 1B). Endoscopic submucosal dissection (ESD) was performed 1 wk after the endoscopy (Figure 1C), and postoperative pathology revealed mucosal ESCC (Figure 1D).

In March 2021, the patient was re-examined 7 mo after ESD. Endoscopic examination showed a 1.0 cm × 2.0 cm scar on the right posterior wall of the esophagus 30 cm from the incisor teeth. Iodine staining showed that the esophageal mucosa was scattered in a patchy light-stained area, with a pink sign (-) (Figure 2A). The mucosa of the gastric fundus and cardia were smooth without any abnormalities (Figure 2B).

In July 2021, the patient was examined again 1 year after ESD. The esophageal mucosa was the same as that at the final endoscopic examination. While gastroendoscopy also showed a 0.6 cm × 0.8 cm IIa + IIc lesion near the anterior wall of the gastric fundus near the cardia, biopsy of this lesion revealed erosion with regeneration and moderate dysplasia locally. The other mucosa of the gastric fundus and cardia were smooth without any abnormalities (Figure 3A). CT also revealed a small cyst in the liver; however, no abnormal thickening was observed in the gastrointestinal wall (Figure 3B). The patient underwent ESD of the fundus lesion (Figure 3C), and postoperative pathology revealed moderate-to-severe dysplasia of the gastric mucosa (Figure 3D).

In November 2021, the patient received a 3rd examination 15 mo after the 1st ESD. Gastroendoscopy revealed patchy light-stained areas throughout the esophagus after iodine staining (Figure 4A). The mucosa of the gastric fundus and cardia was smooth, except for the scar after ESD, and no abnormalities were found on a gastroendoscopy (Figure 4B). CT showed no abnormal thickening of the gastrointestinal wall. However, positron emission tomography (PET)-CT revealed that the metabolism of the lower esophagus increased slightly, the metabolism of the stomach cardia wall increased slightly, and lymph nodes in the retroperitoneal area had high-density shadows and increased metabolism (Figure 4C).

In November 2022, the patient received a 4th endoscopy examination. The esophageal mucosa was smooth, and no advanced cancer was found (Figure 5A). Circumferential submucosal tumor (SMT)-like swelling was observed in the cardia and stomach body; local ulceration was observed, and multiple ulcers were formed. The mucosa surrounding the ulcer was regular and tough, the mucosa surrounding the lesion was clustered, and the lower edge of the lesion involved a minor curvature in the middle of the stomach body (Figure 5B). A biopsy of the cardia revealed SCC (Figure 5C). CT revealed a cardia tumor (Figure 5D), perigastric lymph node enlargement, and multiple metastatic tumors of the liver (Figure 5E) and right adrenal gland (Figure 5F).

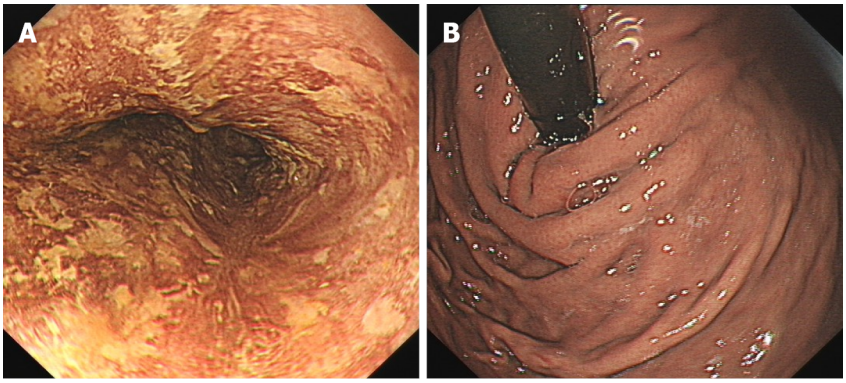

DOI: 10.3748/wjg.v29.i44.5935 **Copyright** ©The Author(s) 2023.

Figure 2 Re-examination of the patient 7 mo after endoscopic submucosal dissection in March 2021. A: Gastroendoscopy revealed a 1.0 cm × 2.0 cm scar on the right posterior wall of the esophagus, 30 cm from the incisor teeth. Iodine staining revealed that the esophageal mucosa was scattered in the patchy, lightly stained area, indicated by the pink sign (-); B: The mucosa of gastric fundus and cardia was smooth without abnormality.

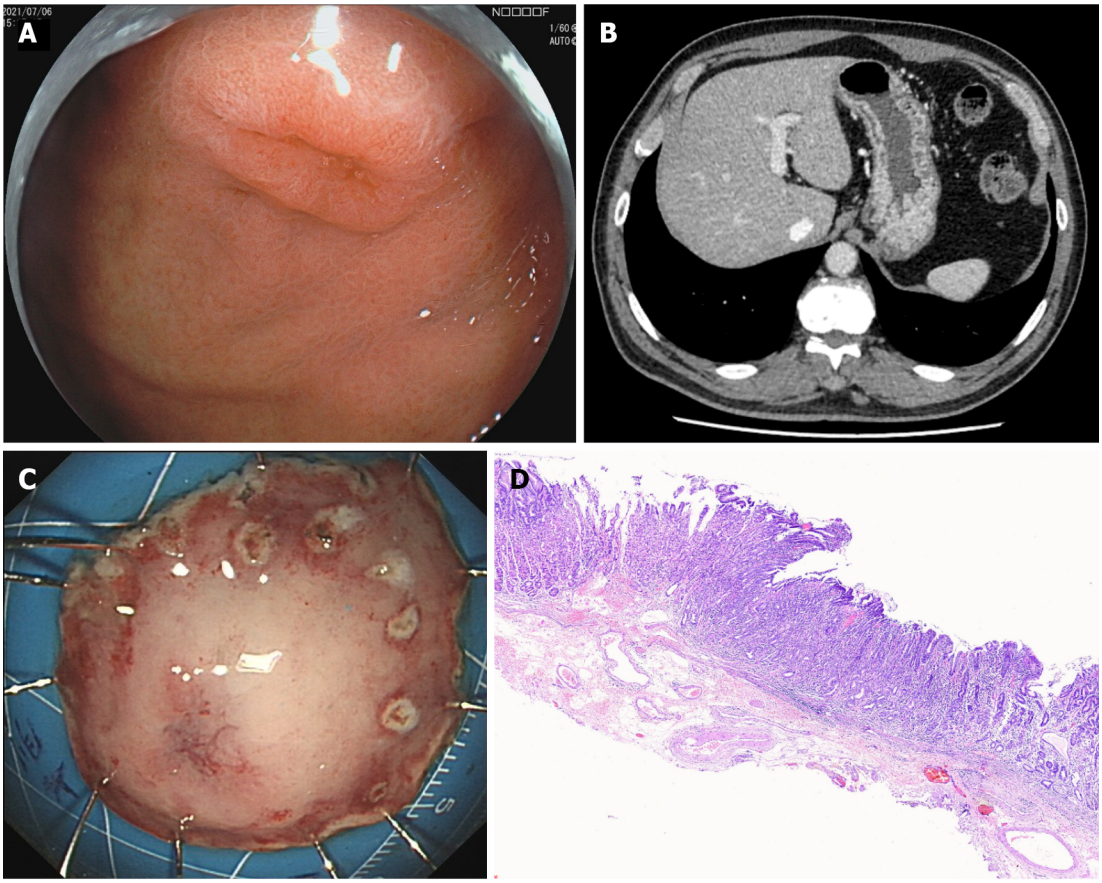

DOI: 10.3748/wjg.v29.i44.5935 **Copyright** ©The Author(s) 2023.

Figure 3 The patient was re-examined for the second time 1 year after endoscopic submucosal dissection in July 2021. A: Gastroendoscopy revealed a 0.6 cm × 0.8 cm IIa + IIc lesion near the anterior wall of the gastric fundus near the cardia. B: Computed tomography showed no abnormal thickening in the gastrointestinal wall; C: The patient underwent Endoscopic submucosal dissection of the fundus lesion; D: Postoperative pathology revealed moderate to severe dysplasia of gastric mucous.

FINAL DIAGNOSIS

The patient was diagnosed as early-stage esophageal carcinoma with giant gastric cardia metastasis.

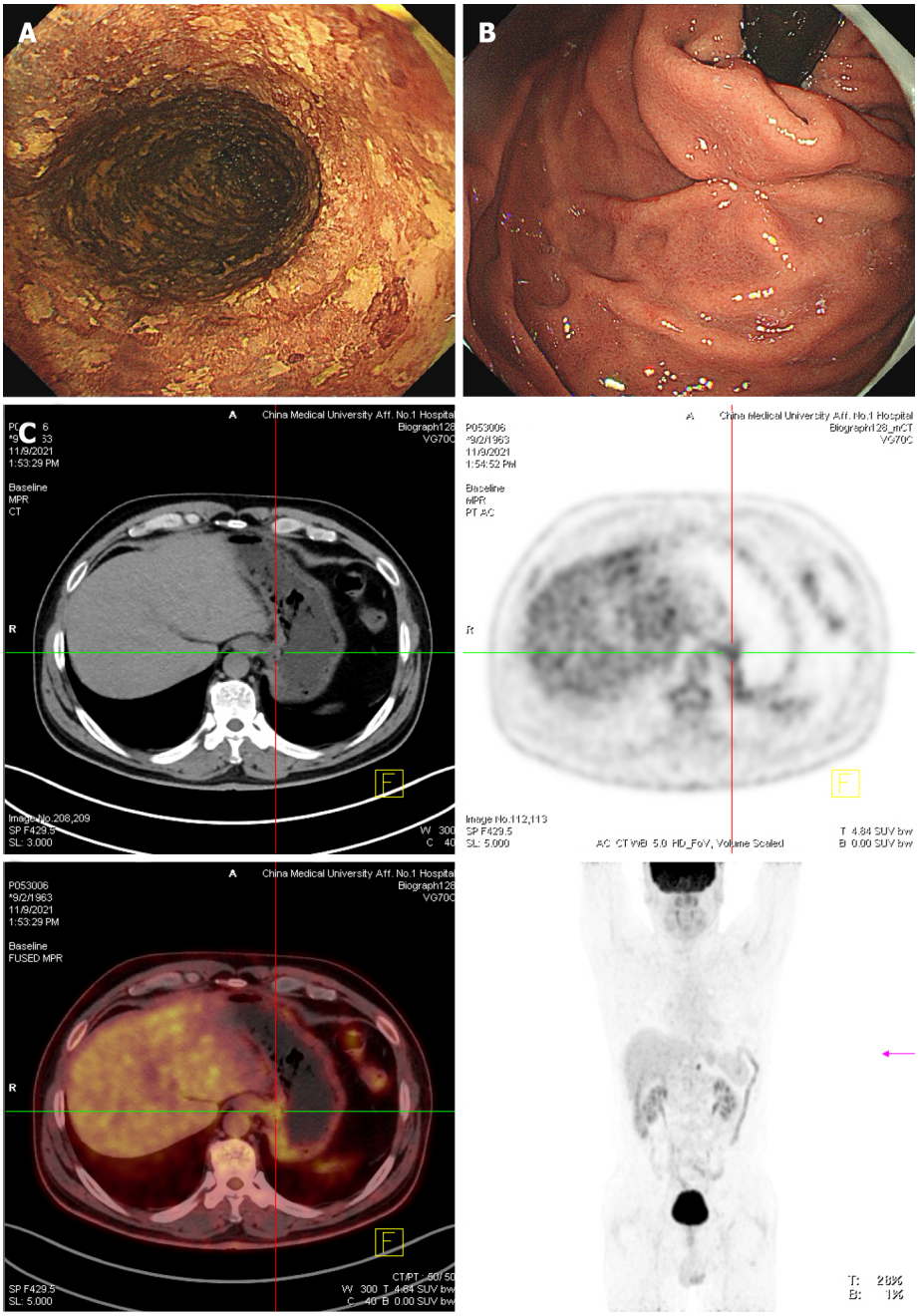

DOI: 10.3748/wjg.v29.i44.5935 **Copyright** ©The Author(s) 2023.

Figure 4 In November 2021, the patient underwent the third re-examination 15 mo after the first endoscopic submucosal dissection. A: The entire esophagus showed patchy, lightly stained areas after iodine staining in gastroendoscopy. B: The mucosa of the gastric fundus and cardia was smooth except for the scar after Endoscopic submucosal dissection operation, and no abnormality was noted on gastroendoscopy. C: Computed tomography (CT) revealed no abnormal thickening in the gastrointestinal wall. However, positron emission tomography-CT revealed that the metabolism of the lower esophagus and stomach cardia wall slightly increased. A lymph node was noted in the retroperitoneal area with high-density shadow and increased metabolism.

TREATMENT

To alleviate the observed multi-organ metastasis, the patient was administered immunochemotherapy (carrelizumab 200 mg D1, albumin paclitaxel 400 mg D1, and carboplatin 450 mg D1) and radiotherapy (30 courses) for esophageal cancer. Six immunochemotherapy and 30 radiotherapy courses were completed.

The development and treatment of the disease in the present case are summarized in Figure 6.

OUTCOME AND FOLLOW-UP

The immunochemotherapy and radiotherapy was completed and the patient was still alive. The follow-up is ongoing.

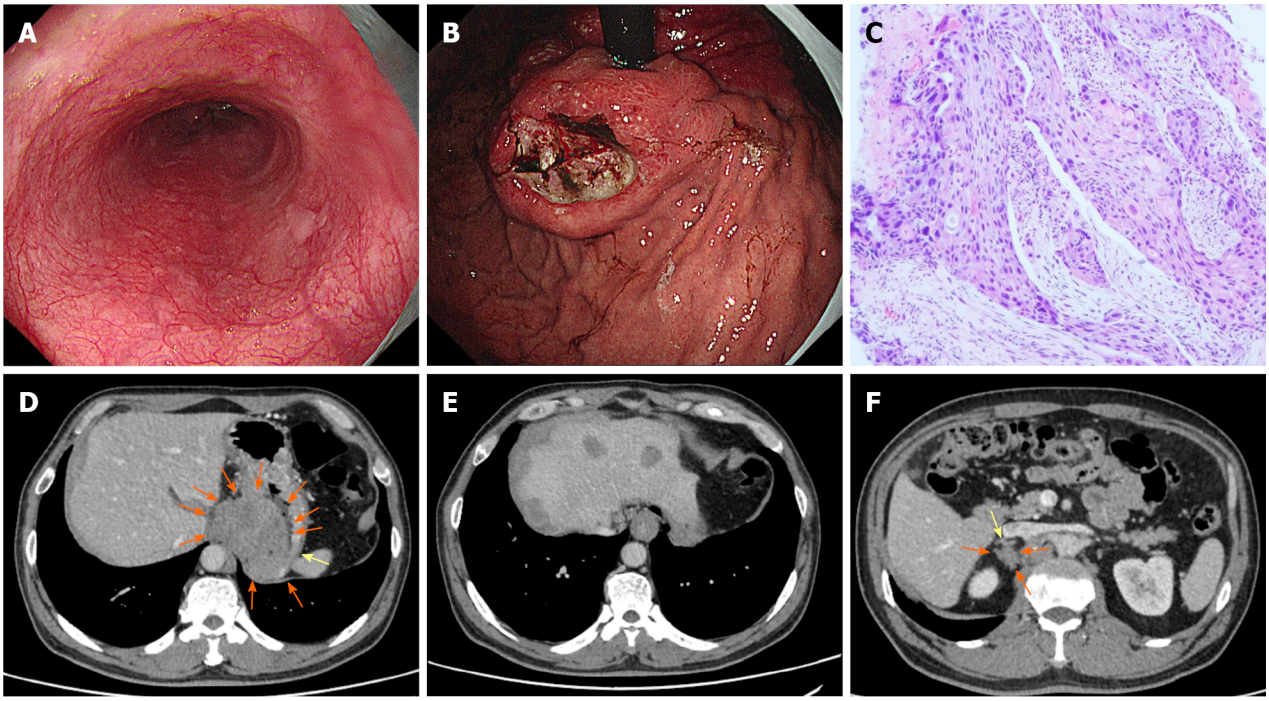

DOI: 10.3748/wjg.v29.i44.5935 **Copyright** ©The Author(s) 2023.

Figure 5 In November 2022, the patient underwent the fourth endoscopy re-examination. A: Esophageal mucosa was smooth, and no advanced cancer was noted; B: Circumferential submucosal tumor-like swelling was observed in the cardia and stomach body, along with local ulceration and the formation of multiple ulcers; C: Biopsy of cardia revealed squamous-cell carcinoma; D: Computed tomography (CT) showed cardia tumor; E: CT revealed multiple metastatic tumors in the liver; F: CT showed metastatic tumors in the right adrenal gland.

DISCUSSION

ESCC is an extremely aggressive cancer and has a poor prognosis owing to its higher propensity for lymph nodes and distant metastases. Historically, cancer-distal metastases are considered as the most important barrier to achieving significant advances in cancer management; moreover, it is responsible for 90% of cancer-related deaths[14,15]. The incidence of distant metastases in newly diagnosed ESCC is approximately 20%–30%. However, this proportion raised to approximately 40%–50% in recurrent cases after radical esophagectomy[16] or concurrent radiochemotherapy[17] in ESCC. IM is another metastasis pathway in esophageal cancer. Based on previous endoscopic findings, clinical IM, including gastric metastasis from ESCC, had mainly three characters: (1) Metastatic tumor often separated distantly from the primary tumor; (2) The metastatic lesion presented in the esophagus or stomach wall; and (3) the SMT lacked of an intraepithelial component, occasionally with an erosive change[6]. Accompanied by these findings, the ESCC strongly suggests an IM tumor[18].

Longitudinal lymphatic vessels contained in the mucosa lamina propria and submucosa of the esophagus are the anatomic basis for IM[19]. The mucosal lymphatic channels in esophagus are not directly connected to those in stomach; however, submucosal channels may have a direct connection with the submucosal gastric lymphatics[20]. Therefore, tumor cells go through the submucosal lymphatic system to the stomach wall and form metastatic loci[20]. Watson and Goodner[21] first reported there existed an interflow of lymphatic channels between the esophagus and stomach through virtue of neo-lymphangiogenesis in the carcinomatous lesion and explained IM as an extension of submucous lymphatics. Kato *et al*[6] documented that the location of the IM toward the primary tumor did not indicate a predilection in the direction of the lymphogenic spread of carcinoma of the esophagus. However, another study[5] showed that among 1259 patients, although the depth of esophageal cancer may be T1, the possibility of IGM still exists. The incidence of IGM is higher in advanced-stage ESCC[5,22], as only a few cases of IGM in the early-stage ESCC have been reported. From mucosal ESCC, to our best knowledge, only 6 cases (including the present one) have been documented[10-13,23]. Therefore, although the probability of lymphatic metastasis is very low, it can still occur even if the tumor is confined to the mucosa.

IGM from esophageal cancer is rare[5,9]; nonetheless, it is considered to be one of the most significant poor prognostic factors due to its higher rate of lymphatic invasion[24,25] and distant metastasis. The correlation between metastatic tumors and lymph node metastasis can be attributed to the fact that gastric metastases occur *via* the lymphatic system. In the middle and lower parts of the esophagus, submucosal lymphatic drainage is regarded to be connected to gastric from the cardia and fundus. At times, the primary esophageal lesion could appear to be small, compared with the gastric metastatic lesion, which is exophytic in morphology because of the submucosal site of implantation[22]. In this report, the primary tumor was in the middle-thoracic esophagus, and the IGM was found in the gastric cardia.

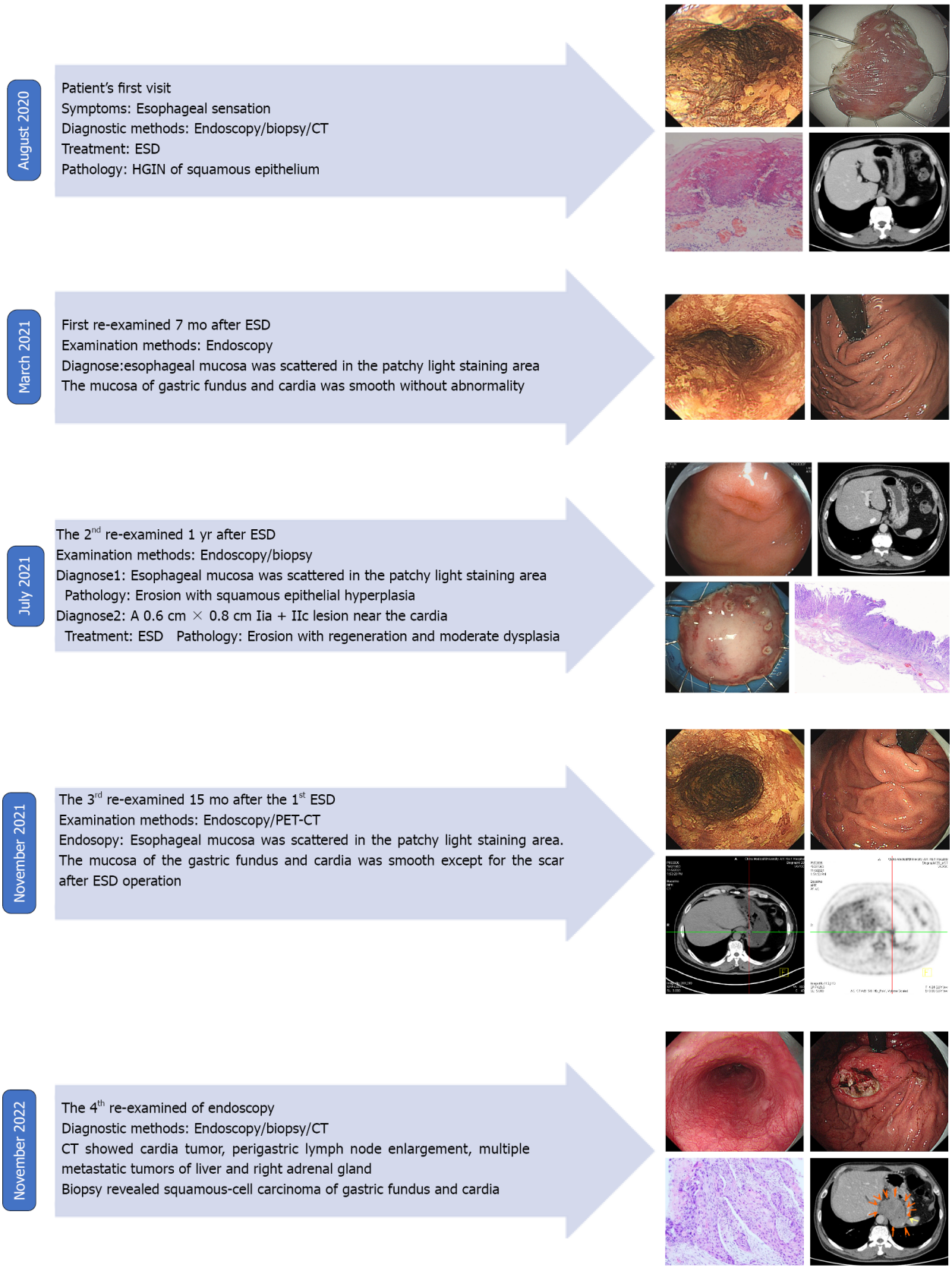

DOI: 10.3748/wjg.v29.i44.5935

Figure 6 Summary of disease development and treatment of the present case.

In addition, IGM plays a role in distant metastasis, particularly in the liver[6]. IGM of ESCC is categorized as distant metastasis, described as M1b stage IVB, according to the Union for International Cancer Control for International Cancer Control Classification[26]. However, other studies have reported metastases in the reconstructed stomach. IGM develops principally in the upper third of the stomach wall; however, it can also appear in the gastric body[5,9]. These mean IGM happen without direct involvement of the lymphatic system[27]. In this report, the tumor cells giving rise to IGM could not have spread *via* the lymphatic system because the primary tumor was confined to the mucosa with no lymphatic connection to the submucosa. Thus, IGM sometimes develops *via* routes other than the lymphatic system, including vascular routes. In addition, we found multiple distant metastases to the liver and right adrenal gland, which indicated that there were hematogenous pathways of metastasis in our case.

In our case, what really surprised us was that from November 2021 (PET-CT suggested abnormal cardiac metabolism) to November 2022 (gastroendoscopy revealed a Borrmann type II lesion in the cardiac area), metastases to the cardia grew rapidly and were so large that no significant primary lesions were found in the esophagus. The cardiac area is rich in blood supply, which is conducive to the root proliferation of squamous cells, and the cardiac area is significantly large [23,24]. Primary gastric adenocarcinoma sometimes has a similar gross appearance but a higher incidence in the lower part of the stomach. Gastrointestinal stromal tumors also appear as exophytic lesions. The detection rate of IM of ESCC ranges 5.5% between 16.6%[6,28]. General endoscopy has certain limitations when the metastases are confined below the mucosa without breaking through the surface. The radiological imaging, especially fluorodeoxyglucose-PET, can detect out early metastatic lesions in time[29-31]. Therefore, preoperative and postoperative radiographic follow-up is conducive to indicating the presence of IM[20,32]. The five-year disease-free survival rate of patients with ESCC with IM is significantly lower than that of patients without IM[6,33]. Therefore, multimodal treatments with strong antitumor effects should be administered.

CONCLUSION

In conclusion, preoperative and postoperative endoscopic follow-up of patients with ESCC of any stage, although the depth of an esophageal cancer may be T1, in addition to paying attention to esophageal lesions, the stomach should also be carefully examined, especially for the submucosal eminence in the upper part of the stomach, to consider the possibility of IGM, and the nature of the submucosal eminence can be clarified by combining endoscopic ultrasonography and ultrasonic puncture biopsy. Therefore, enhancing the preoperative and postoperative imaging and endoscopic ultrasonography are beneficial for indicating the existence of IM.

FOOTNOTES

Co-corresponding authors: Sun MJ and Zhang HJ.

Author contributions: Zhang HJ and Sun MJ had full access to all the content in the study and takes responsibility for the integrity and the accuracy of the data analysis; Yang MQ and Sun MJ performed information collection; Yang MQ and Zhang HJ wrote the paper and performed editing. Sun MJ and Zhang HJ contributed equally to this work as co-corresponding authors. The reasons for designating Sun MJ and Zhang HJ as co-corresponding authors are threefold. Firstly, our research project is a collaborative effort. Throughout the entire research process, we worked closely together, sharing responsibilities in experimental design, data analysis, and result interpretation. Each of us made significant contributions in different aspects, whether it be in experimental operations, data processing, or writing and revising the manuscript. Therefore, we believe that designating two corresponding authors accurately reflects our collective efforts and academic contributions. Secondly, the selection of two corresponding authors is also driven by our commitment to academic fairness and transparency. This also promotes the most comprehensive and in-depth examination of the research topic, ultimately enriching readers' understanding by offering various expert perspectives. Thirdly, Sun MJ and Zhang HJ contributed efforts of equal substance throughout the research process. Sun MJ made a significant contribution to the diagnostic process of this case. The choice of these researchers as co-corresponding authors acknowledges and respects this equal contribution, while recognizing the spirit of teamwork and collaboration of this study. In summary, we believe that designating Sun MJ and Zhang HJ as co-corresponding authors of is fitting for our manuscript as it accurately reflects our team's collaborative spirit, equal contributions, and diversity.

Supported by Natural Science Foundation of Liaoning Science, No. 2022-YGJC-71.

Informed consent statement: All procedures involving human participants performed in this study were in accordance with the ethical standards of the institutional and/or national research committee(s) and the Helsinki Declaration (as revised in 2013). Written informed consent was obtained from all patients.

Conflict-of-interest statement: All the authors report no relevant conflicts of interest for this article.

CARE Checklist (2016) statement: The authors have read the CARE Checklist (2016), and the manuscript was prepared and revised according to the CARE Checklist (2016).

Country/Territory of origin: China

ORCID number: Mei-Qi Yang 0000-0003-0886-3196; Ming-Jun Sun 0009-0001-0538-597X; Hui-Jing Zhang 0000-0002-6322-2335.

S-Editor: Lin C
L-Editor: A
P-Editor: Lin C

REFERENCES

1 **Siegel RL**, Miller KD, Jemal A. Cancer statistics, 2016. *CA Cancer J Clin* 2016; **66**: 7-30 [PMID: 26742998 DOI: 10.3322/caac.21332]
2 **Takubo K**, Sasajima K, Yamashita K, Tanaka Y, Fujita K. Prognostic significance of intramural metastasis in patients with esophageal carcinoma. *Cancer* 1990; **65**: 1816-1819 [PMID: 2317758 DOI: 10.1002/1097-0142(19900415)65:8<1816::aid-cncr2820650825>3.0.co;2-l]
3 **Seki M**. [Clinicopathological study on the intramural metastasis of the esophageal cancer]. *Nihon Geka Gakkai Zasshi* 1991; **92**: 1426-1435 [PMID: 1961180]
4 **Shaheen O**, Ghibour A, Alsaid B. Esophageal Cancer Metastases to Unexpected Sites: A Systematic Review. *Gastroenterol Res Pract* 2017; **2017**: 1657310 [PMID: 28659974 DOI: 10.1155/2017/1657310]
5 **Ebihara Y**, Hosokawa M, Kondo S, Katoh H. Thirteen cases with intramural metastasis to the stomach in 1259 patients with oesophageal squamous cell carcinoma. *Eur J Cardiothorac Surg* 2004; **26**: 1223-1225 [PMID: 15541989 DOI: 10.1016/j.ejcts.2004.08.019]
6 **Kato H**, Tachimori Y, Watanabe H, Itabashi M, Hirota T, Yamaguchi H, Ishikawa T. Intramural metastasis of thoracic esophageal carcinoma. *Int J Cancer* 1992; **50**: 49-52 [PMID: 1728612 DOI: 10.1002/ijc.2910500111]
7 **Kuwano H**, Baba K, Ikebe M, Kitamura K, Adachi Y, Mori M, Sugimachi K. Gastric involvement of oesophageal squamous cell carcinoma. *Br J Surg* 1992; **79**: 328-330 [PMID: 1576500 DOI: 10.1002/bjs.1800790415]
8 **Oda**, Kondo H, Yamao T, Saito D, Ono H, Gotoda T, Yamaguchi H, Yoshida S, Shimoda T. Metastatic tumors to the stomach: analysis of 54 patients diagnosed at endoscopy and 347 autopsy cases. *Endoscopy* 2001; **33**: 507-510 [PMID: 11437044 DOI: 10.1055/s-2001-14960]
9 **Saito T**, Iizuka T, Kato H, Watanabe H. Esophageal carcinoma metastatic to the stomach. A clinicopathologic study of 35 cases. *Cancer* 1985; **56**: 2235-2241 [PMID: 4052968 DOI: 10.1002/1097-0142(19851101)56:9<2235::aid-cncr2820560917>3.0.co;2-0]
10 **Ebihara Y**, KT, Kobayashi M, Hosokawa M, Kato H. A case of esophageal carcinoma with giant intramural gastric metastasis. *Jpn J Surg Assoc* 2002; **63**: 8
11 **Yoshida K**, Ide H, Murata Y, Kobayashi A, Hanyuu H, Yamada A. [A case of mucosal esophageal carcinoma with a large intramural metastasis in the stomach]. *Nihon Kyobu Geka Gakkai Zasshi* 1989; **37**: 1430-1435 [PMID: 2794606]
12 **Nishimura T**, TT, Shibuya Y, Nakamura T, Goto M, Fukui Y. A case of mucosal esophageal carcinoma with metastasis to the gastric wall. *Jpn J Surg Assoc* 2008; **69**: 5
13 **Nabeki B**, O. H., Omoto I, Matsumoto M, Uchikado Y, Setoyama T *et al*, A case of upper thoracic superficial esophageal carcinoma with intramural metastasis to the stomach and lymph node metastasis along the common hepatic artery. *Jpn J Gastroenterol Surg* 2012; **45**: 7
14 **Chaffer CL**, Weinberg RA. A perspective on cancer cell metastasis. *Science* 2011; **331**: 1559-1564 [PMID: 21436443 DOI: 10.1126/science.1203543]
15 **Gupta GP**, Massagué J. Cancer metastasis: building a framework. *Cell* 2006; **127**: 679-695 [PMID: 17110329 DOI: 10.1016/j.cell.2006.11.001]
16 **Sudo K**, Kato K, Kuwabara H, Sasaki Y, Takahashi N, Shoji H, Iwasa S, Honma Y, Okita NT, Takashima A, Hamaguchi T, Yamada Y, Ito Y, Itami J, Fukuda T, Tobinai K, Boku N. Patterns of Relapse after Definitive Chemoradiotherapy in Stage II/III (Non-T4) Esophageal Squamous Cell Carcinoma. *Oncology* 2018; **94**: 47-54 [PMID: 29080886 DOI: 10.1159/000480515]
17 **Yamashita K**, Watanabe M, Mine S, Kurogochi T, Okamura A, Hayami M, Imamura Y. Patterns and Outcomes of Recurrent Esophageal Cancer After Curative Esophagectomy. *World J Surg* 2017; **41**: 2337-2344 [PMID: 28432391 DOI: 10.1007/s00268-017-4024-5]
18 **Okamura A**, Yoshimizu S, Kanamori J, Imamura Y, Asari T, Nakayama I, Ogura M, Ishiyama A, Yoshio T, Chin K, Fujisaki J, Watanabe M. Treatment Strategy for Esophageal Squamous Cell Carcinoma With Endoscopic Intramural Metastasis. *Cureus* 2022; **14**: e23028 [PMID: 35464586 DOI: 10.7759/cureus.23028]
19 **Wang Y**, Zhu L, Xia W, Wang F. Anatomy of lymphatic drainage of the esophagus and lymph node metastasis of thoracic esophageal cancer. *Cancer Manag Res* 2018; **10**: 6295-6303 [PMID: 30568491 DOI: 10.2147/CMAR.S182436]
20 **Riquet M**, Saab M, Le Pimpec Barthes F, Hidden G. Lymphatic drainage of the esophagus in the adult. *Surg Radiol Anat* 1993; **15**: 209-211 [PMID: 8235965 DOI: 10.1007/BF01627708]
21 **WATSON WL**, GOODNER JT. Carcinoma of the esophagus. *J Int Coll Surg* 1957; **28**: 715-723 [PMID: 13481411]
22 **Roul PK**, Saran S, Poonia DR, Paul P. Intramural Gastric Metastasis: A Rare Presentation of Esophageal Squamous Cell Carcinoma. *J Med Ultrasound* 2022; **30**: 47-49 [PMID: 35465584 DOI: 10.4103/JMU.JMU_1_21]
23 **Nakazawa N**, Fukuchi M, Sakurai S, Naitoh H, Kiriyama S, Fukasawa T, Tabe Y, Yamauchi H, Suzuki M, Yoshida T, Kuwano H. Mucosal esophageal squamous cell carcinoma with intramural gastric metastasis invading liver and pancreas: a case report. *Int Surg* 2014; **99**: 458-462 [PMID: 25058784 DOI: 10.9738/INTSURG-D-13-00069.1]
24 **Sun K**, Lv H, Chen B, Nie C, Zhao J, Wang S, Wang J, Xu W, Chen X. Dawning precision treatment for gastric cancer: The latest biomarkers. *J Transl Int Med* 2021; **9**: 228-230 [PMID: 35136720 DOI: 10.2478/jtim-2021-0023]
25 **Abnet CC**, Arnold M, Wei WQ. Epidemiology of Esophageal Squamous Cell Carcinoma. *Gastroenterology* 2018; **154**: 360-373 [PMID: 28823862 DOI: 10.1053/j.gastro.2017.08.023]
26 **Okumura T**, Shimada Y, Hojo S, Sekine S, Hirano K, Moriyama M, Miwa S, Nagata T, Tsukada K. Perforation of intramural gastric metastasis during preoperative chemotherapy in a patient with thoracic esophageal squamous cell carcinoma. *Int J Surg Case Rep* 2015; **17**: 23-27 [PMID: 26519812 DOI: 10.1016/j.ijscr.2015.10.024]
27 **Matsutani T**, SK, Yoshida H, Hosone M, Katayama H, Uchida EA. A case of intramural gastric tube metastasis from esophageal squamous

cell carcinoma. *Esophagus* 2012; **9**: 239-242

28 **Nishimaki T**, Suzuki T, Tanaka Y, Aizawa K, Hatakeyama K, Muto T. Intramural metastases from thoracic esophageal cancer: local indicators of advanced disease. *World J Surg* 1996; **20**: 32-37 [PMID: 8588409 DOI: 10.1007/s002689900006]

29 **Nishida K**, Okuyama C, Kubota T, Matsushima S, Oda M, Akazawa K, Nishimura T. Intramural metastasis of esophageal carcinoma to the reconstructed gastric tube detected by FDG PET/CT. *Clin Nucl Med* 2009; **34**: 523-525 [PMID: 19617734 DOI: 10.1097/RLU.0b013e3181abb791]

30 **Liu P**, Zhu H, Zhang X, Feng A, Zhu X, Sun Y. Predicting Survival for Hepatic Arterial Infusion Chemotherapy of Unresectable Colorectal Liver Metastases: Radiomics Analysis of Pretreatment Computed Tomography. *J Transl Int Med* 2022; **10**: 56-64 [PMID: 35702189 DOI: 10.2478/jtim-2022-0004]

31 **Lee GD**, Kim YH, Kim JB, Choi SH, Kim HR, Kim DK, Park SI. Esophageal Cancer Associated with Multiple Primary Cancers: Surgical Approaches and Long-term Survival. *Ann Surg Oncol* 2013; **20**: 4260-4266 [PMID: 23904006 DOI: 10.1245/s10434-013-3183-3]

32 **Szántó I**, Vörös A, Nagy P, Gonda G, Gamal EM, Altorjay A, Banai J, Kiss J. Esophageal intramural metastasis from adenocarcinoma of the gastroesophageal junction. *Endoscopy* 2002; **34**: 418-420 [PMID: 11972277 DOI: 10.1055/s-2002-25294]

33 **Watanabe M**, Kuwano H, Araki K, Kawaguchi H, Saeki H, Kitamura K, Ohno S, Sugimachi K. Prognostic factors in patients with submucosal carcinoma of the oesophagus. *Br J Cancer* 2000; **83**: 609-613 [PMID: 10944600 DOI: 10.1054/bjoc.2000.1288]

Published by **Baishideng Publishing Group Inc**
7041 Koll Center Parkway, Suite 160, Pleasanton, CA 94566, USA
Telephone: +1-925-3991568
E-mail: bpgoffice@wjgnet.com
Help Desk: https://www.f6publishing.com/helpdesk
https://www.wjgnet.com